Indirect searches for dark matter – Lec IV

Christoph Weniger

IMPRS PhD block course

23-25 Nov 2015, MPP, Munich

GRAPPA

GRavitation AstroParticle Physics Amsterdam

Cosmic rays

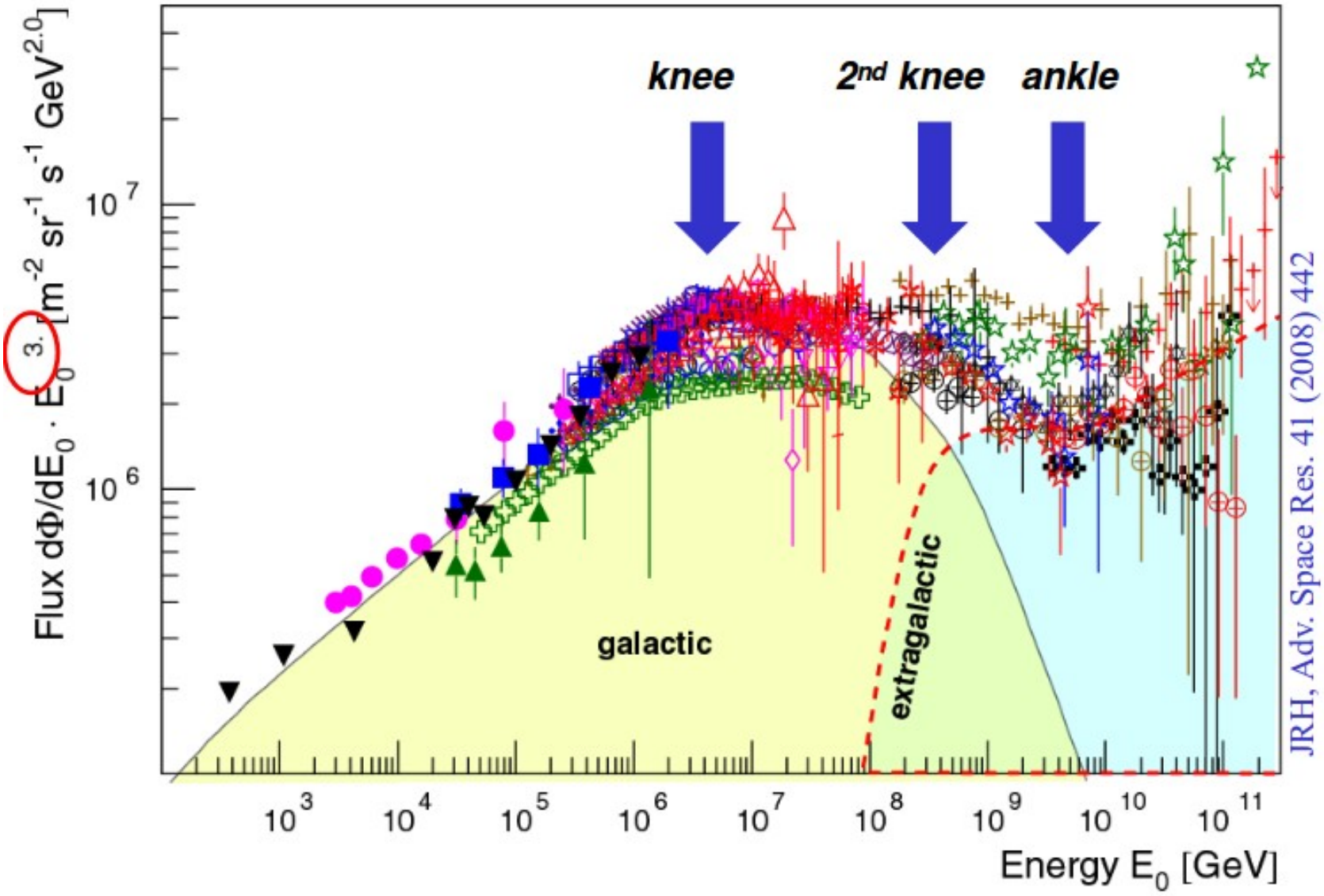
knee
2nd knee
ankle
galactic
extragalactic
Flux dΦ/dE0 · E0^3 [m^-2 sr^-1 s^-1 GeV^2.0]
Energy E0 [GeV]
JRH, Adv. Space Res. 41 (2008) 442

Cosmic ray propagation

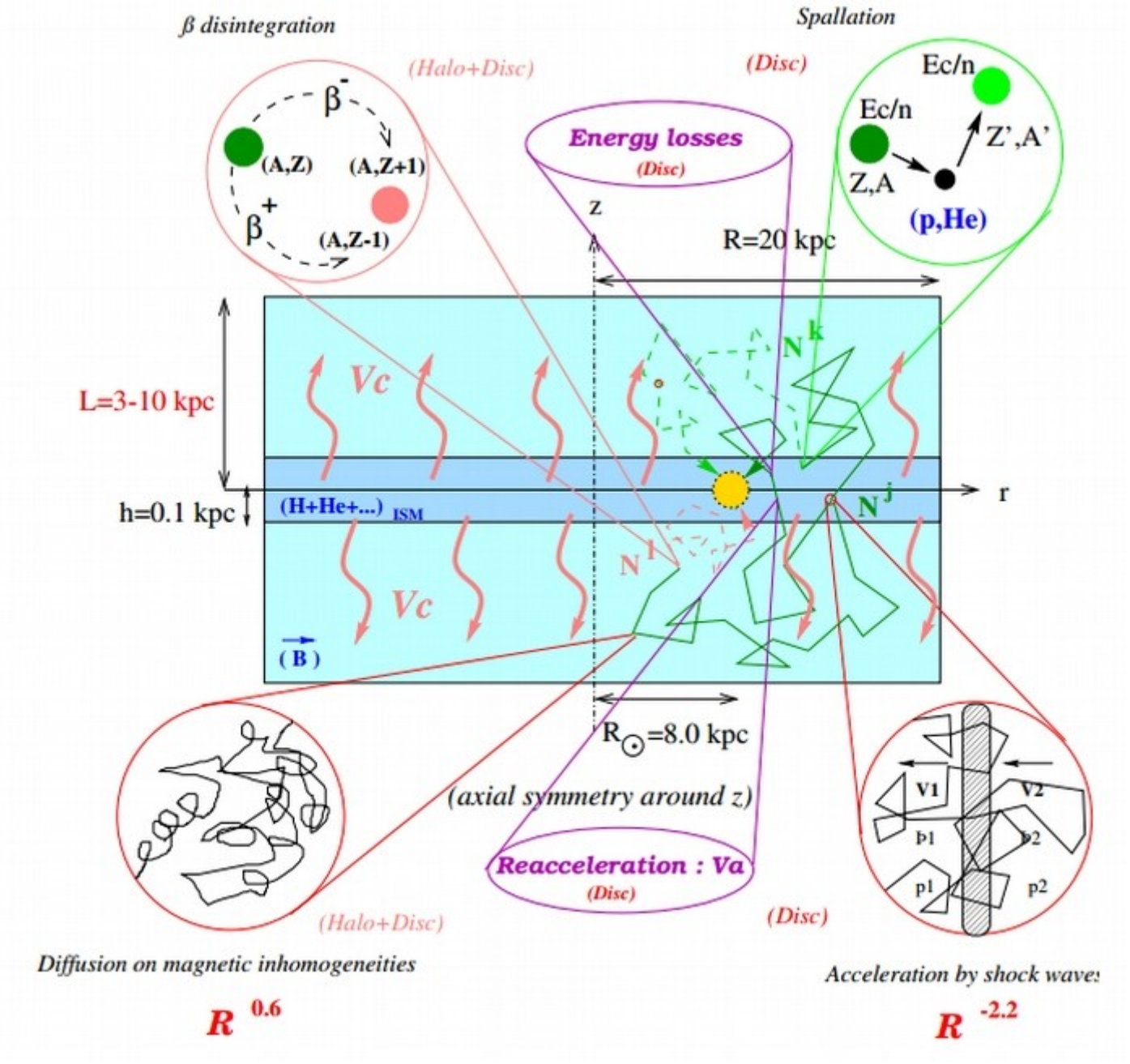

Cosmic ray composition

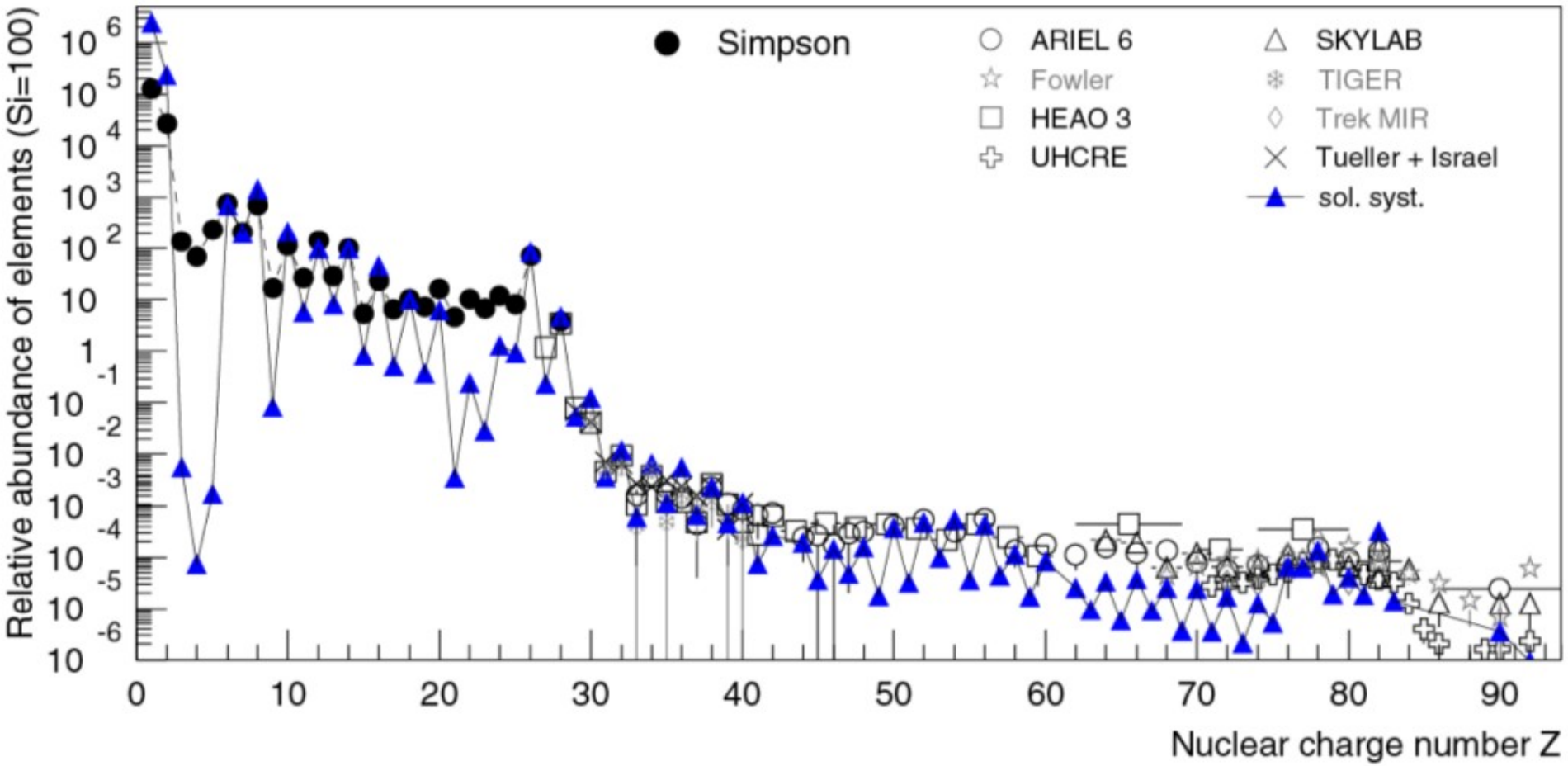

The “grammage” matters

Two sources for cosmic rays

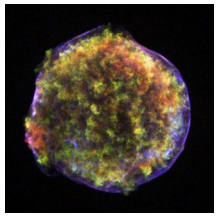

Primary cosmic rays from supernova remnants (likely)

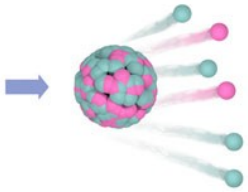

Secondary cosmic rays from spallation etc

Diffusion in a box

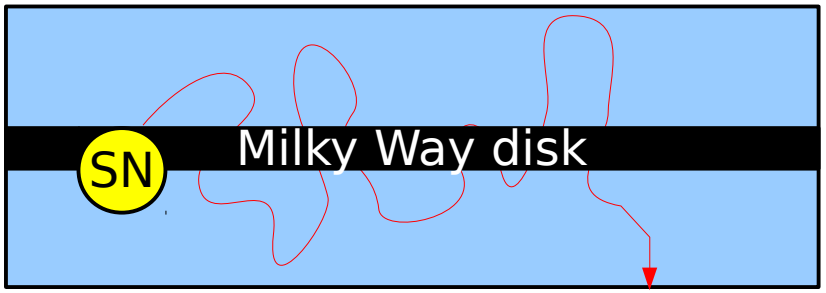

Chemical composition of CRs vs solar system

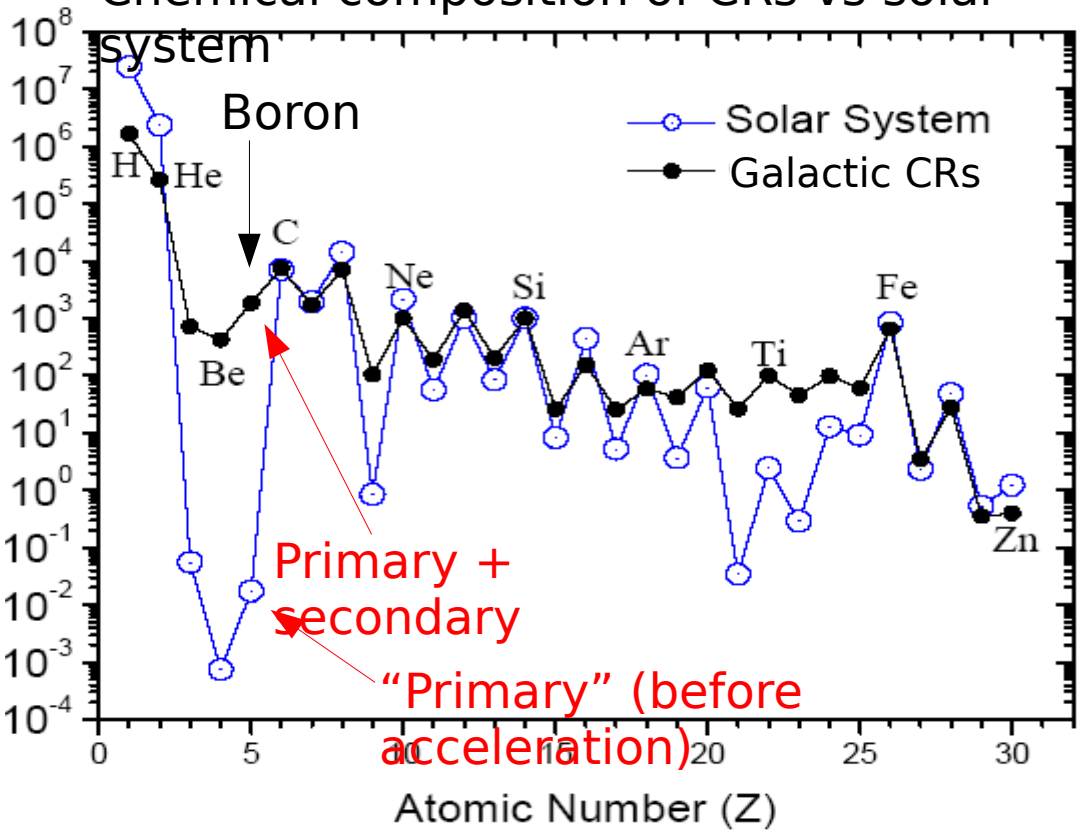

Total grammage (column density along propagation path)

$$G_{\text{total}} = n_{\text{crossings}} G_{\text{disk}}$$

Secondary Boron:

$$n_B = n_C \sigma(C \to B) \cdot G_{\text{total}} \quad \Rightarrow G_{\text{total}}$$

Secondary antiprotons:

$$n_{\bar{p}} = n_p \sigma(p \to \bar{p}) \cdot G_{\text{total}} \quad \Rightarrow n_{\bar{p}}$$

Fit to B/C, predictions for anti-protons

Viable parameters for the propagation model: (fit to B/C and p data)

Model	z_t(kpc)	δ	$D_0(10^{28}\mathrm{cm}^2/\mathrm{s})$	η	v_A(km/s)	γ	dv_c/dz(km/s/kpc)	$\chi^2_{B/C}$	χ^2_p	Φ (GV)	$\chi^2_{\bar{p}}$	Color in Fig.s
KRA	4	0.50	2.64	−0.39	14.2	2.35	0	0.6	0.47	0.67	0.59	Red
KOL	4	0.33	4.46	1.	36.	1.78/2.45	0	0.4	0.3	0.36	1.84	Blue
THN	0.5	0.50	0.31	−0.27	11.6	2.35	0	0.7	0.46	0.70	0.73	Green
THK	10	0.50	4.75	−0.15	14.1	2.35	0	0.7	0.55	0.69	0.62	Orange
CON	4	0.6	0.97	1.	38.1	1.62/2.35	50	0.4	0.53	0.21	1.32	Gray

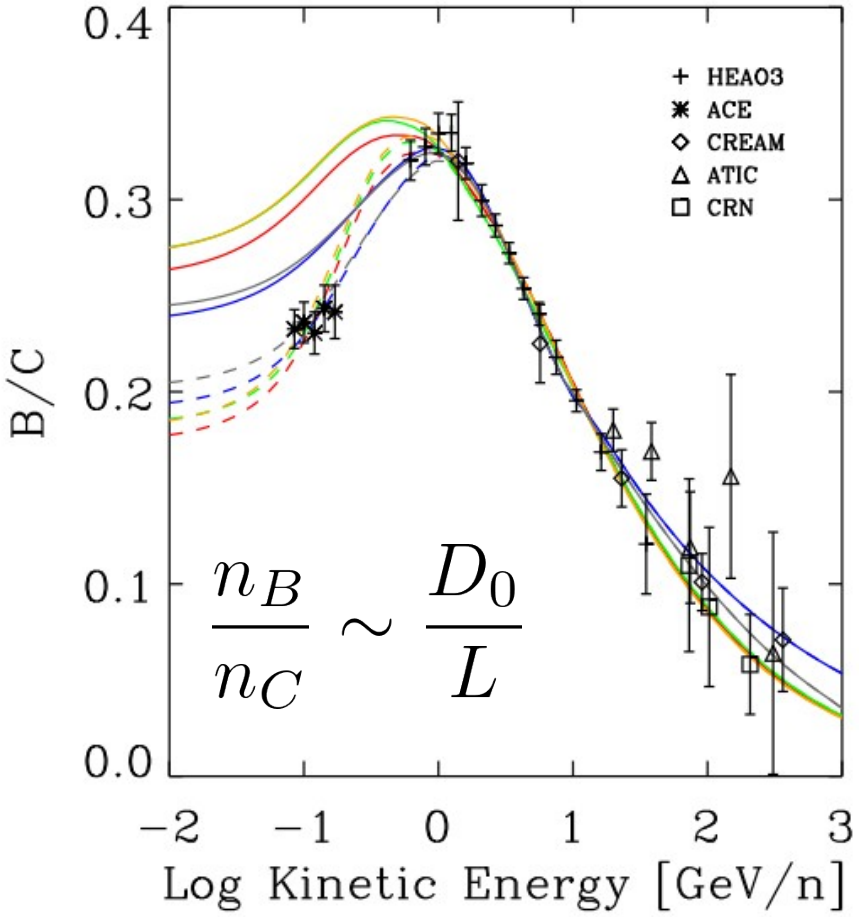

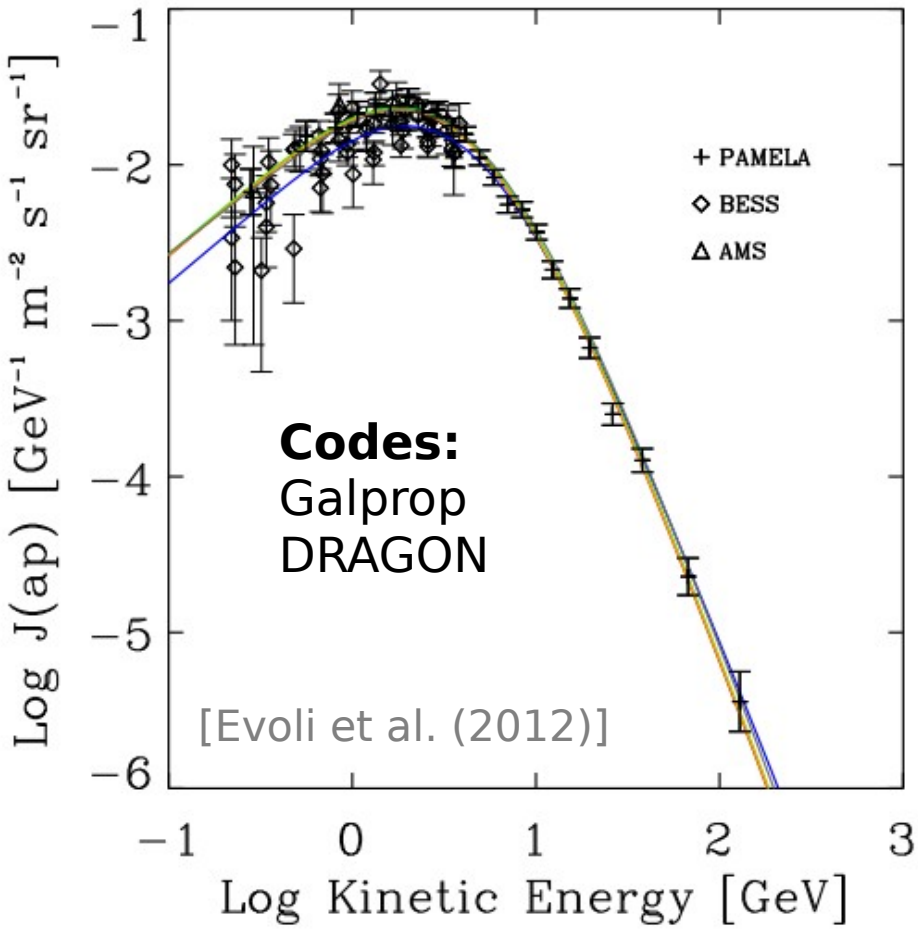

The LAT view on the gamma-ray sky

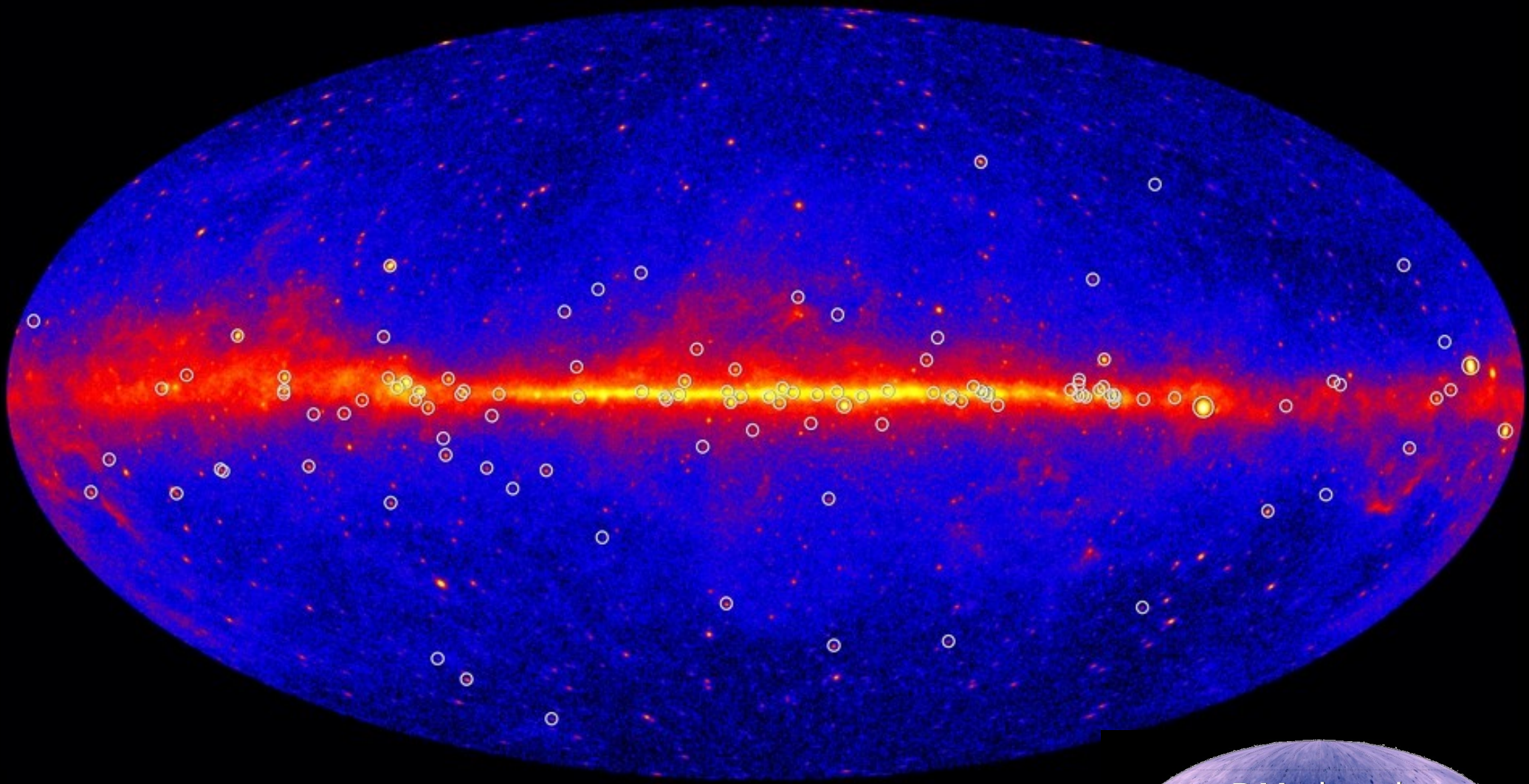

Five years of data taking > 1 GeV
Gamma-ray pulsar positions are indicated as circles

http://svs.gsfc.nasa.gov/vis/a010000/a011300/a011342/

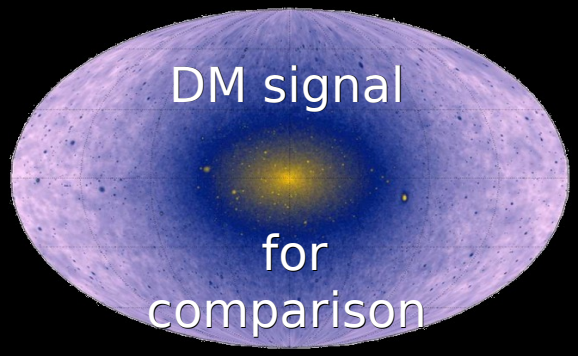

Fermi LAT sky in pseudo colors

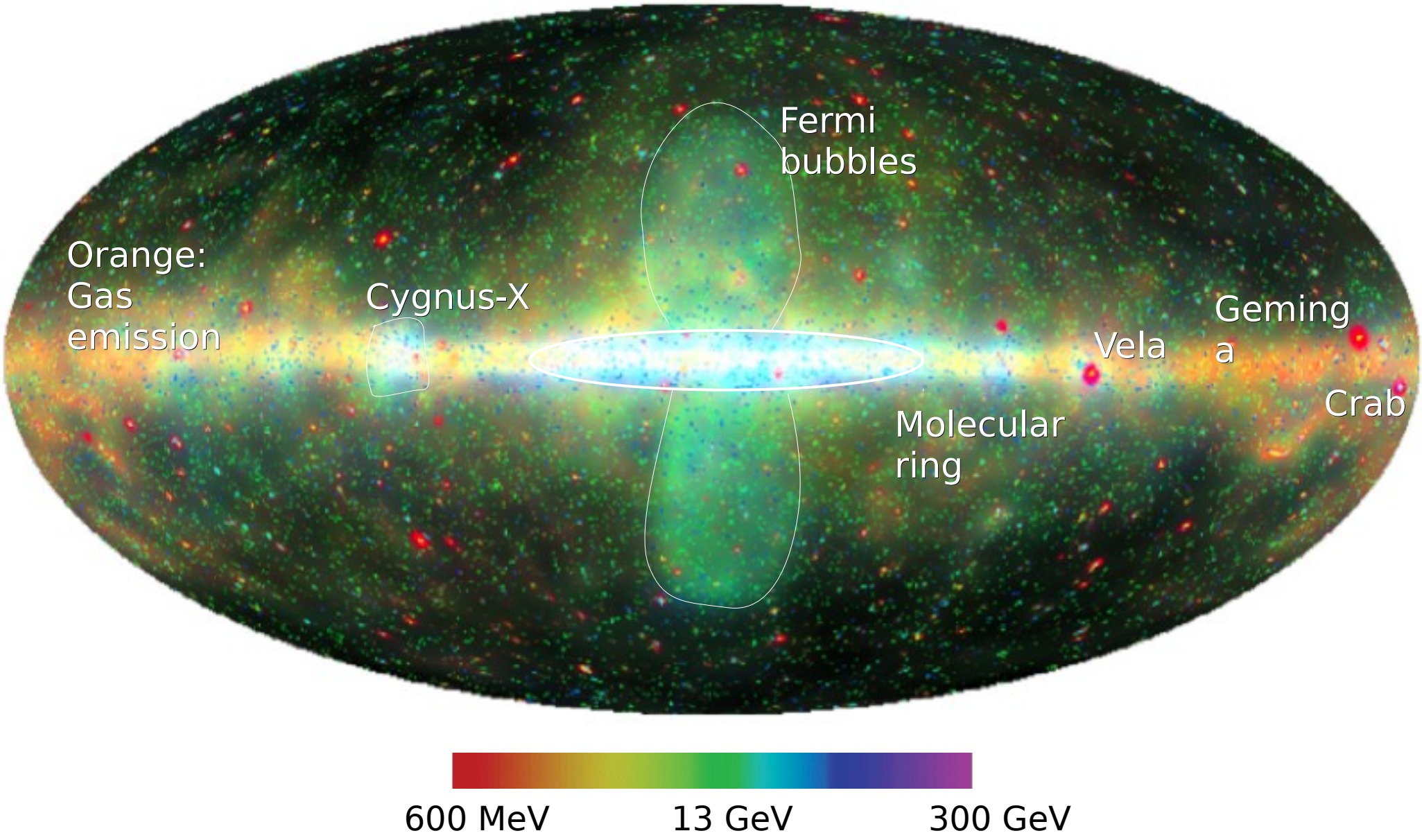

Selig+ 2014, 6.5 years of data, using D^{3}PO algorithm

Contributions to Galactic diffuse gamma rays

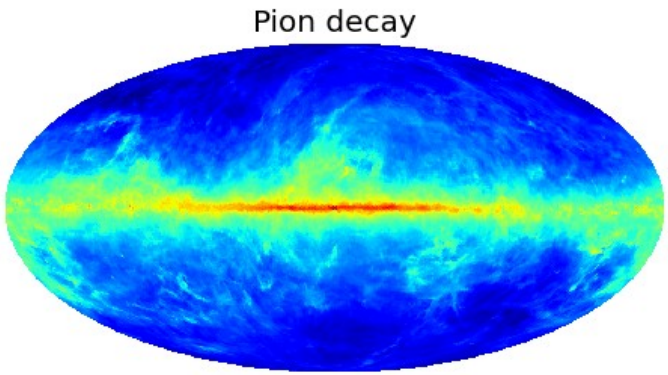

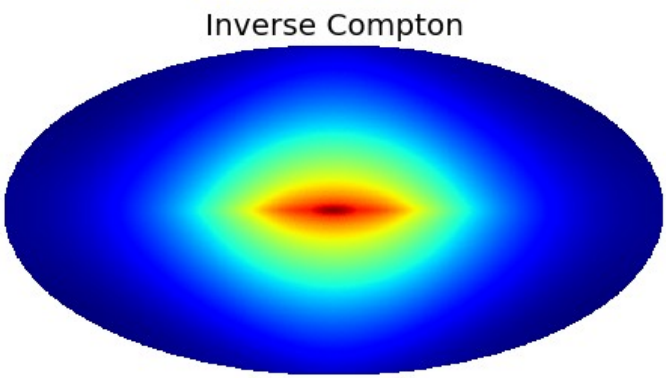

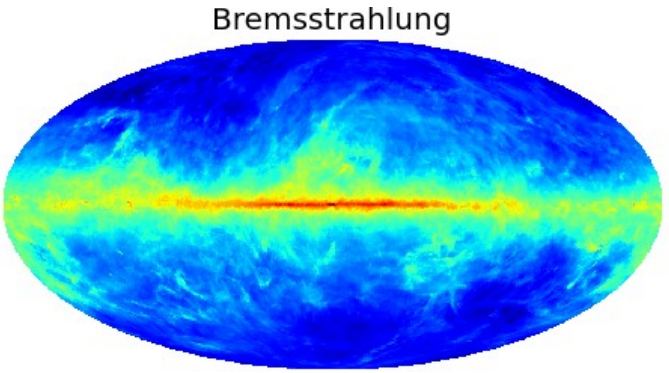

Neutral pions

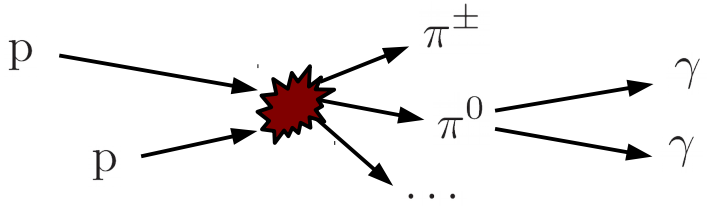

Inverse Compton

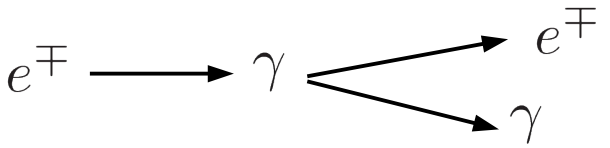

Predictions rely on

- Distribution and composition of interstellar medium
- Distribution and spectrum of interstellar radiation field
- Distribution and injection spectra of cosmic ray sources
- Average Galactic magnetic field
- Properties of diffusion halo
- Hadronic scattering cross-sections
- ...

Distribution of cosmic-ray sources

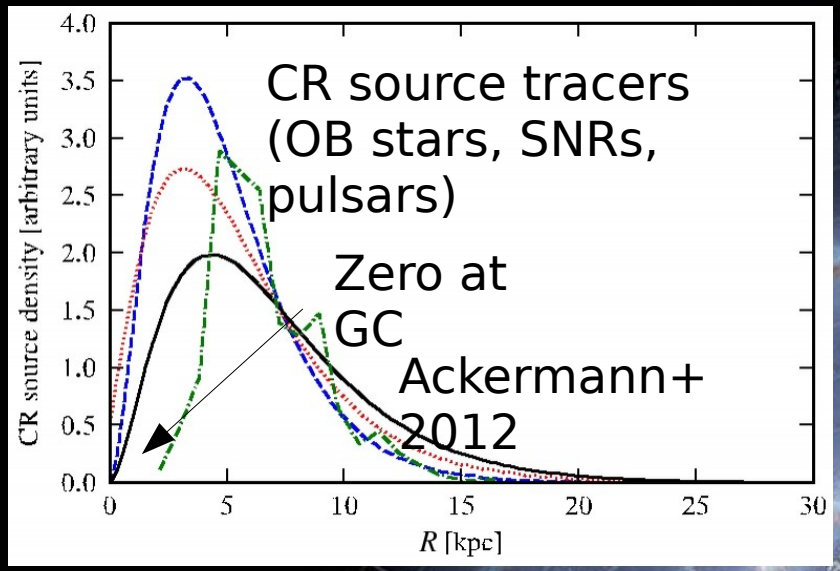

Typical travel distance (at 1 – 100 GeV)

CR electrons: O(1 kpc)

CR protons: O(10 kpc)

http://www.nasa.gov/mission_pages/sunearth/news/gallery/galaxy-location.html

Neutral hydrogen (H I) from 21 cm line

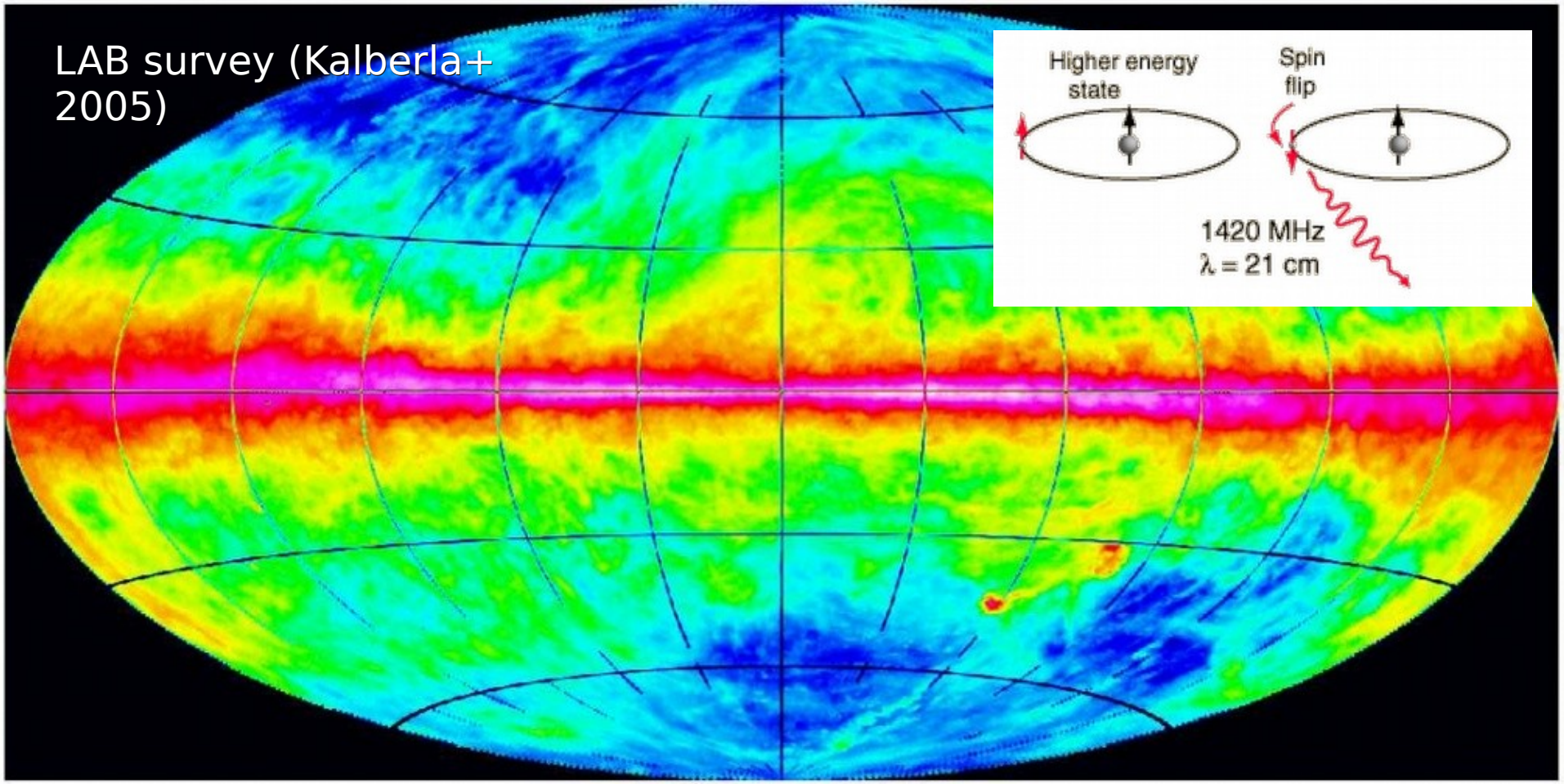

H I tracer

- LAB survey (Kalberla+ 2005)
- Decomposition along line-of-sight using Doppler shift

GALPROP; Ackermann+ 2012

$$v_{\rm LSR} = R_\odot \left(\frac{V(R)}{R} - \frac{V_\odot}{R_\odot} \right) \sin(l) \cos(b)$$

- Distributed in rings (boundaries: 0.0, 1.5, 2.0, 2.5, ..., 6.5, 7.0, 8.0, 10.0, kpc)

Example: Spatial decomposition of CO map

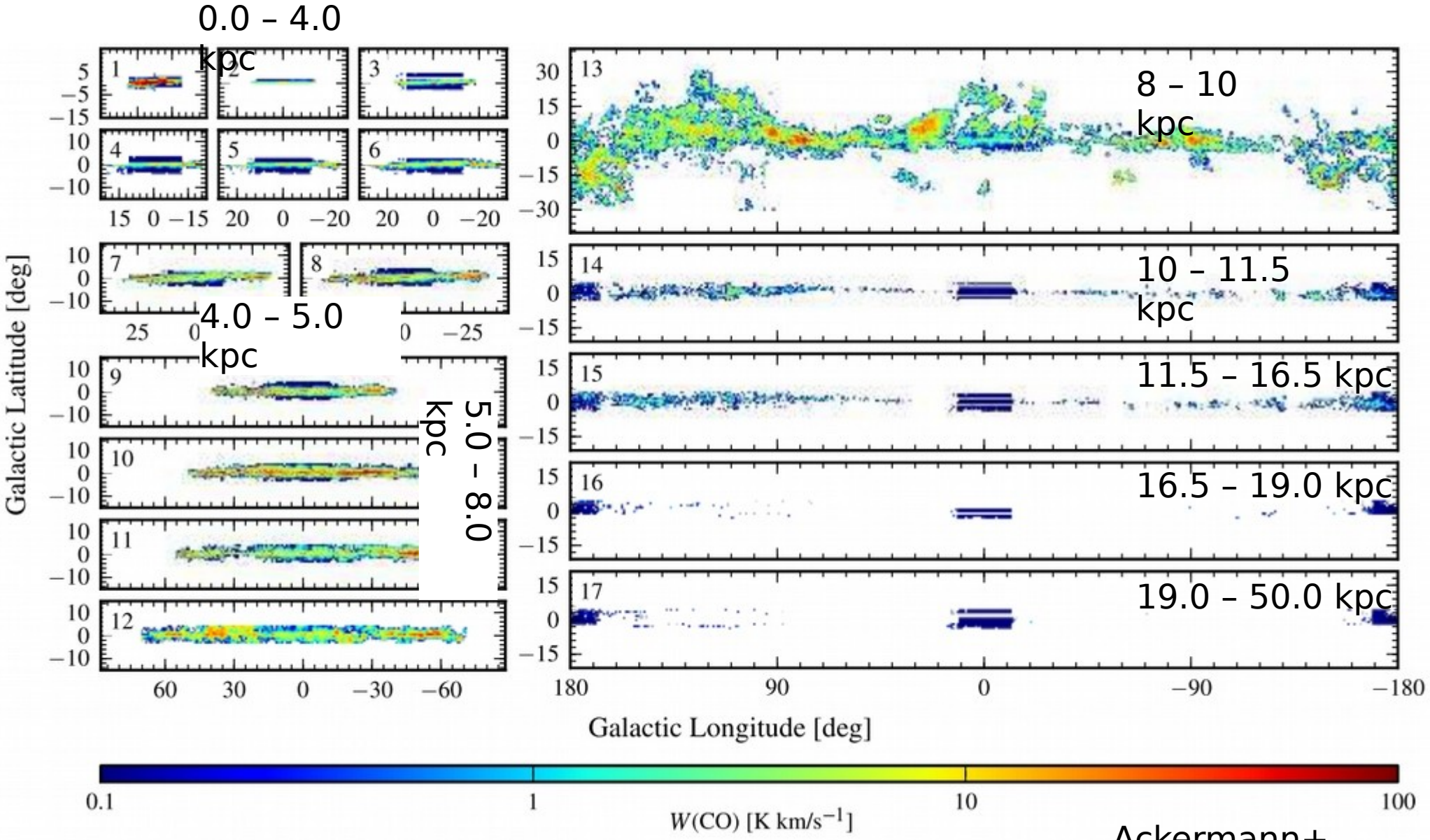

Ackermann+ 2012

Spatial decomposition

- Significant column densities all the way towards the GC (inner degrees)
- No molecular hydrogen above 5 deg in the inner ~5 kpc

Interstellar radiation field

Strong+ 2000; Porter & Strong 2005; Moskalenko+ 2006; Porter+ 2008

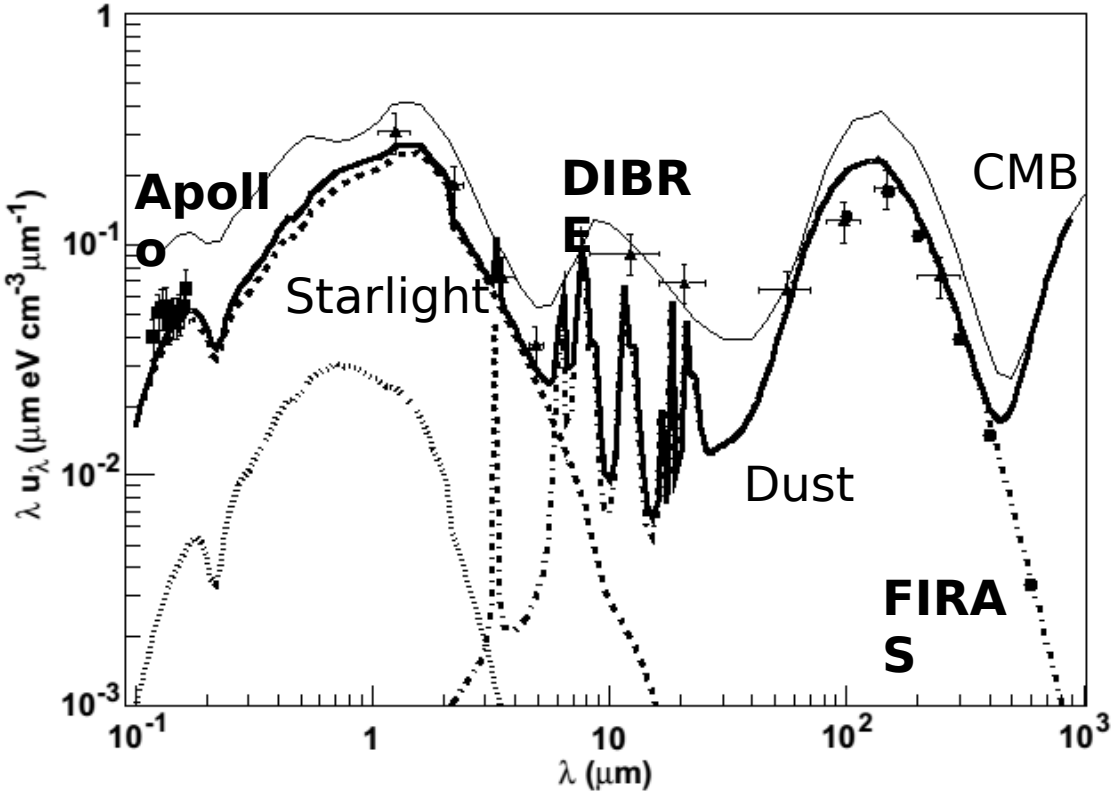

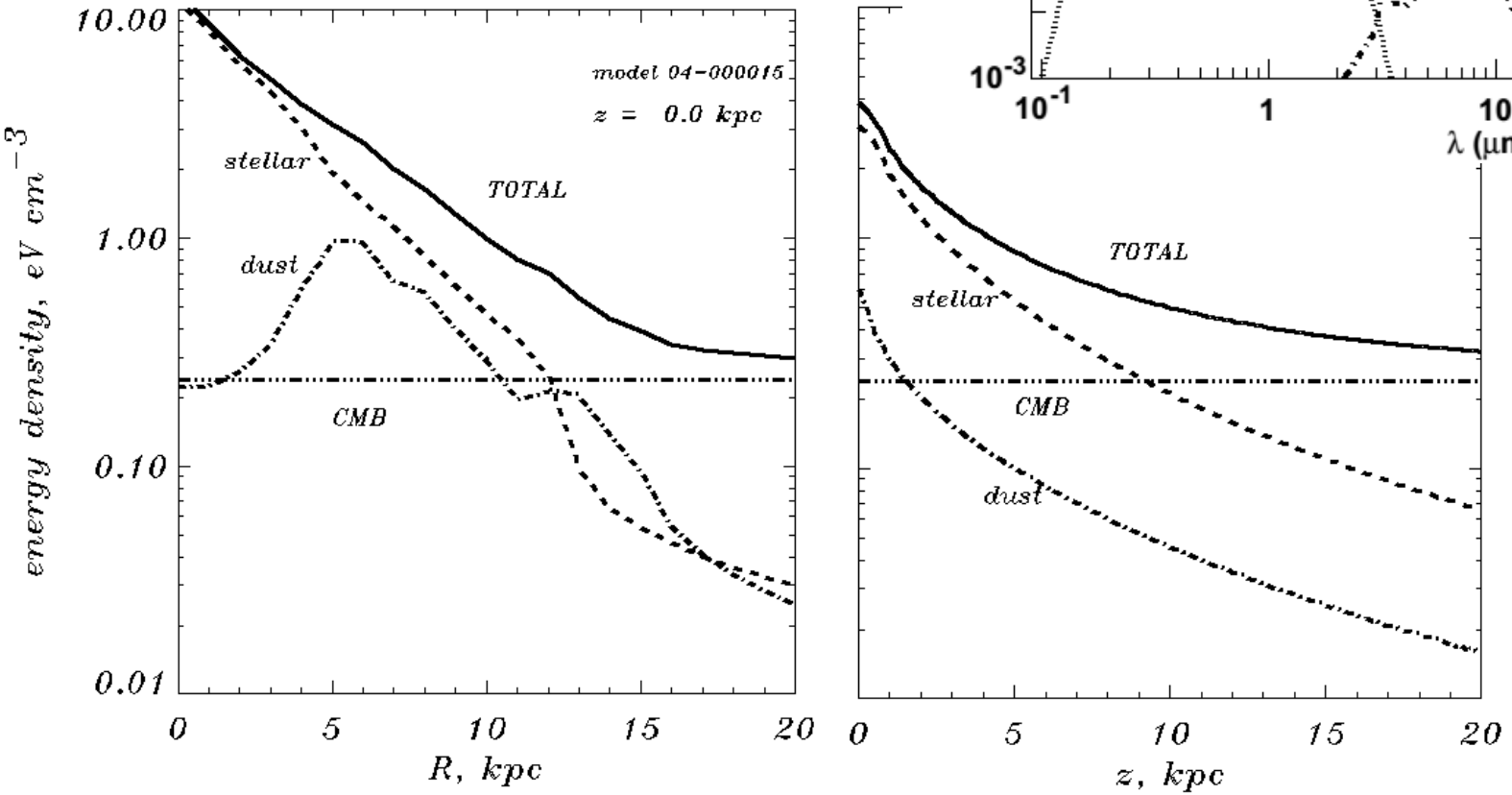

The Fermi Bubbles

Fermi Bubbles
[Su+ 2010; Dobler+ 2010; Ackermann+ 2014]

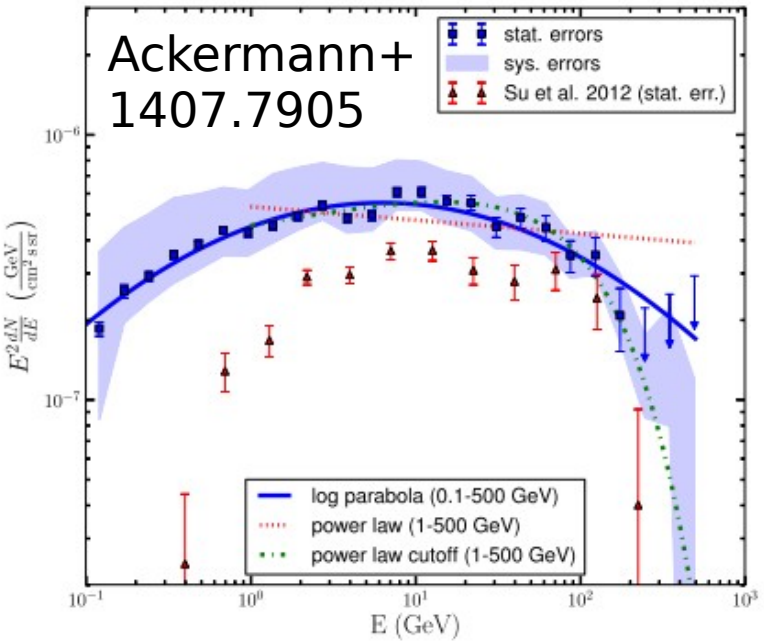

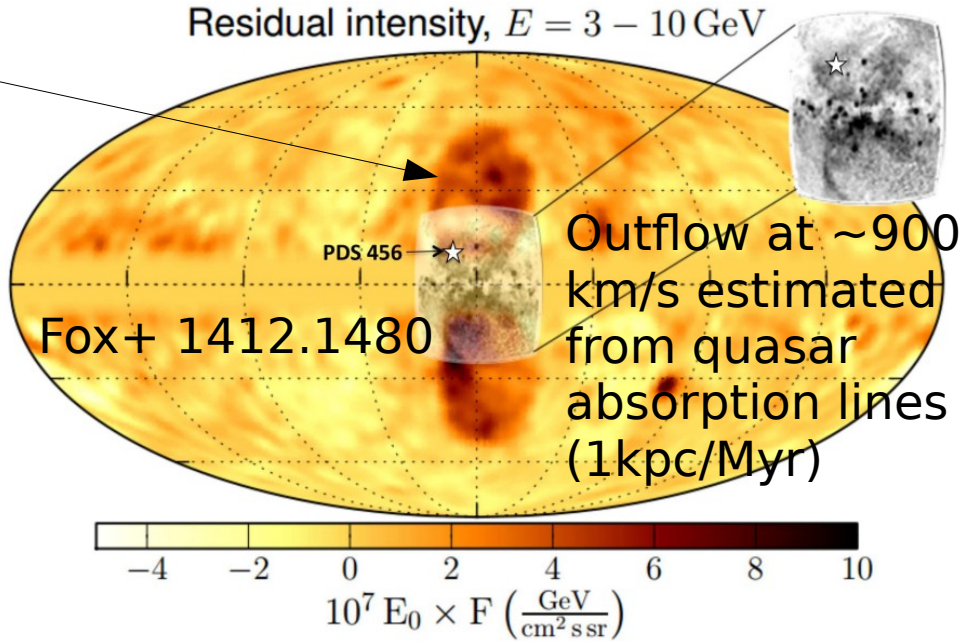

Possible explanations

- Jets from the black hole
  [Guo & Mathews 2012, Yang+ 2012]
- Feedback from nuclear star formation
  [Crocker & Aharonian 2011, Carretti+ 2013; Lacki 2014]
- Shocks from accretion flows onto Sgr A*
  [Cheng+ 2011, Mou+ 2014]
- Spherical outflow from Sgr A*
  [Zubovas+ 2011]

Are modeled with simple template.

Blazars

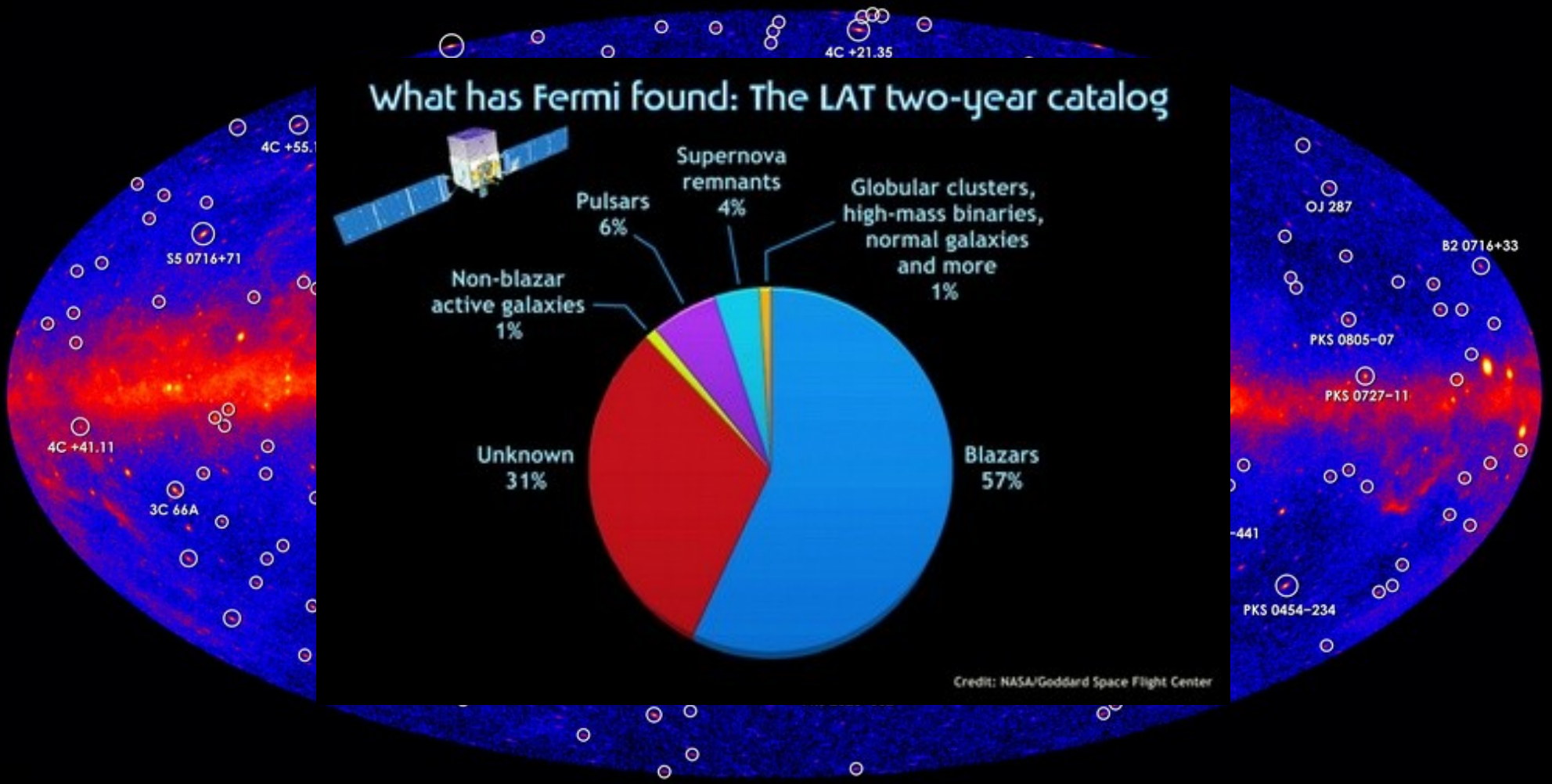
What has Fermi found: The LAT two-year catalog
Supernova remnants 4%
Pulsars 6%
Globular clusters, high-mass binaries, normal galaxies and more 1%
Non-blazar active galaxies 1%
Unknown 31%
Blazars 57%
Credit: NASA/Goddard Space Flight Center
4C +21.35
4C +55.
S5 0716+71
4C +41.11
3C 66A
OJ 287
B2 0716+33
PKS 0805-07
PKS 0727-11
PKS 0454-234

Pulsars

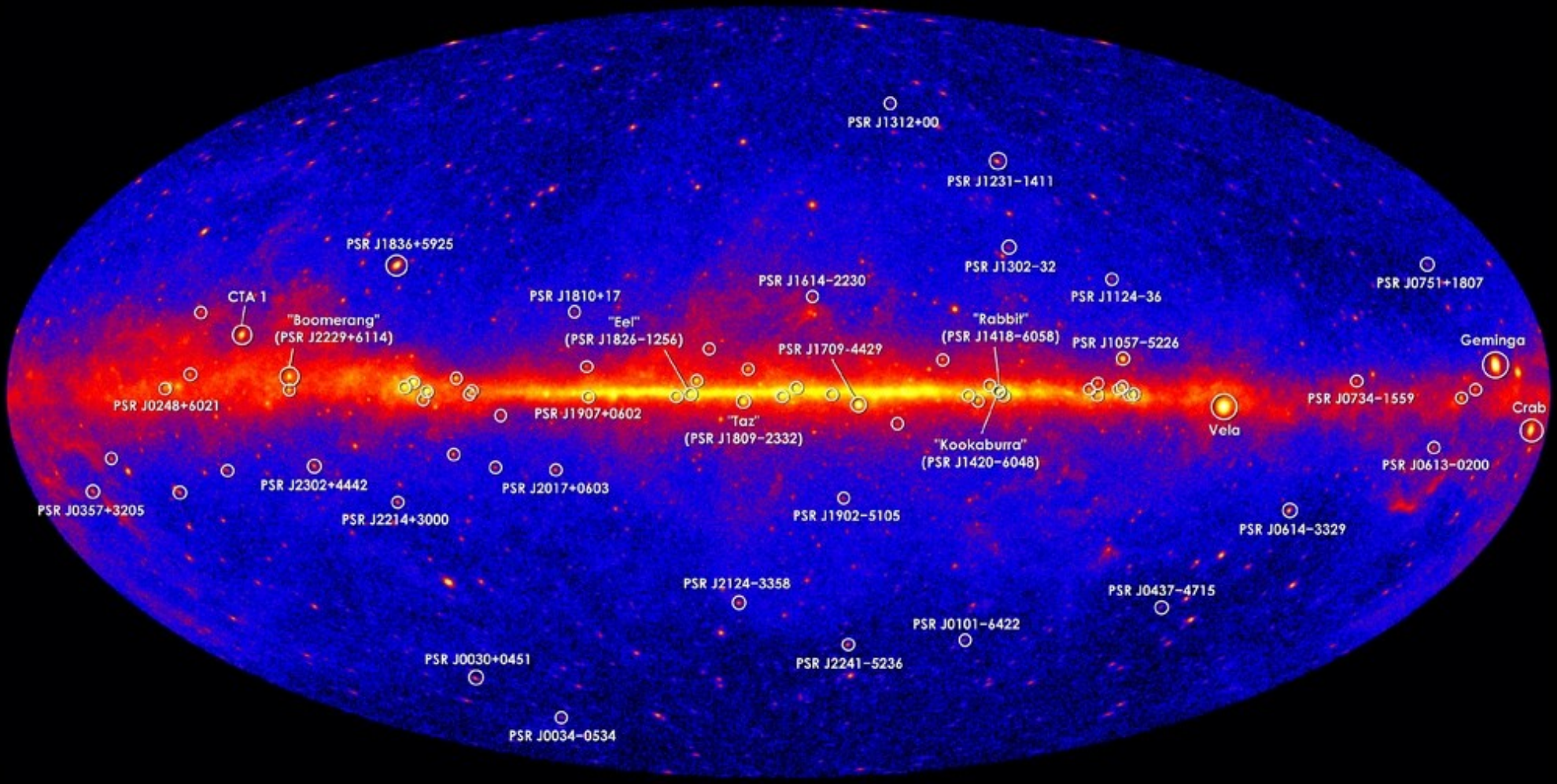
PSR J1312+00
PSR J1231−1411
PSR J1836+5925
PSR J1302−32
PSR J0751+1807
PSR J1614−2230
PSR J1124−36
CTA 1
PSR J1810+17
"Boomerang"
(PSR J2229+6114)
"Eel"
(PSR J1826−1256)
"Rabbit"
(PSR J1418−6058)
PSR J1057−5226
Geminga
PSR J1709−4429
PSR J0248+6021
PSR J1907+0602
PSR J0734−1559
Crab
"Taz"
(PSR J1809−2332)
Vela
"Kookaburra"
(PSR J1420−6048)
PSR J0613−0200
PSR J2302+4442
PSR J2017+0603
PSR J0357+3205
PSR J2214+3000
PSR J1902−5105
PSR J0614−3329
PSR J2124−3358
PSR J0437−4715
PSR J0101−6422
PSR J0030+0451
PSR J2241−5236
PSR J0034−0534

Results spatial and spectral

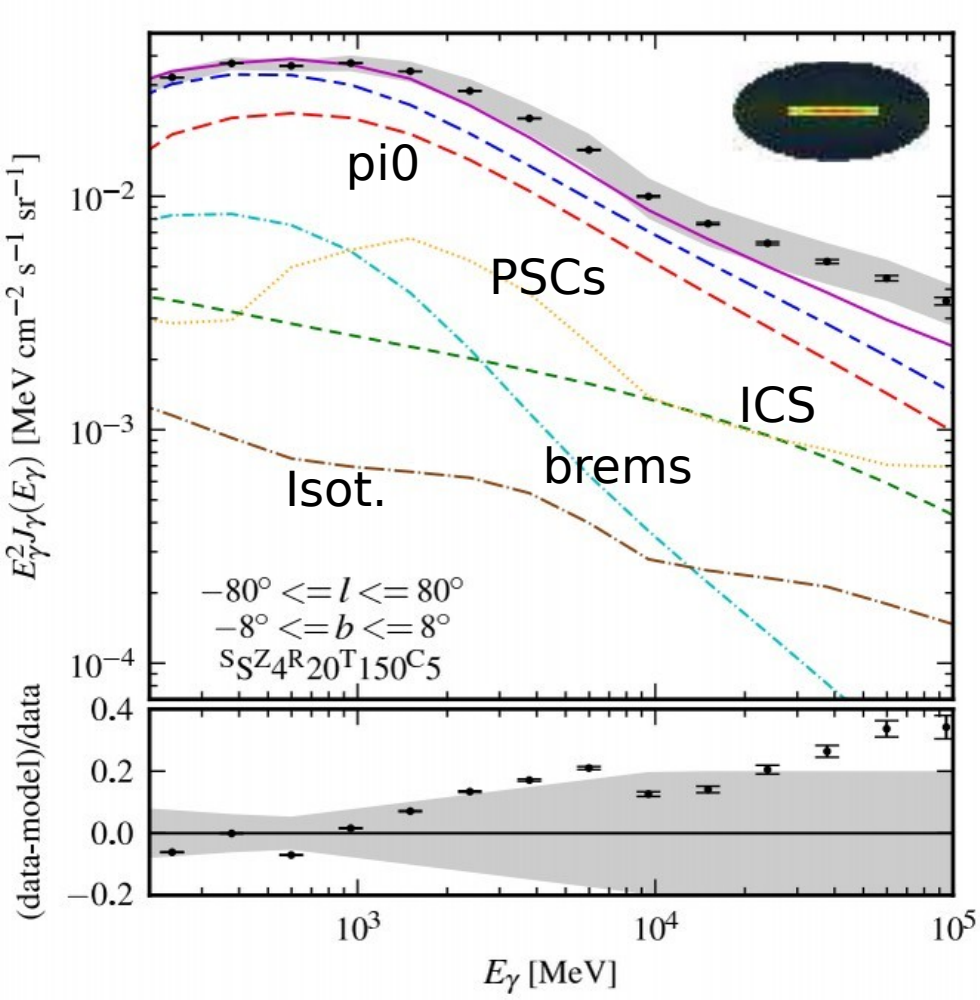

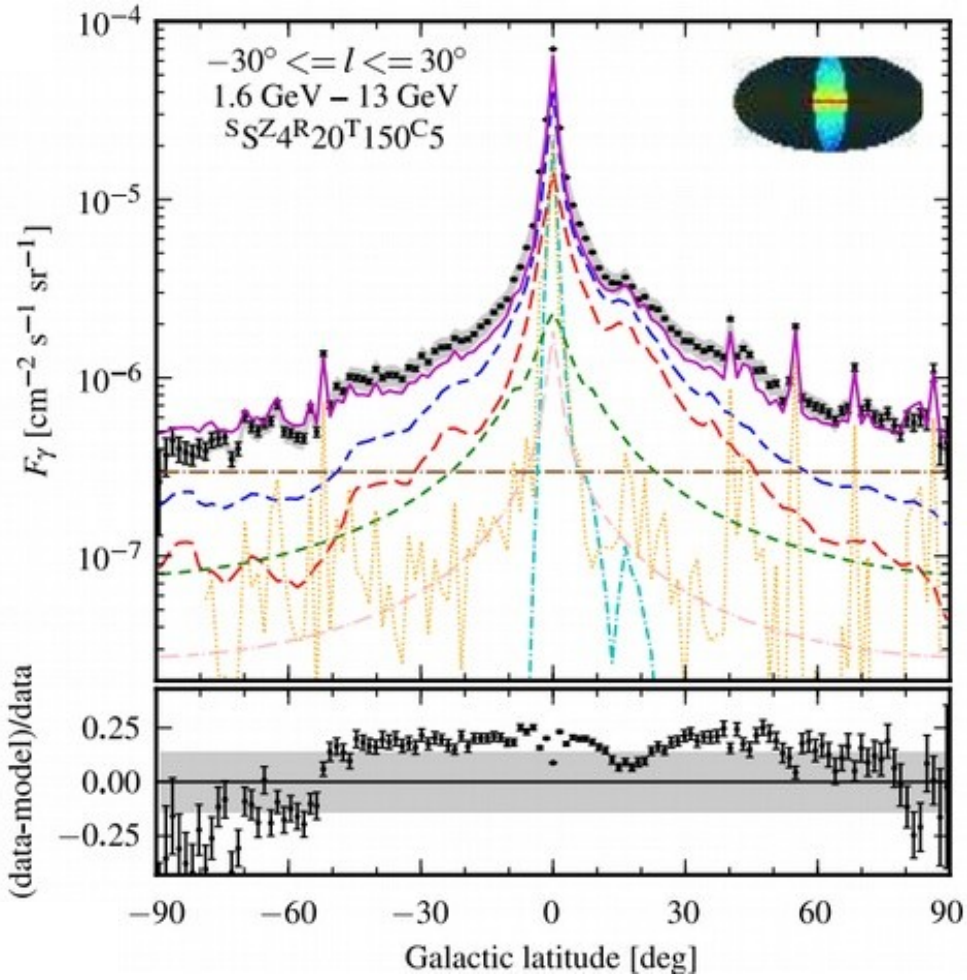

Ackermann+ 2012

General performance of models

- Models that reproduce the local cosmic ray measurements reproduce gamma-ray observations in the Galaxy reasonably well
- Residuals at high energies remain, possibly indicating variations in the diffusion properties towards the inner Galaxy [e.g. Gaggero+ 2014]

Fractional residuals

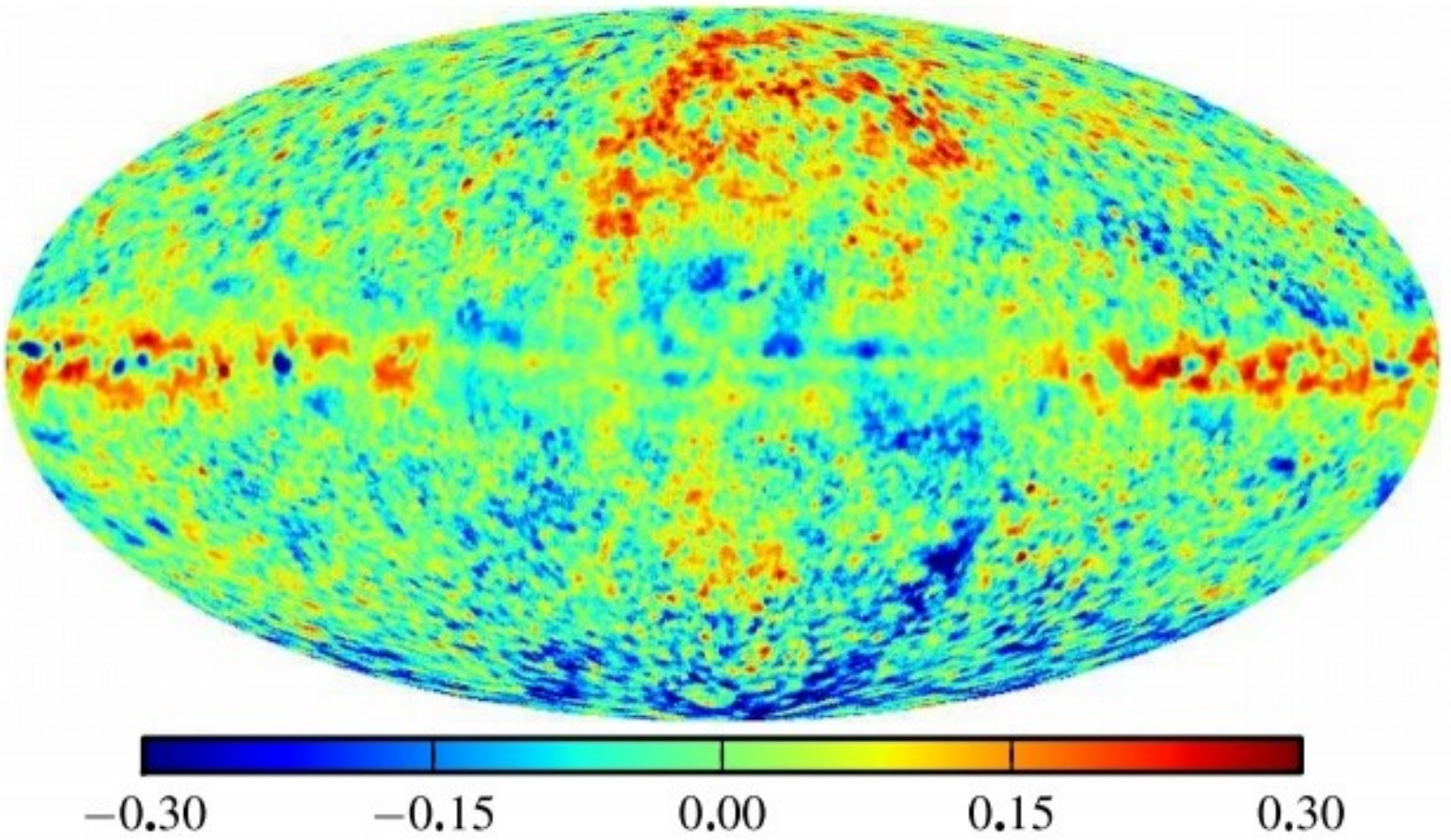

(model-data)/data (200 MeV – 100 GeV)

The Fermi Galactic center GeV excess

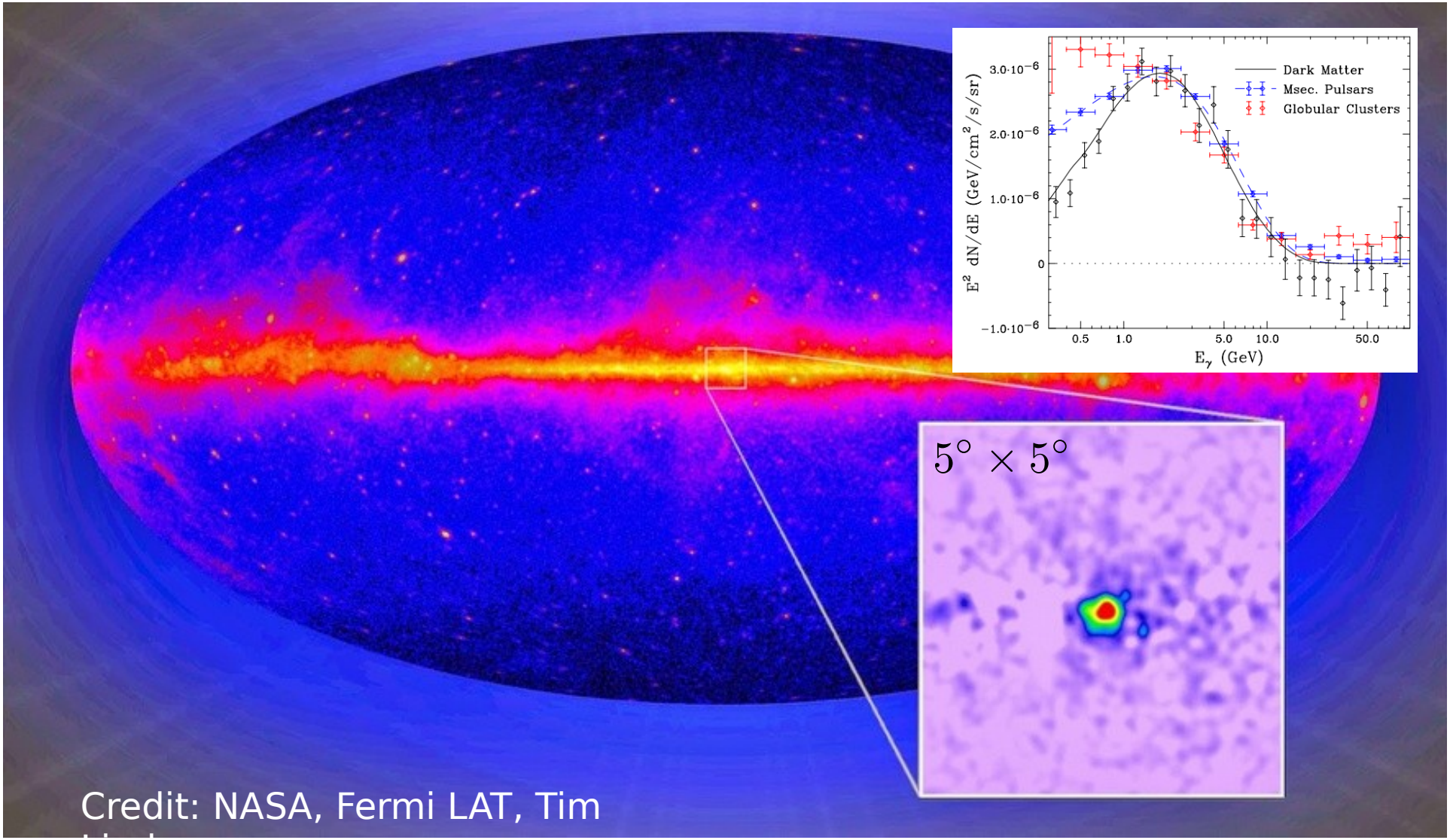

Goodenough & Hooper 2009, Vitale+ (Fermi coll.) 2009, Hooper & Goodenough 2011, Hooper & Linden 2011, Boyarsky+ 2011 (no signal), Abazajian & Kaplinghat 2012, Hooper & Slatyer 2013, Huang+ 2013, Gordon & Macias 2013, Macias & Gordon 2014, Zhou+ 2014, Abazajian+ 2014, Daylan+2014, Calore+ 2014, Gaggero+ 2015

The Galactic Center

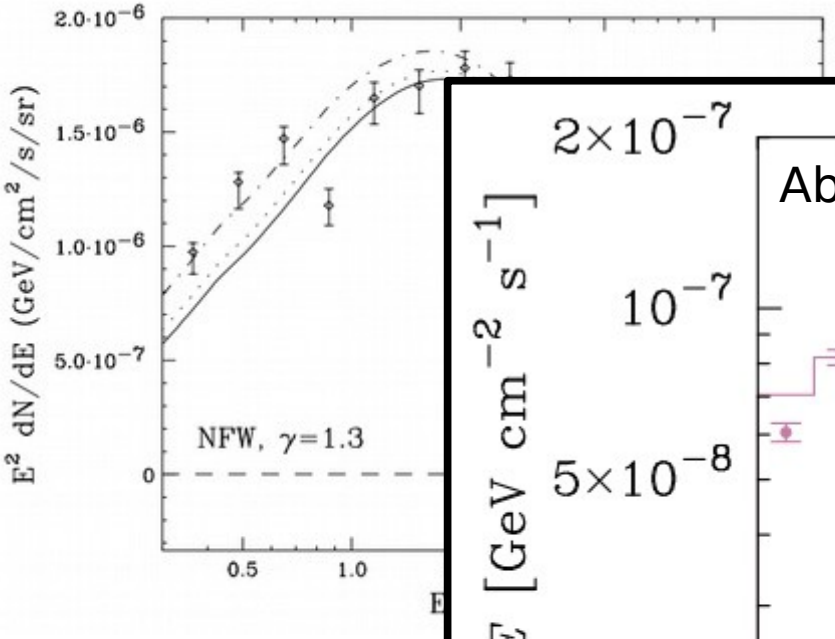

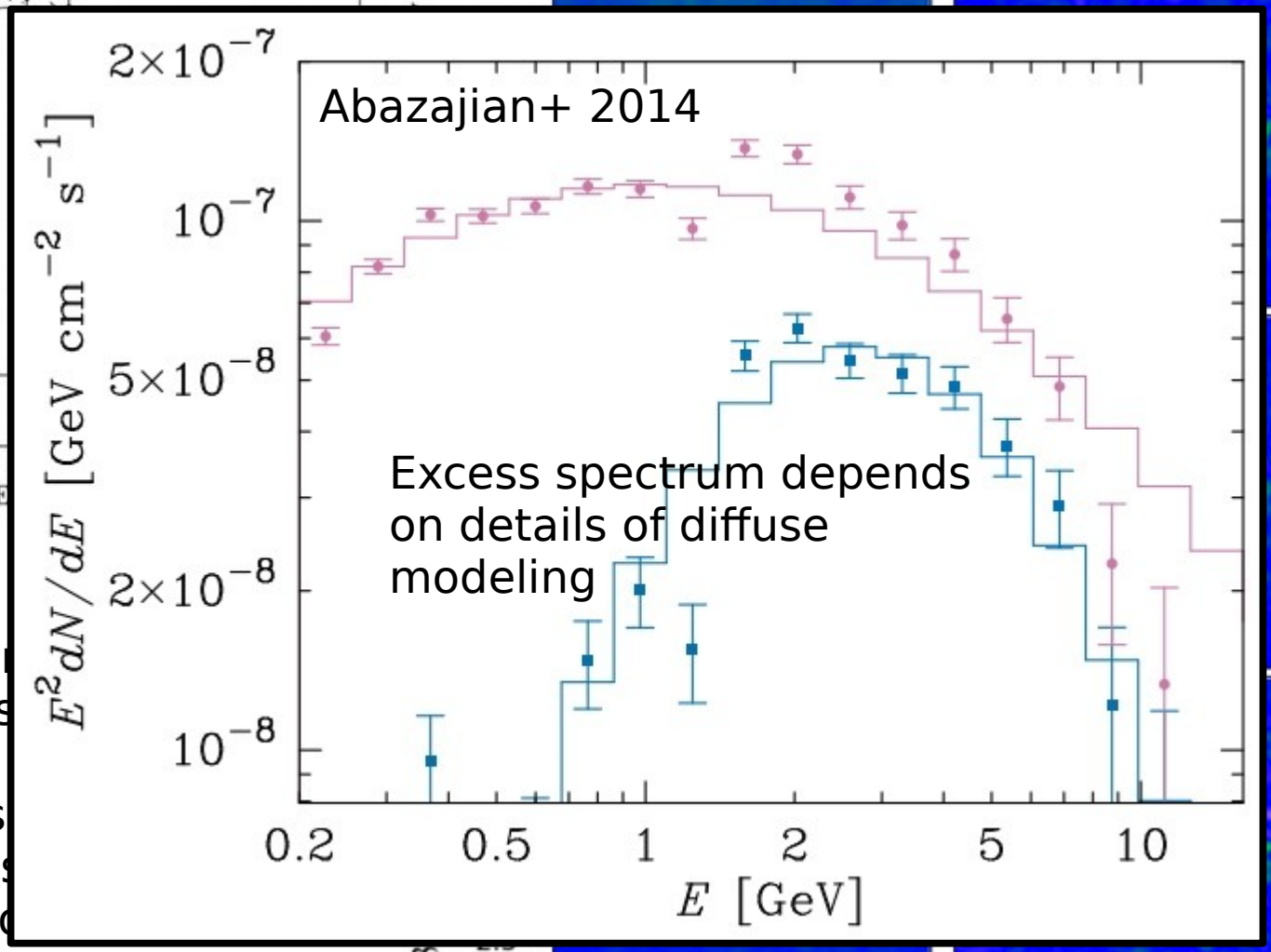

Daylan+ 2014

- Extended exces
  above
  - Diffuse emiss
  - Sgr A* Fermi
  - Other 2FGL s
- Morphology

$$\frac{dn}{dV} \sim r^{-\Gamma} \qquad \Gamma \sim 2.5$$

The excess at low and mid-latitudes

Excess at the Galactic center $|\ell|, |b| \lesssim 2^\circ$

Goodenough & Hooper 2009
Hooper & Goodenough 2011
Hooper & Linden 2011
Boyarsky+ 2011
Abazajian & Kaplinghat 2012
Gordon & Macias 2013
Macias & Gordon 2014
Abazajian+ 2014
Daylan+2014

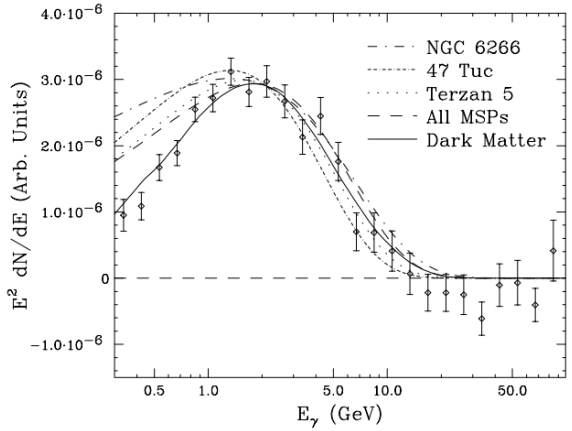

Excess at mid-latitudes (as expected for an extended DM signal)

Hooper & Slatyer 2013
Huang+ 2013
Zhou+ 2014
Daylan+ 2014

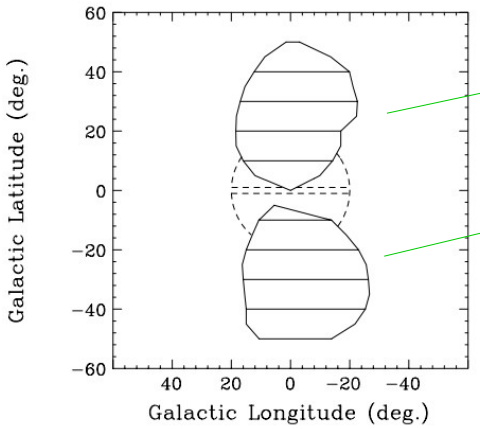

[Hooper & Slatyer 2013]

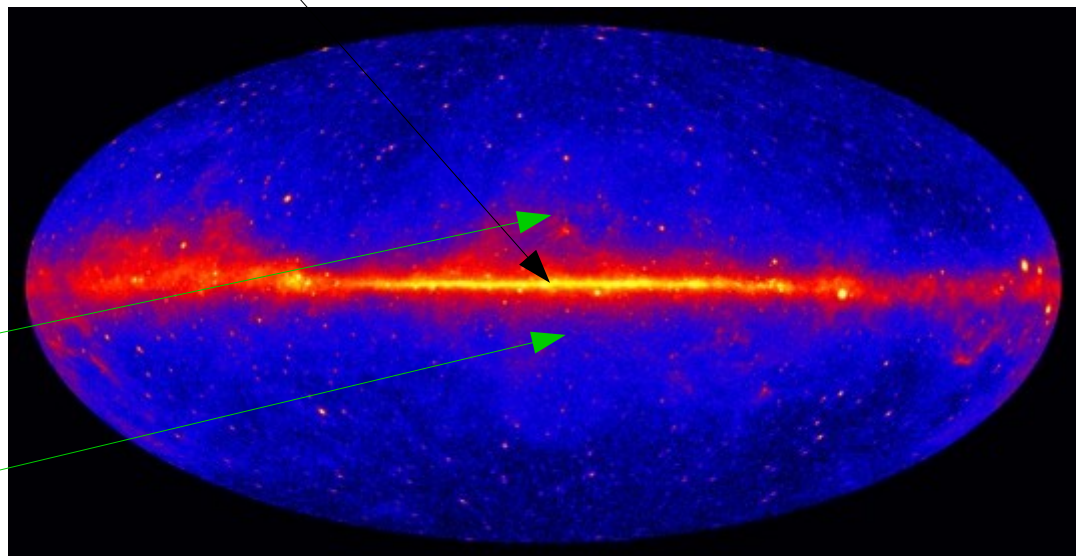

$|\ell| \lesssim 20^\circ, \quad 2^\circ \lesssim |b| \lesssim 2^\circ$

Fluxes at low latitudes

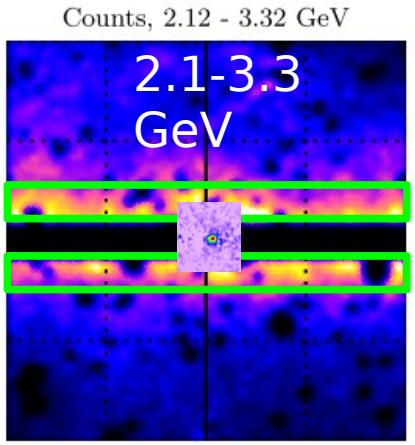

Calore, Cholis, CW 2014

- Reanalysis of “inner Galaxy” ROI
- We allow for extreme variations in ISRF, magnetic field, diffusion properties
- The “excess” is relatively robust w.r.t. all variations
  → Seems to be genuine emission from the Galactic bulge

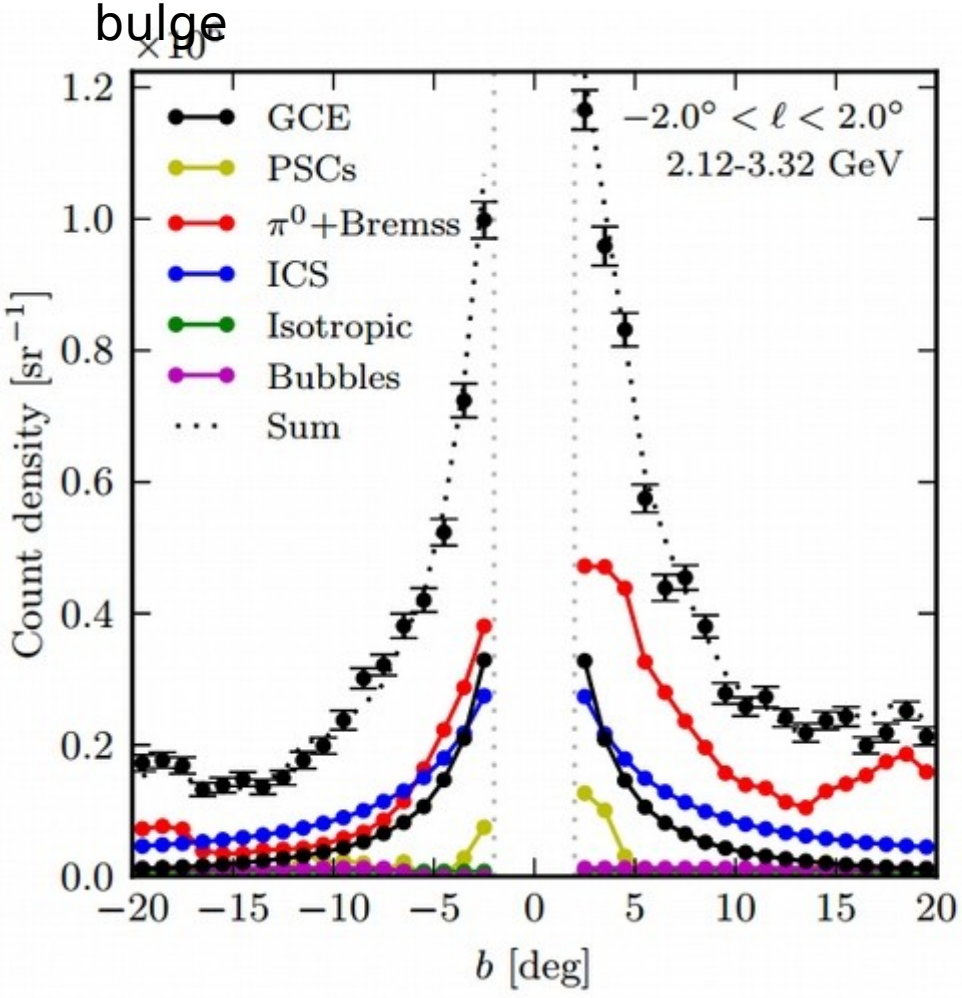

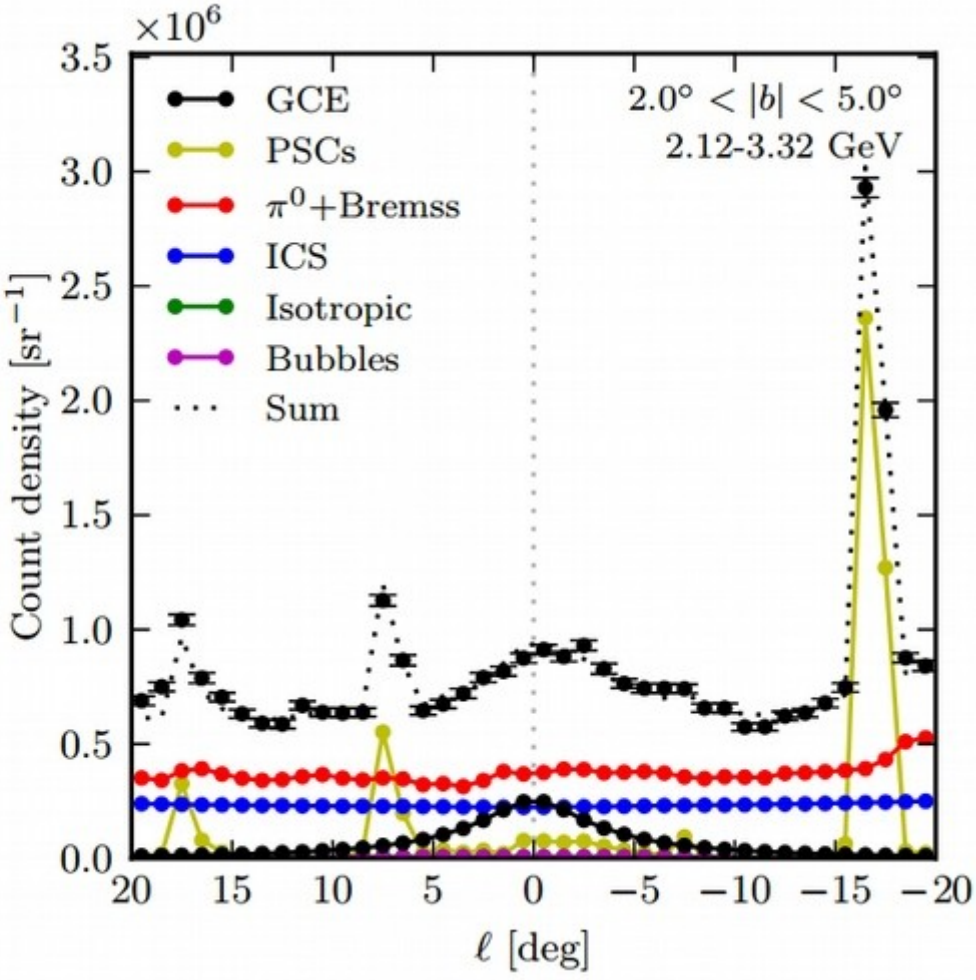

Typical residuals after foreground subtraction

Calore, Cholis, CW 2014

40 deg x 40 deg

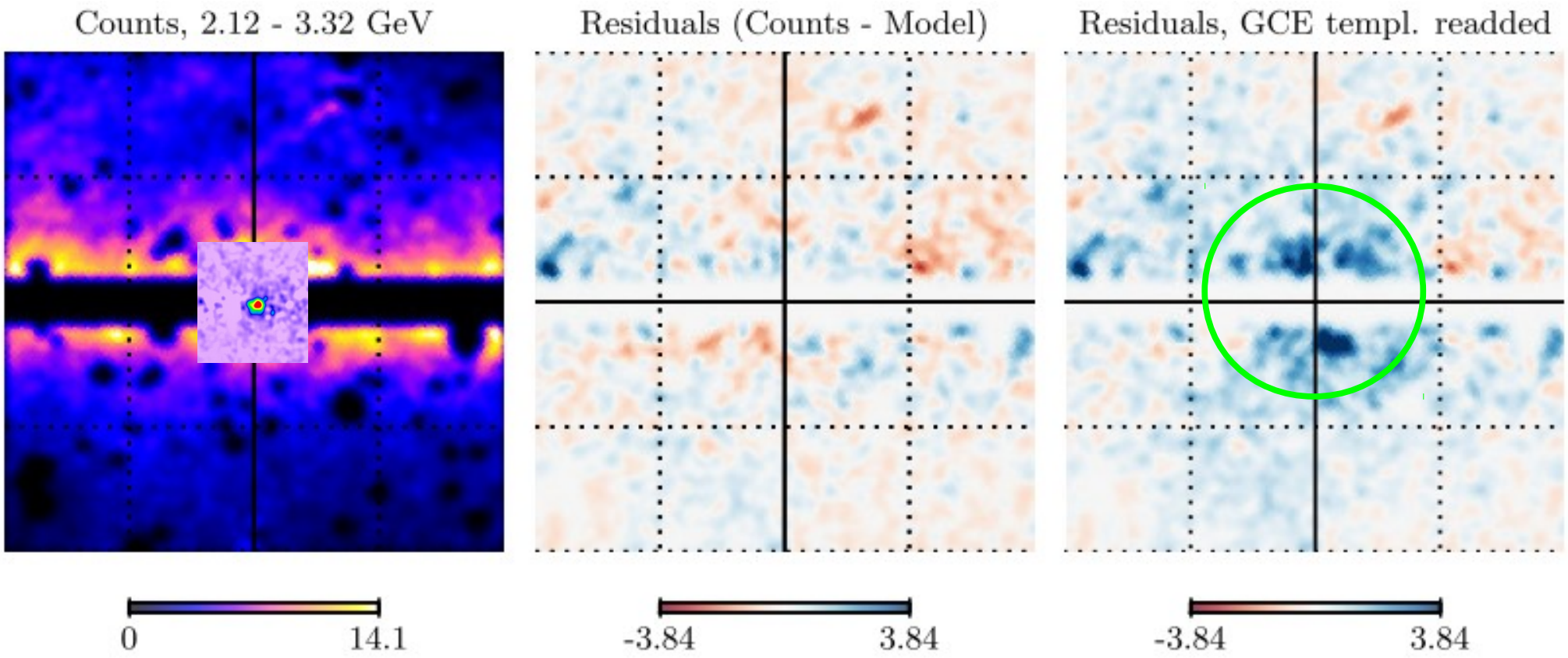

- Left: Point source mask clearly visible
- Middle: Residuals at the level of <20% are observed
- Right: Re-adding the DM template clearly shows an extended excess around the GC

Component spectra

$$\left.\frac{dN}{dE}\right|_{\text{meas. res.}}$$

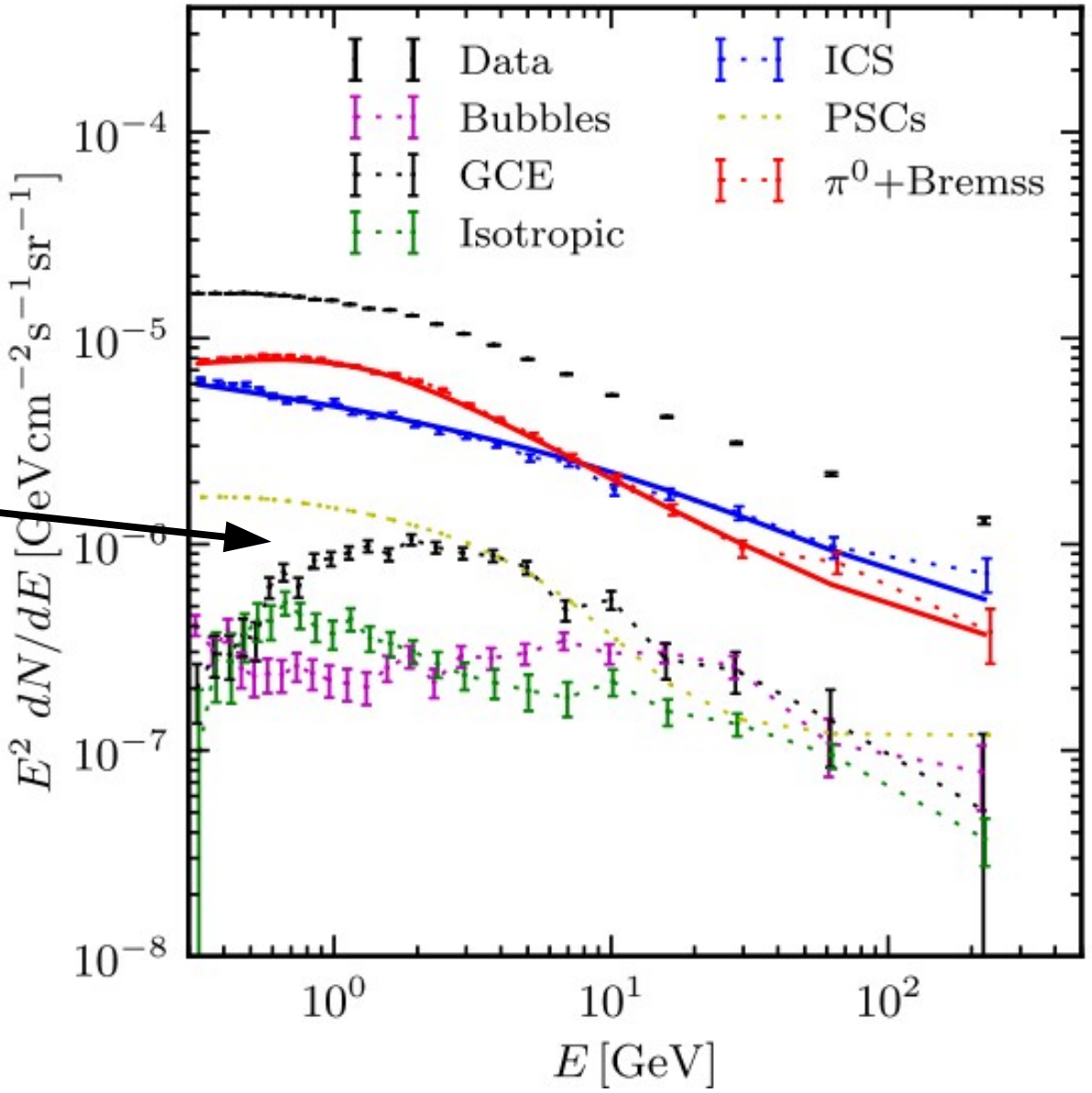

$$\left.\frac{dN}{dE}\right|_{\text{real}} = \left.\frac{dN}{dE}\right._{\text{meas. res.}} + \delta \left.\frac{dN}{dE}\right|_{\pi_0} + \delta \left.\frac{dN}{dE}\right|_{ICS} + \delta \left.\frac{dN}{dE}\right|_{rest}$$

Excess spectra in control regions

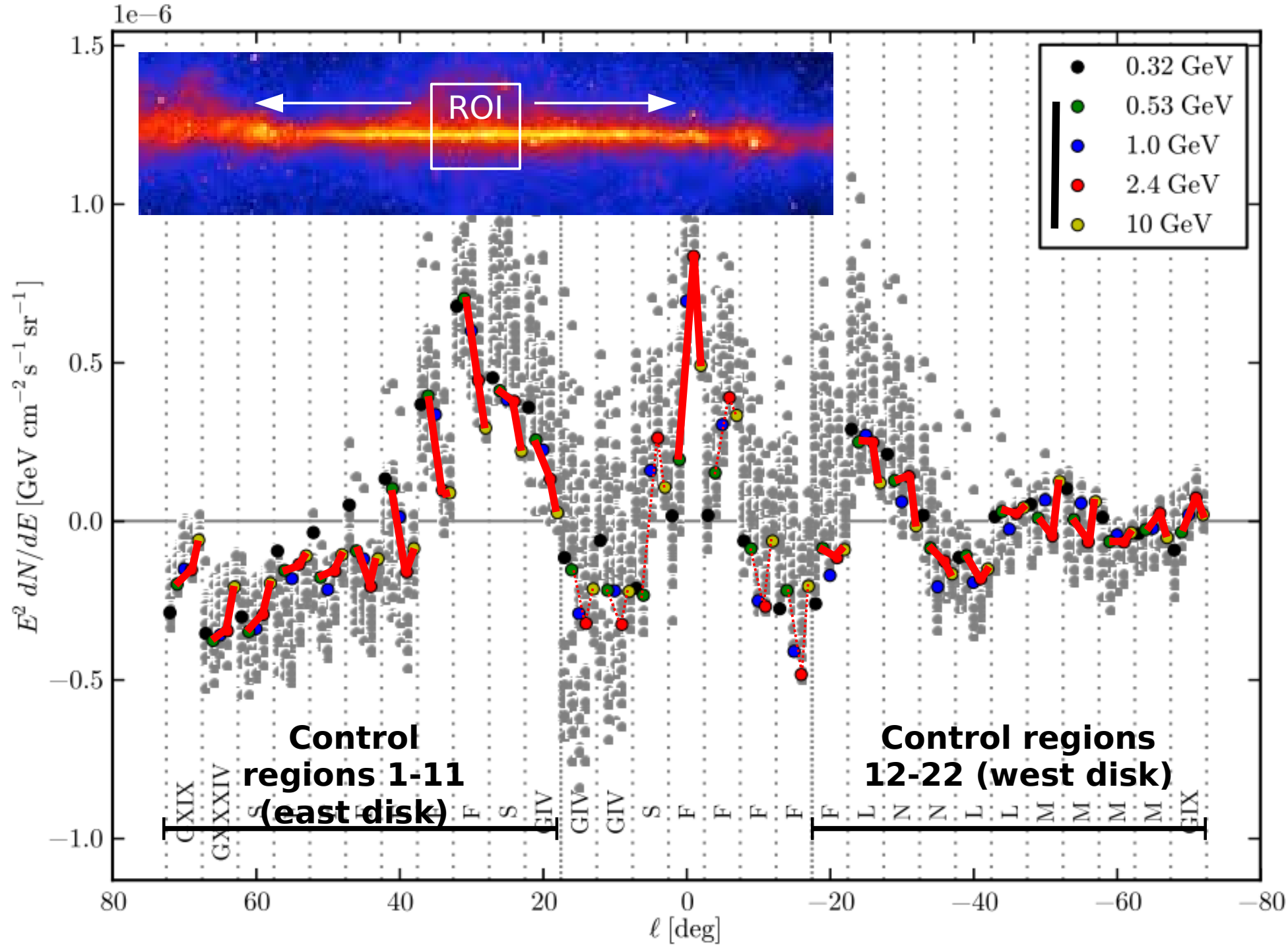

Low/high energy tails of spectrum very uncertain

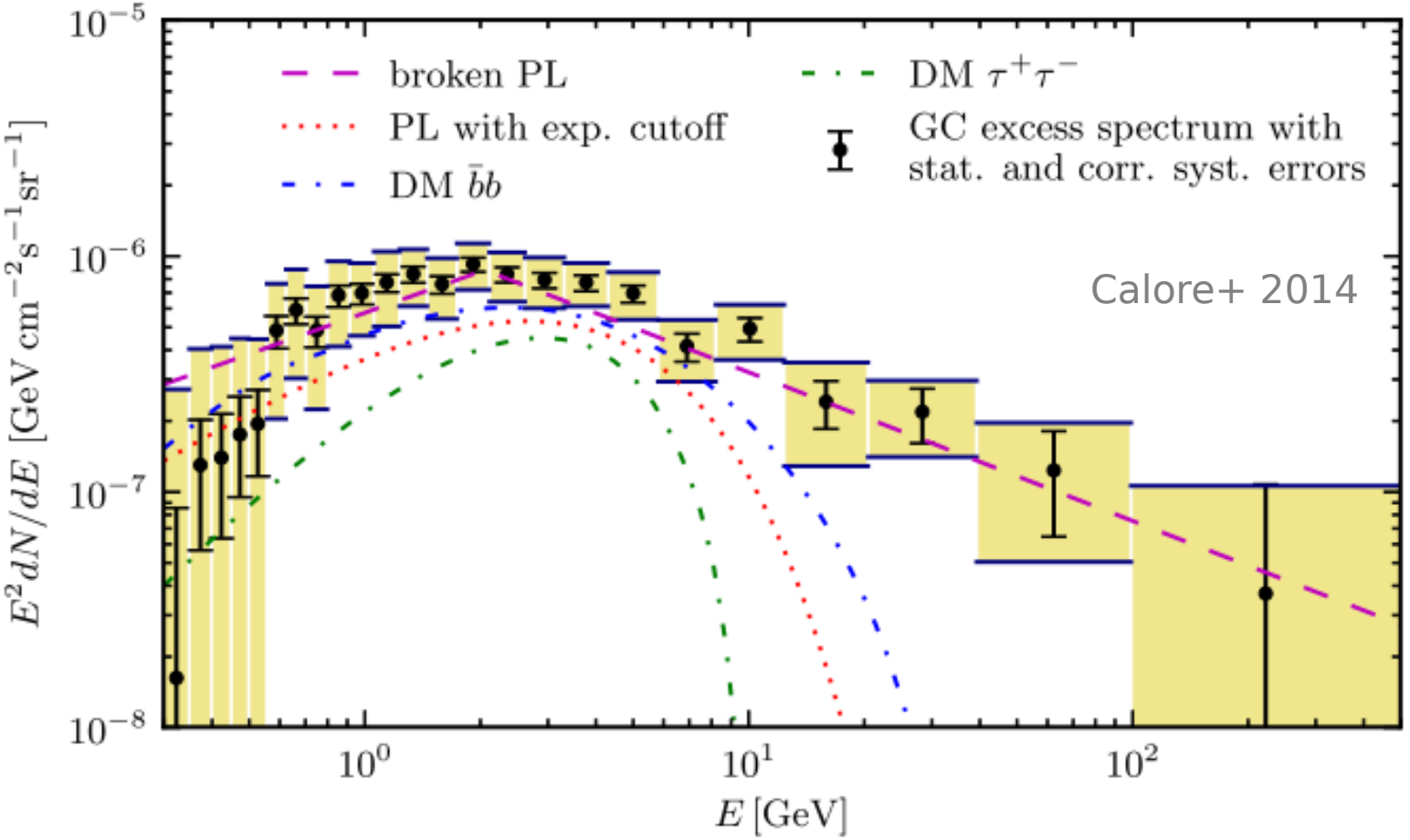

Spectrum	Parameters	χ^2/dof	p-value
broken PL	$\alpha_1 = 1.42^{+0.22}_{-0.31}$, $\alpha_2 = 2.63^{+0.13}_{-0.095}$, $E_{\rm break} = 2.06^{+0.23}_{-0.17}$ GeV	1.06	0.47
DM $\chi\chi \to \bar{b}b$	$\langle\sigma v\rangle = 1.76^{+0.28}_{-0.27} \times 10^{-26}$ cm^3 s^{-1}, $m_\chi = 49^{+6.4}_{-5.4}$ GeV	1.08	0.43
DM $\chi\chi \to \bar{c}c$	$\langle\sigma v\rangle = 1.25^{+0.2}_{-0.18} \times 10^{-26}$ cm^3 s^{-1}, $m_\chi = 38.2^{+4.6}_{-3.9}$ GeV	1.07	0.44
PL with exp. cutoff	$E_{\rm cut} = 2.53^{+1.1}_{-0.77}$ GeV, $\alpha = 0.945^{+0.36}_{-0.5}$	1.37	0.16
DM $\chi\chi \to \tau^+\tau^-$	$\langle\sigma v\rangle = 0.337^{+0.047}_{-0.048} \times 10^{-26}$ cm^3 s^{-1}, $m_\chi = 9.96^{+1.1}_{-0.91}$ GeV	1.52	0.065

Spatial distribution of excess emission

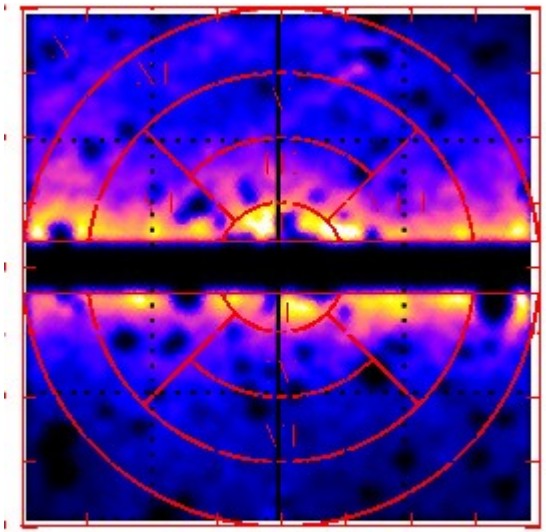

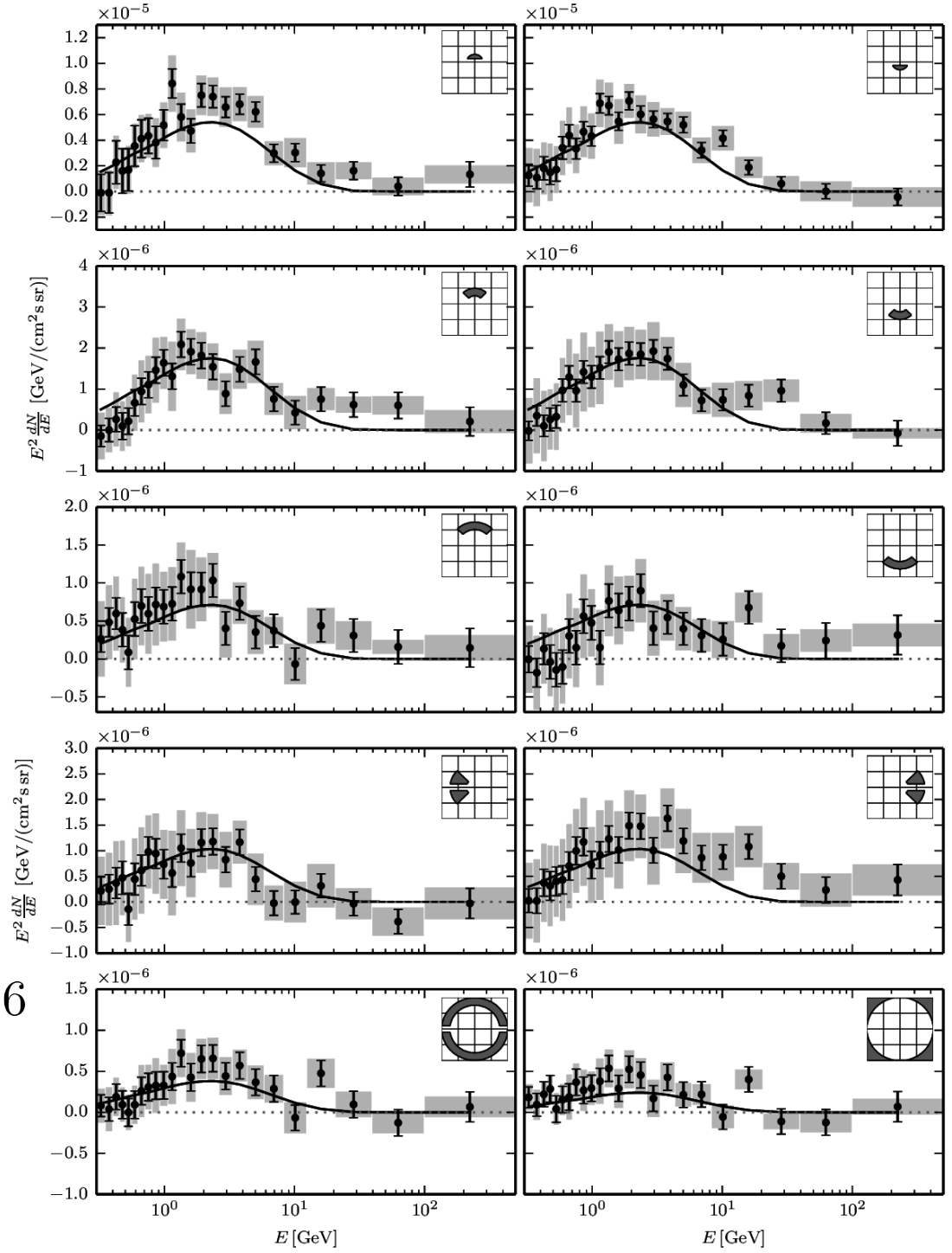

Can be fit with a contracted NFW profile and DM annihilation into b-quarks, for DM masses around 50 GeV

$$\rho_{\rm DM} = \frac{1}{r^{\gamma}(r_s + r)^{2-\gamma}} \qquad \gamma \simeq 1.26$$

(based on Calore+ 2014)

The D^{3}PO version of the GeV excess

“Cloud-like” component

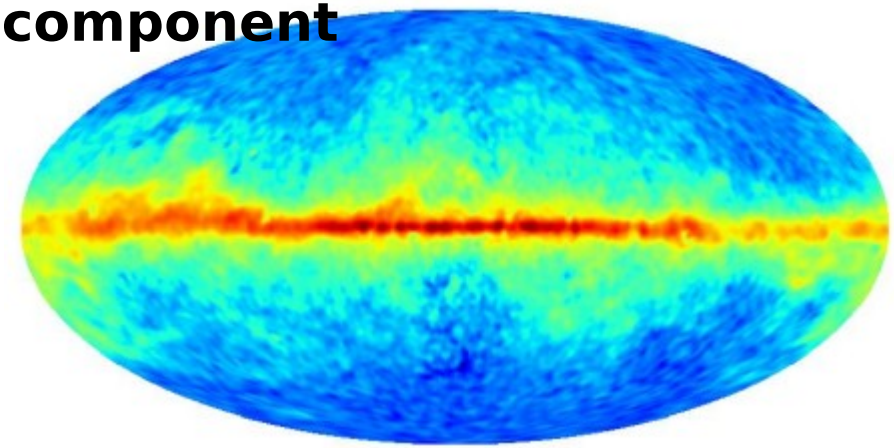

“Bubble-like” component

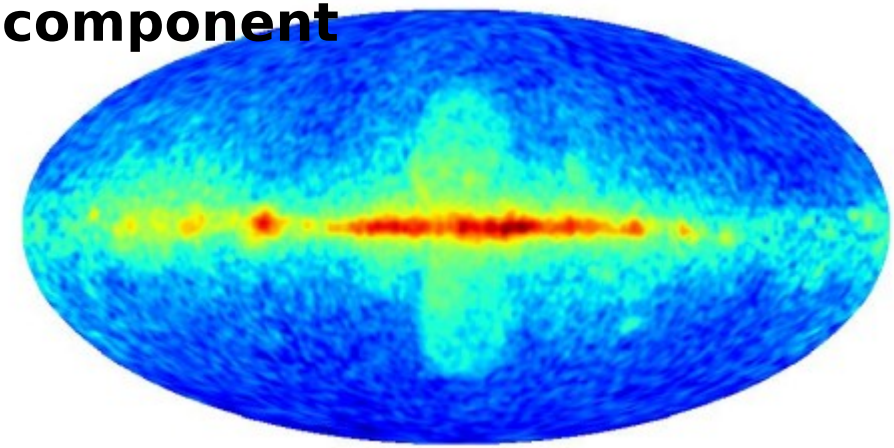

“DM-like” component (GeV excess)

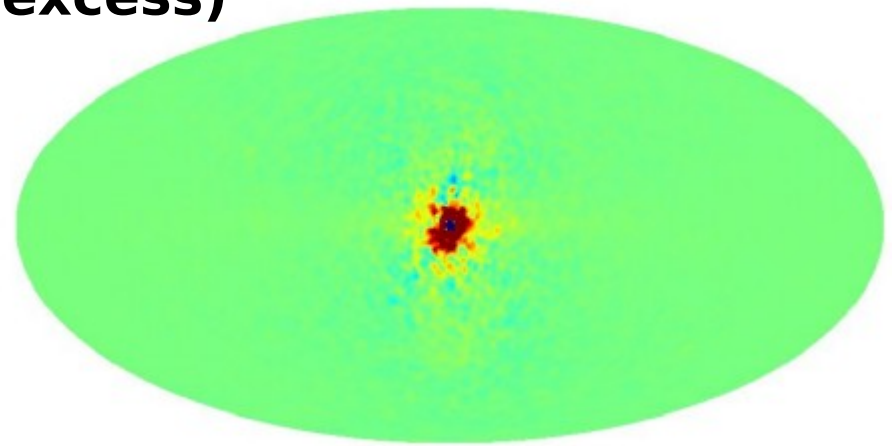

Local significance for contribution from bb spectrum

Pixel-by-pixel spectral decomposition:

$$\frac{dN}{dE} = \alpha_1 \left.\frac{dN}{dE}\right|_{\mathrm{Bu}} + \alpha_2 \left.\frac{dN}{dE}\right|_{\mathrm{Cl}} + \alpha_3 \left.\frac{dN}{dE}\right|_{b\bar{b}} + \mathrm{PSC}$$

Huang+ 2015

The poor-man GeV excess

Bartels & CW

Residuals w.r..t. 300 MeV longitudinal morphology

$$RES(E,\ell,b) = \bar{D}(E,\ell,b) - \mathcal{R}(b)\bar{D}(300\ \mathrm{MeV},\ell,b)$$

Point-source correction (3FGL):

$$\bar{D}(E,\ell,b) = D(E,\ell,b) - \mathrm{PSC}(E,\ell,b)$$

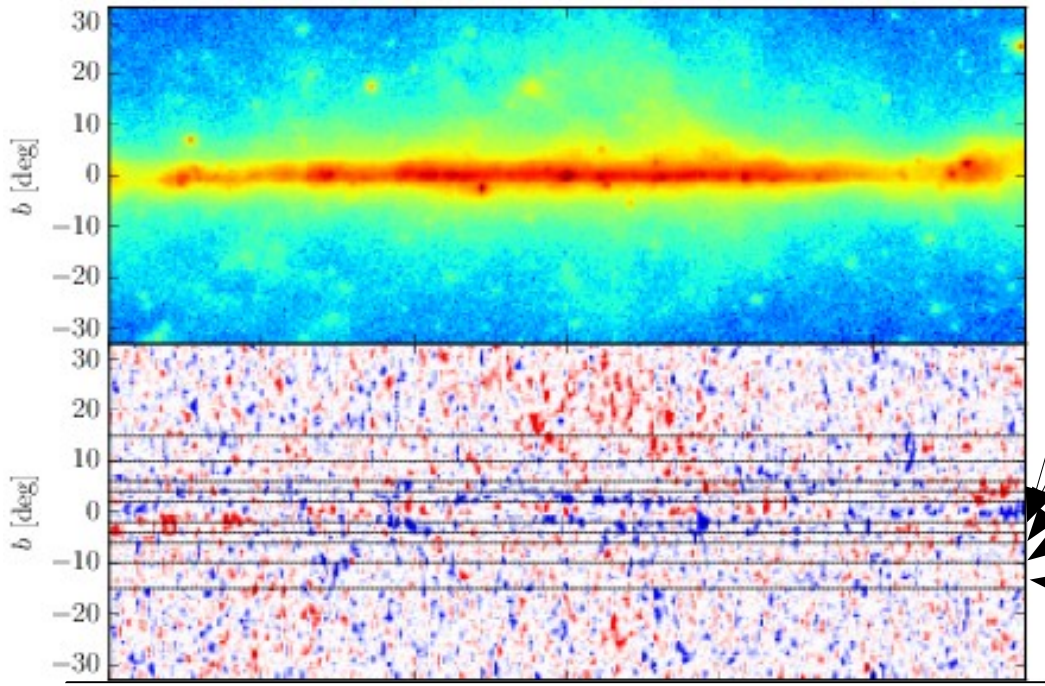

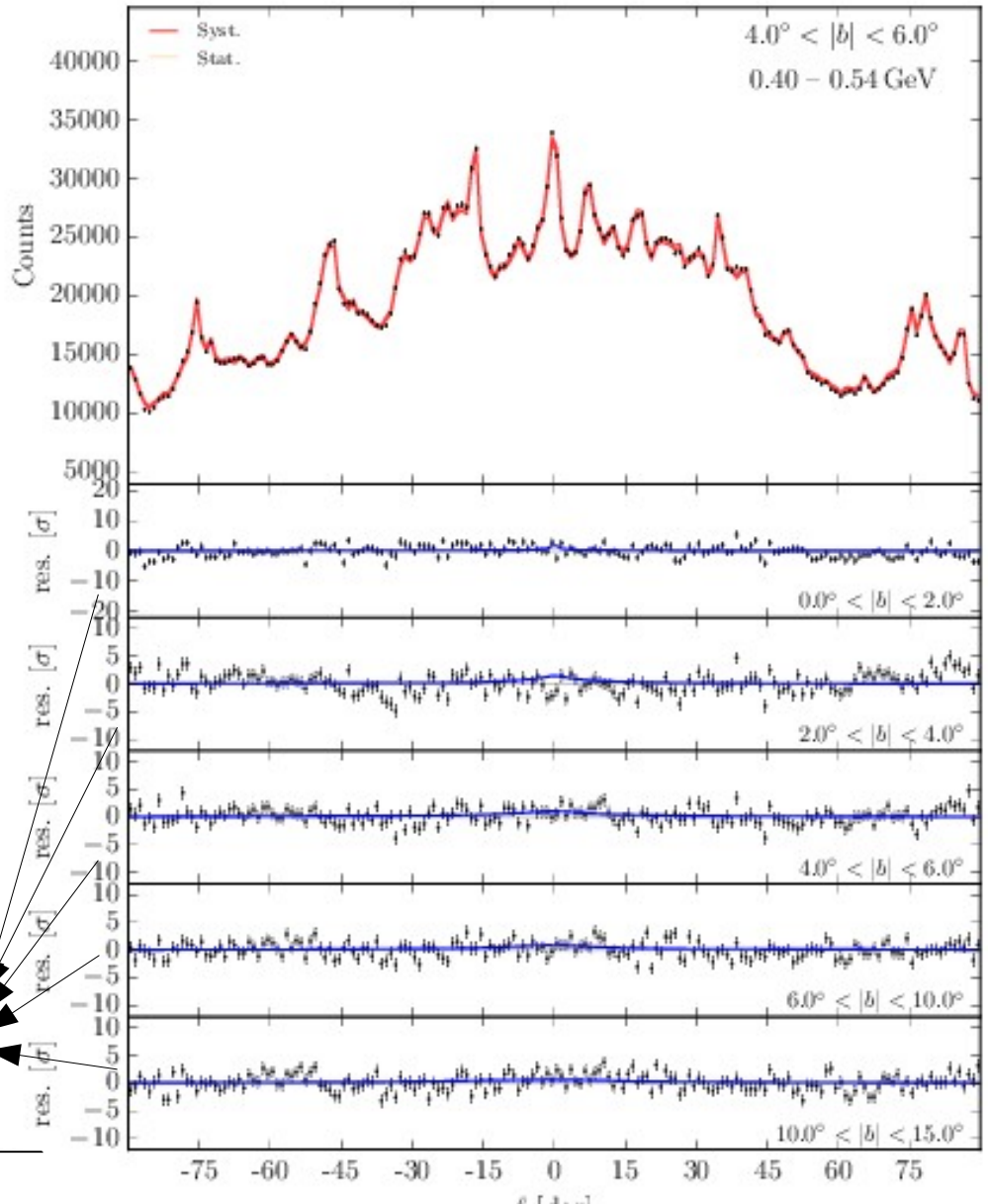

Blue: stacked MSP spectrum

The poor man version of the GeV excess

Bartels & CW

Residuals w.r..t. 300 MeV longitudinal morphology

$$RES(E,\ell,b) = \bar{D}(E,\ell,b) - \mathcal{R}(b)\bar{D}(300\ \mathrm{MeV},\ell,b)$$

Point-source correction:

$$\bar{D}(E,\ell,b) = D(E,\ell,b) - \mathrm{PSC}(E,\ell,b)$$

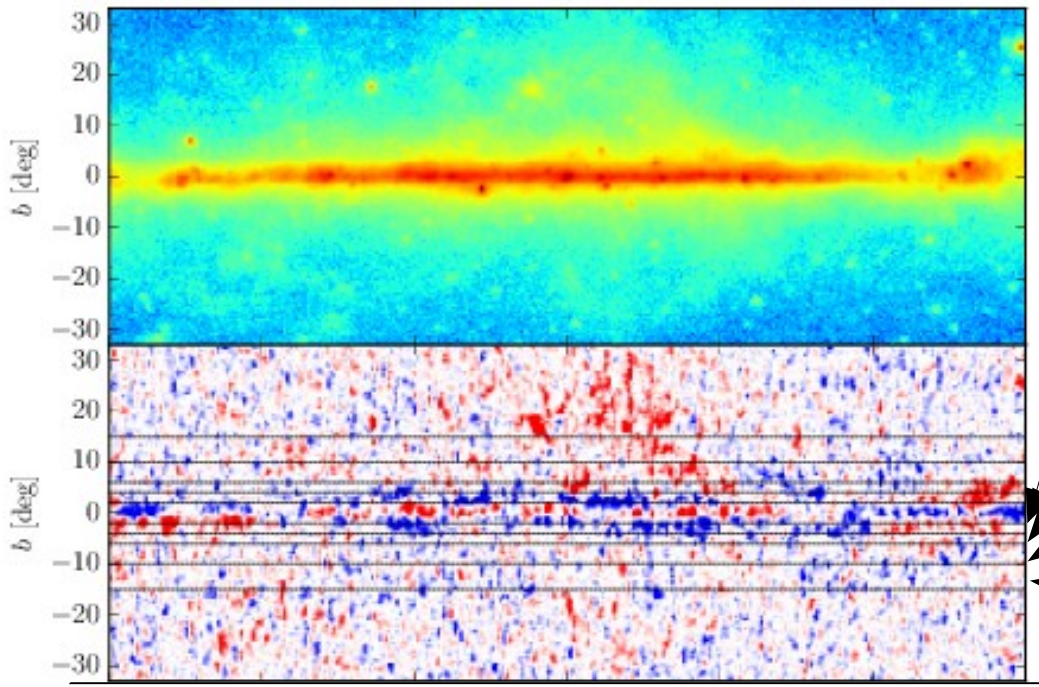

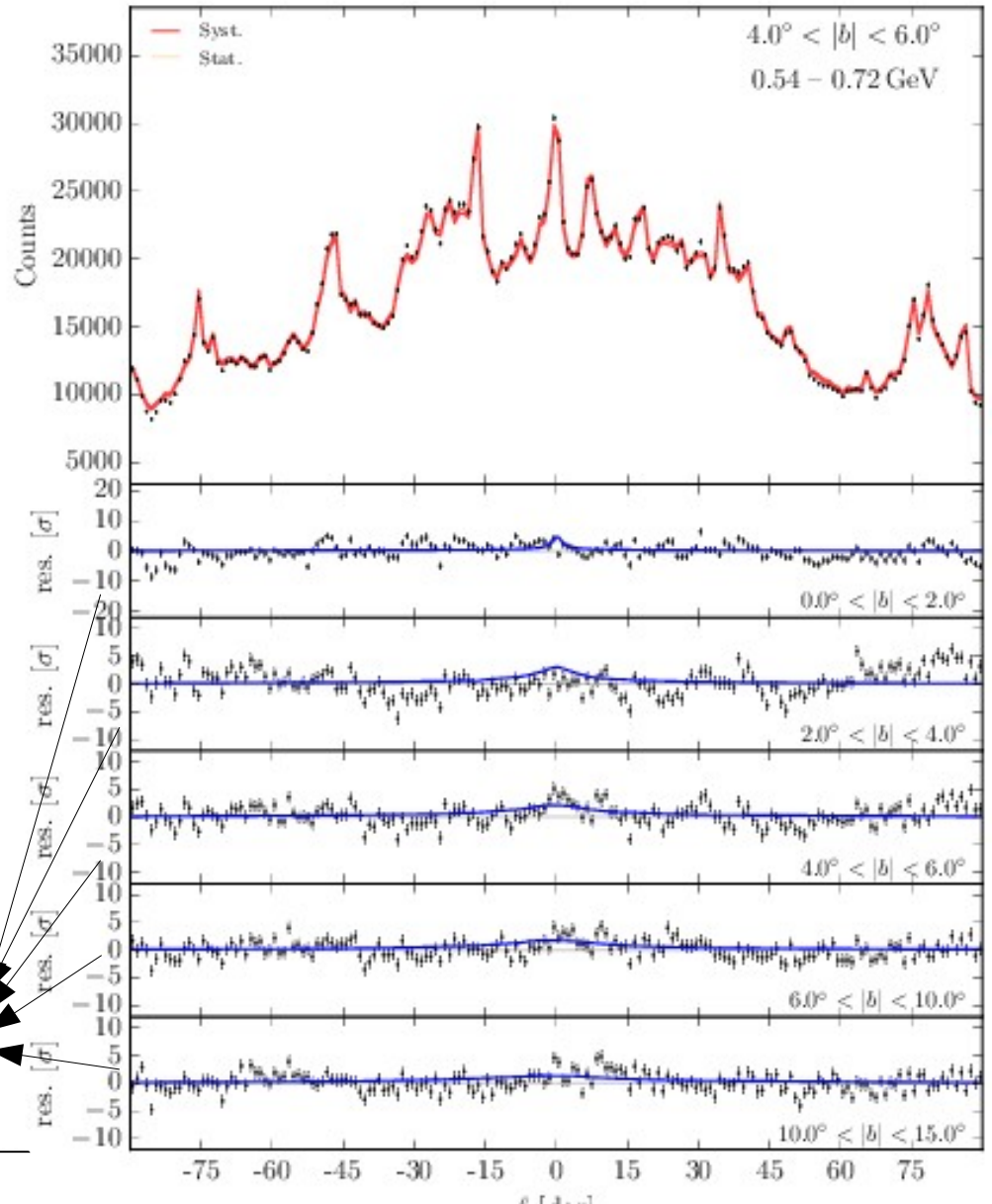

Blue: stacked MSP spectrum

The poor man version of the GeV excess

Bartels & CW

Residuals w.r..t. 300 MeV longitudinal morphology

$$RES(E,\ell,b) = \bar{D}(E,\ell,b) - \mathcal{R}(b)\bar{D}(300\ \mathrm{MeV},\ell,b)$$

Point-source correction:

$$\bar{D}(E,\ell,b) = D(E,\ell,b) - \mathrm{PSC}(E,\ell,b)$$

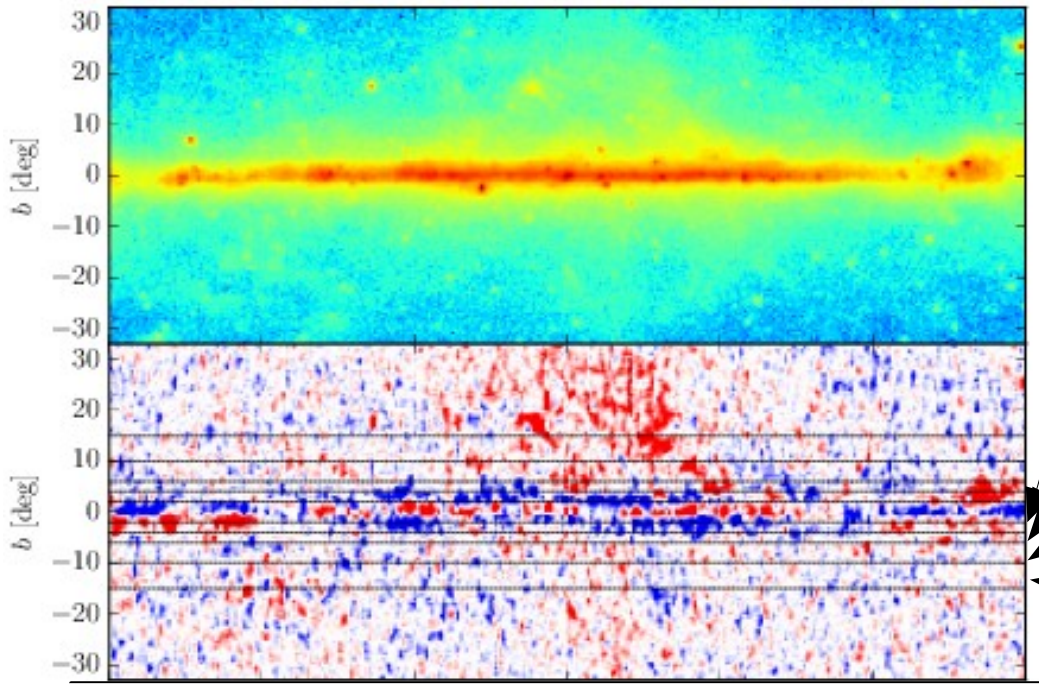

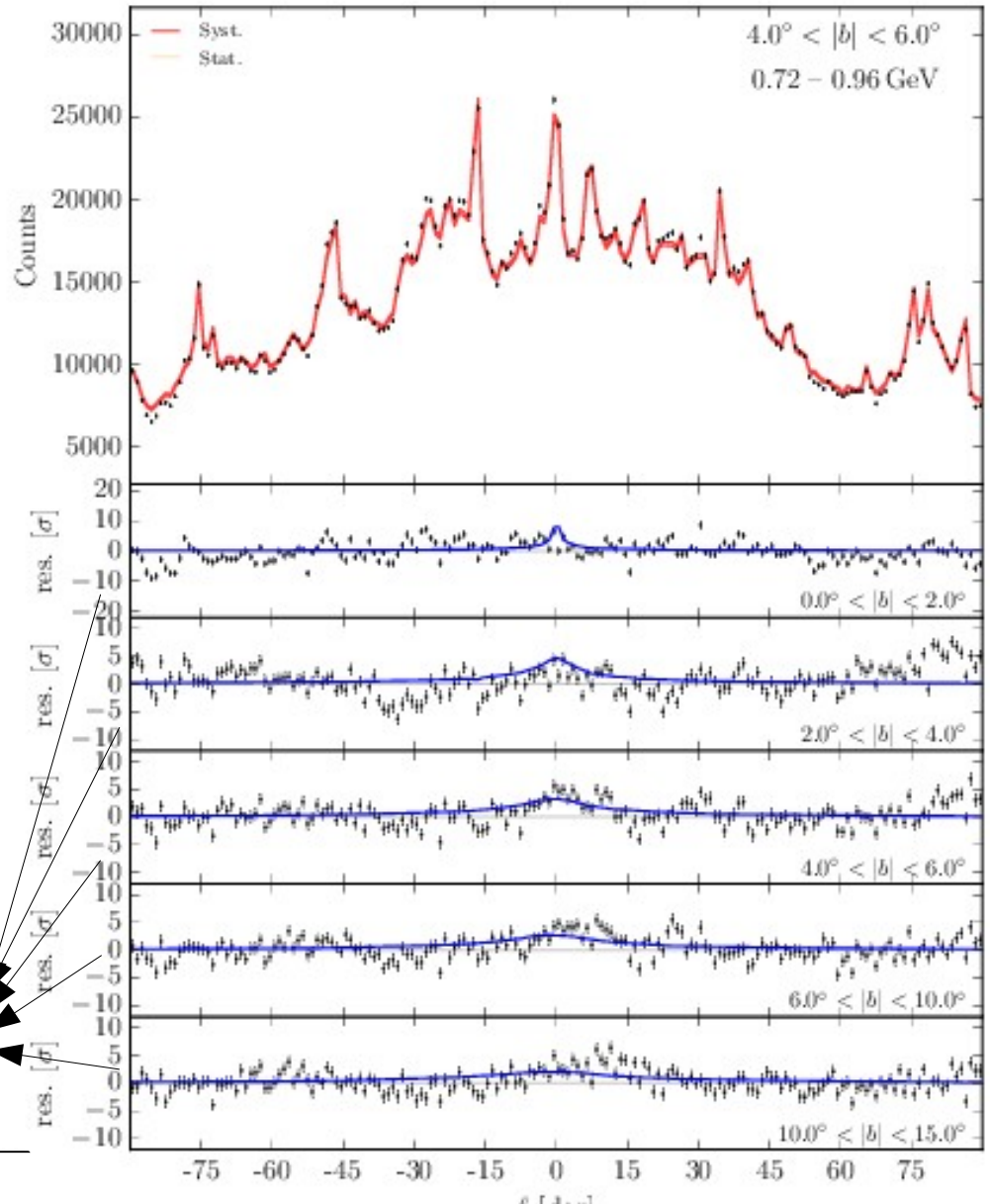

Blue: stacked MSP spectrum

The poor man version of the GeV excess

Bartels & CW

Residuals w.r..t. 300 MeV longitudinal morphology

$$RES(E,\ell,b) = \bar{D}(E,\ell,b) - \mathcal{R}(b)\bar{D}(300\ \mathrm{MeV},\ell,b)$$

Point-source correction:

$$\bar{D}(E,\ell,b) = D(E,\ell,b) - \mathrm{PSC}(E,\ell,b)$$

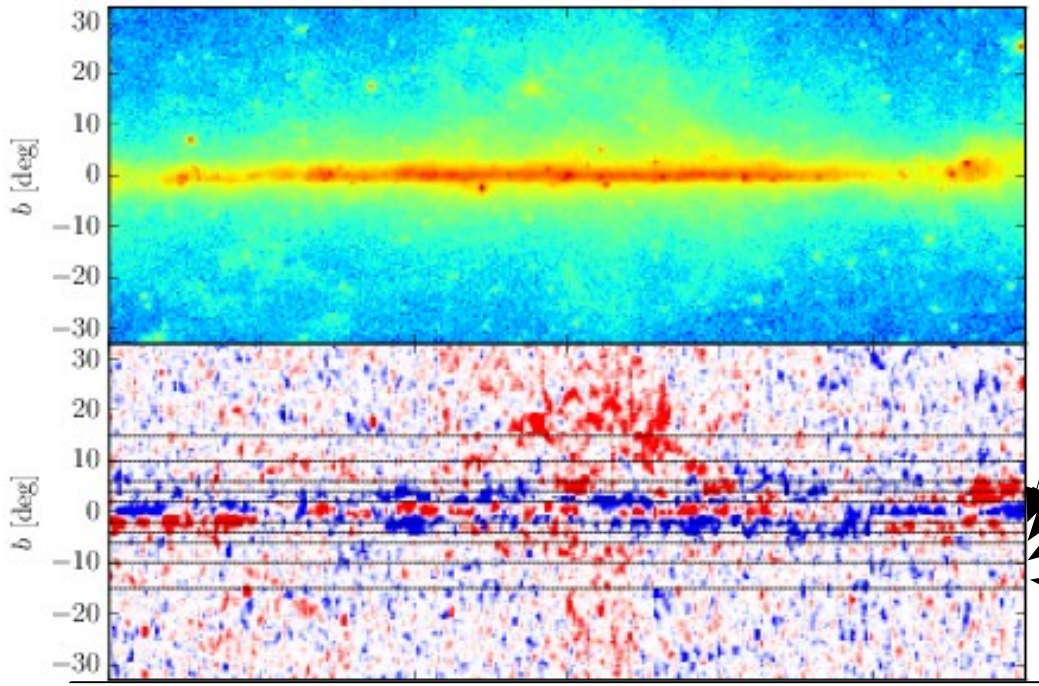

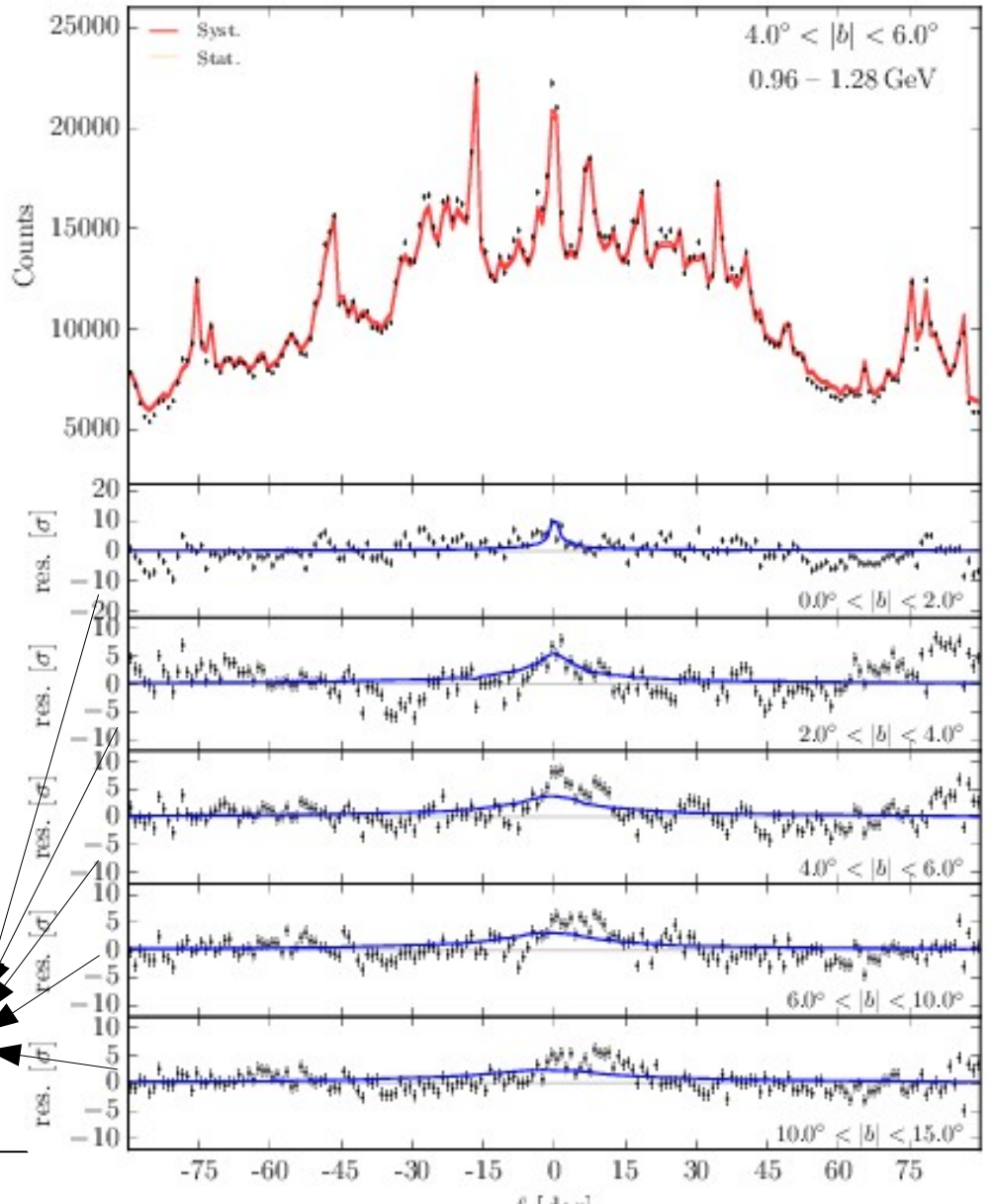

Blue: stacked MSP spectrum

The poor man version of the GeV excess

Bartels & CW

Residuals w.r..t. 300 MeV longitudinal morphology

$$RES(E,\ell,b) = \bar{D}(E,\ell,b) - \mathcal{R}(b)\bar{D}(300\ \mathrm{MeV},\ell,b)$$

Point-source correction:

$$\bar{D}(E,\ell,b) = D(E,\ell,b) - \mathrm{PSC}(E,\ell,b)$$

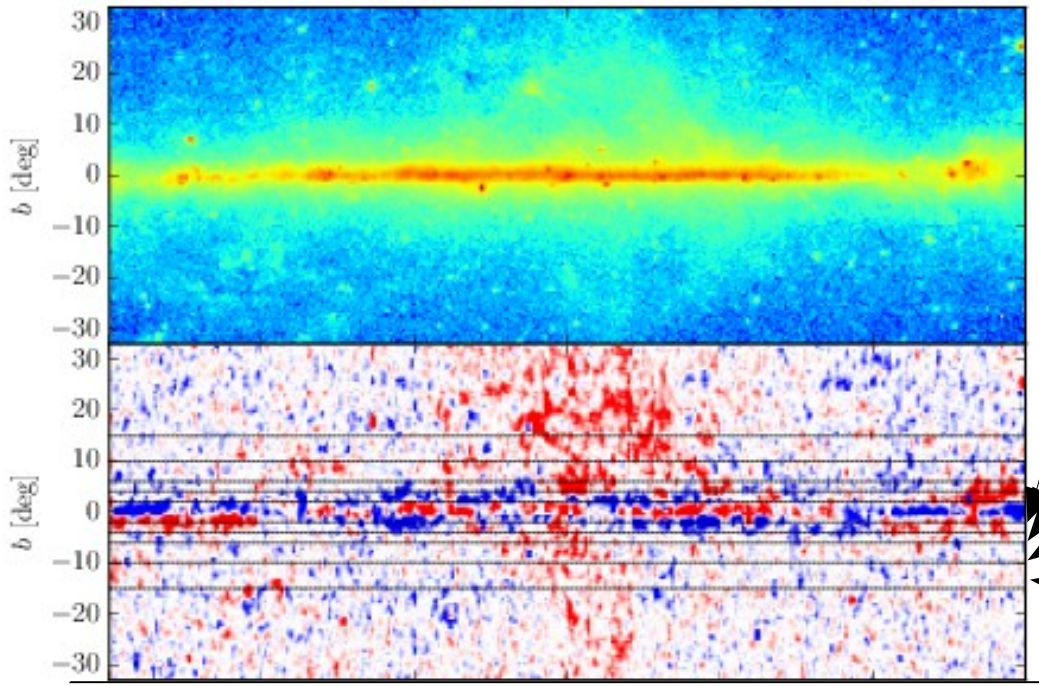

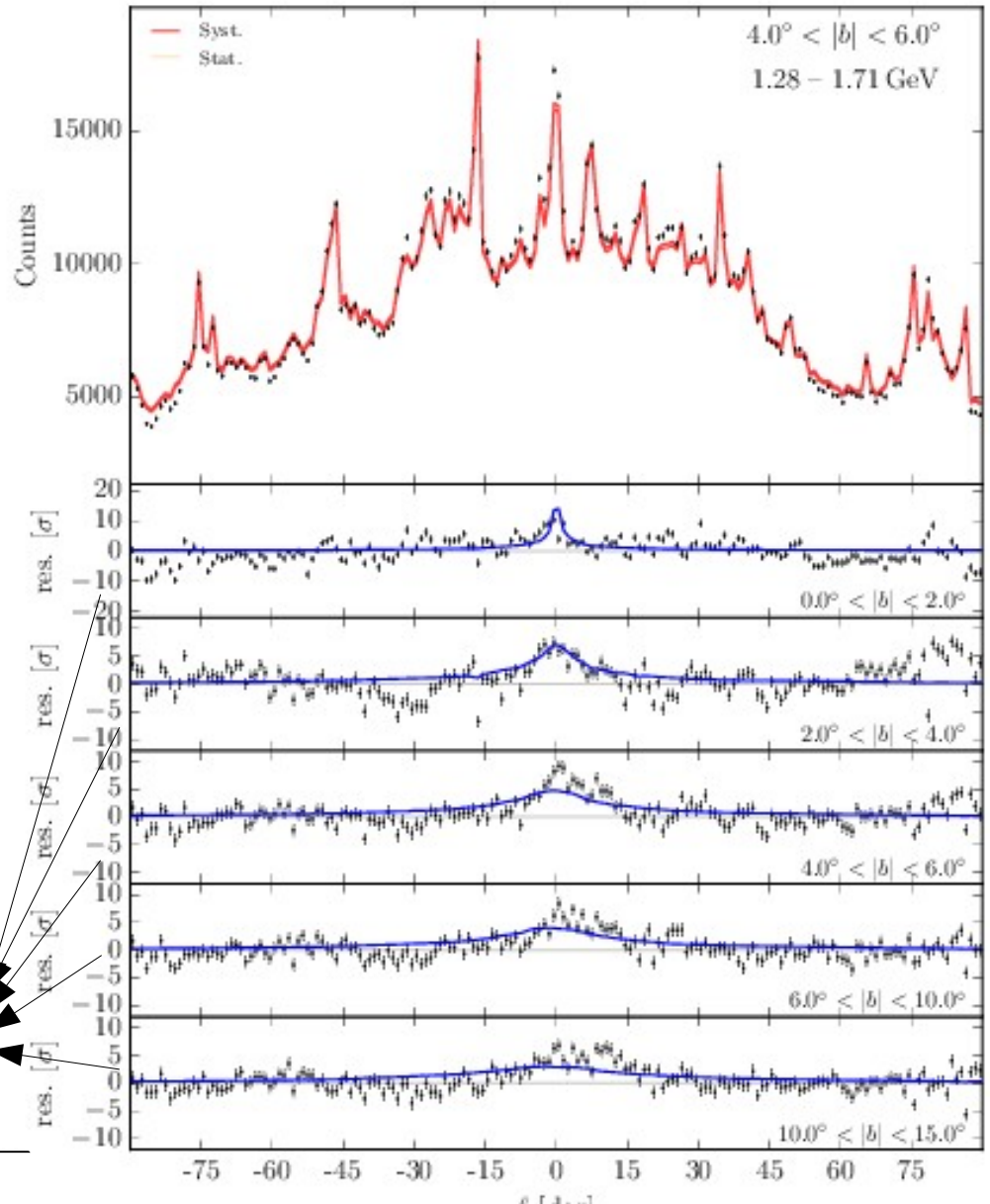

Blue: stacked MSP spectrum

The poor man version of the GeV excess

Bartels & CW

Residuals w.r..t. 300 MeV longitudinal morphology

$$RES(E,\ell,b) = \bar{D}(E,\ell,b) - \mathcal{R}(b)\bar{D}(300\ \mathrm{MeV},\ell,b)$$

Point-source correction:

$$\bar{D}(E,\ell,b) = D(E,\ell,b) - \mathrm{PSC}(E,\ell,b)$$

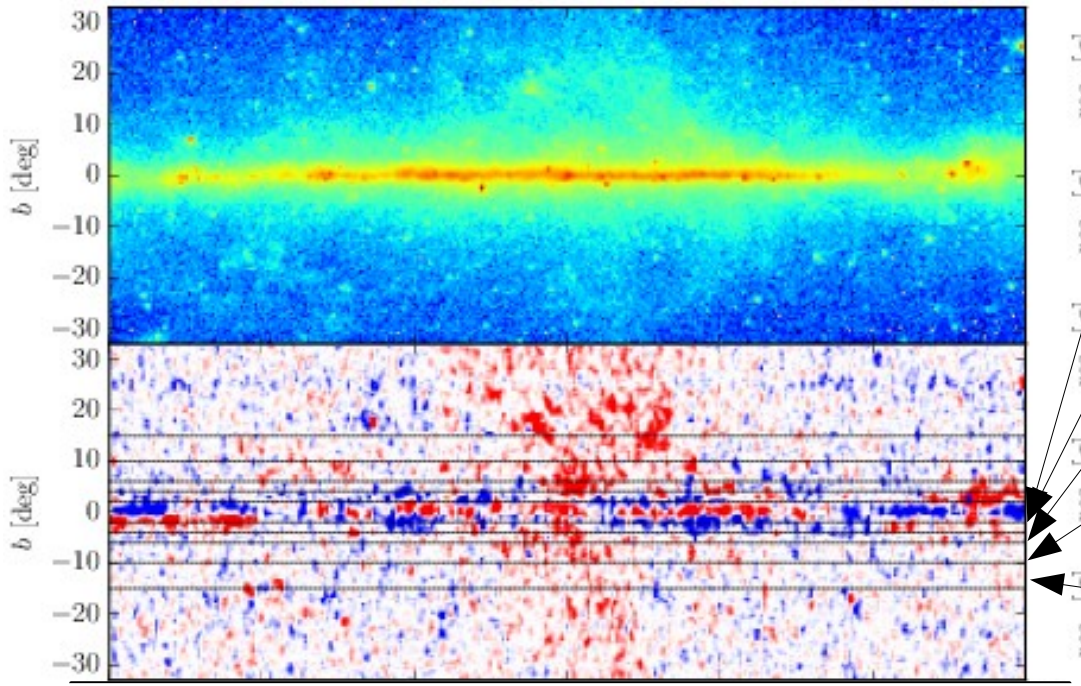

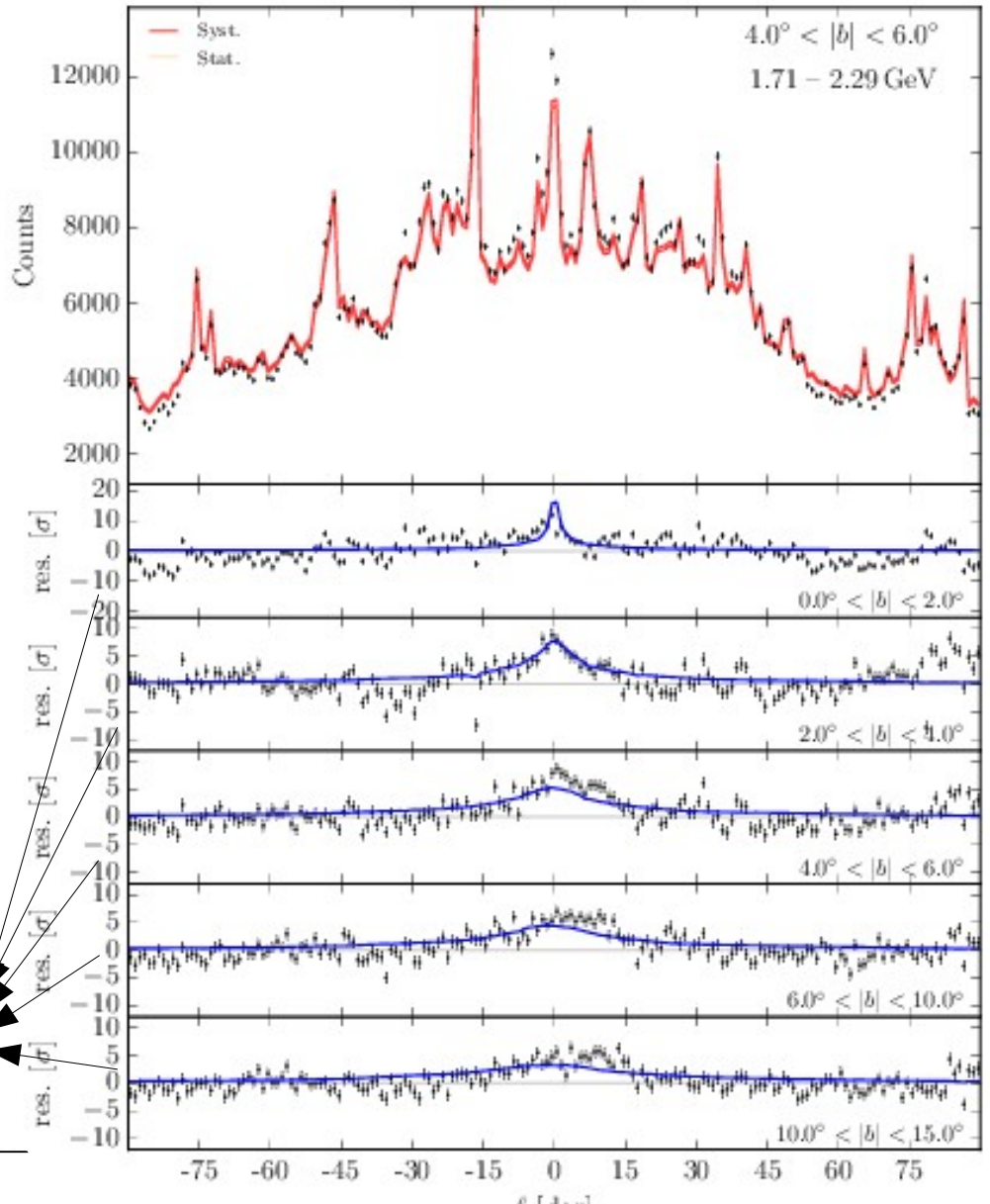

Blue: stacked MSP spectrum

The poor man version of the GeV excess

Bartels & CW

Residuals w.r..t. 300 MeV longitudinal morphology

$$RES(E,\ell,b) = \bar{D}(E,\ell,b) - \mathcal{R}(b)\bar{D}(300\ \mathrm{MeV},\ell,b)$$

Point-source correction:

$$\bar{D}(E,\ell,b) = D(E,\ell,b) - \mathrm{PSC}(E,\ell,b)$$

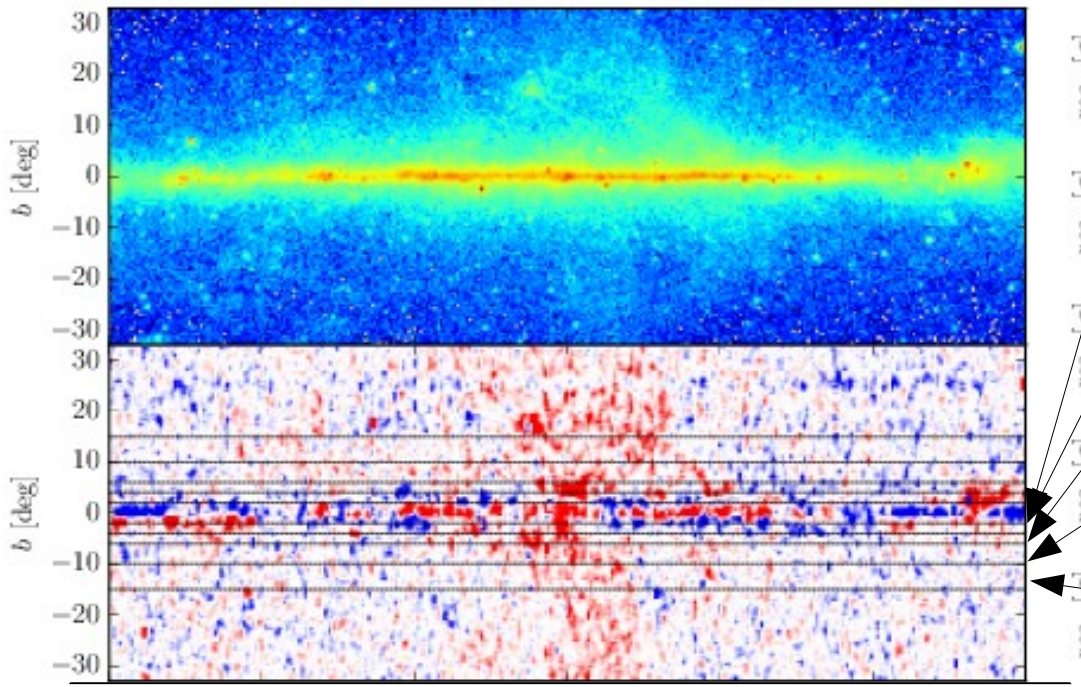

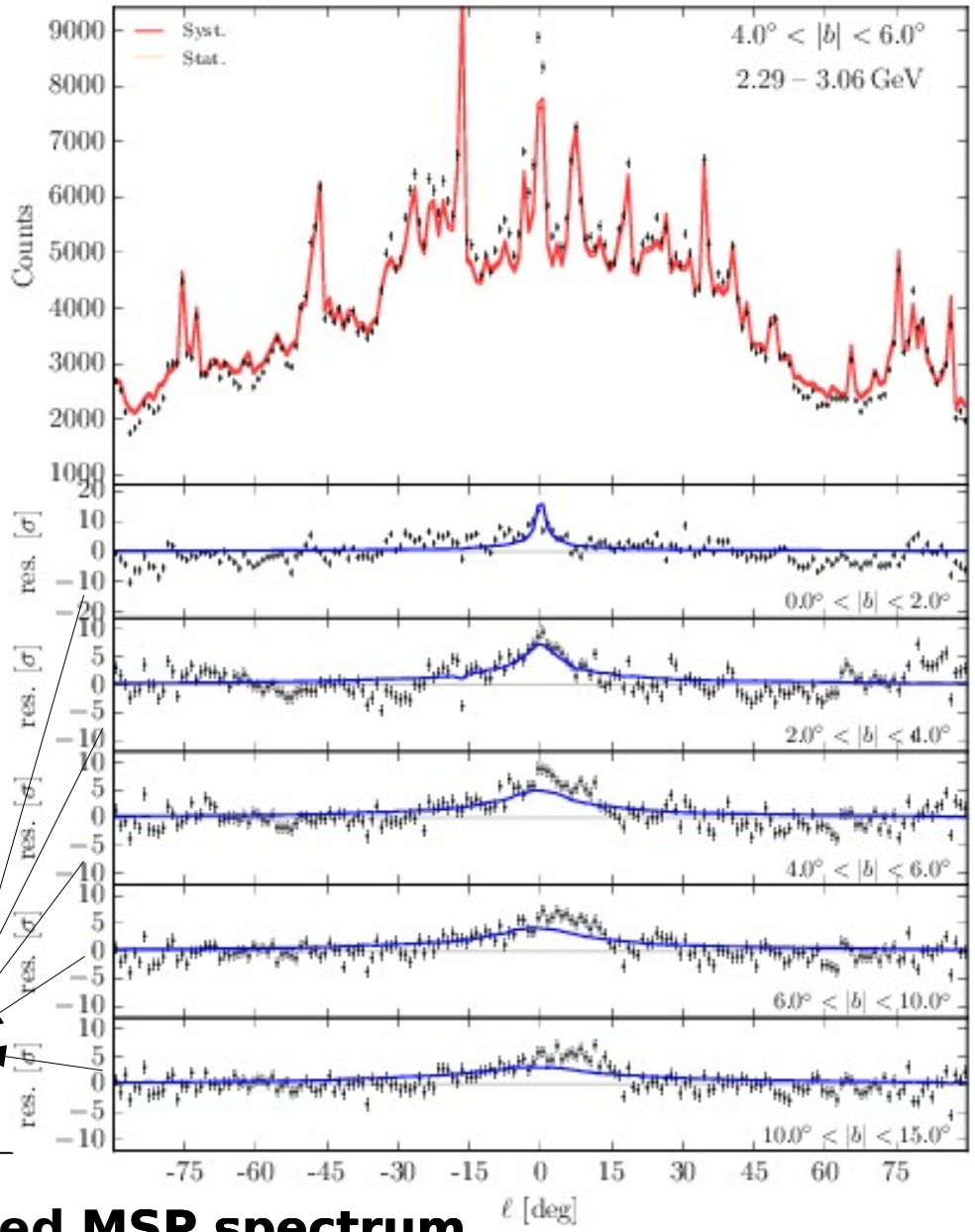

Blue: stacked MSP spectrum

The poor man version of the GeV excess

Bartels & CW

Residuals w.r..t. 300 MeV longitudinal morphology

$$RES(E,\ell,b) = \bar{D}(E,\ell,b) - \mathcal{R}(b)\bar{D}(300\ \mathrm{MeV},\ell,b)$$

Point-source correction:

$$\bar{D}(E,\ell,b) = D(E,\ell,b) - \mathrm{PSC}(E,\ell,b)$$

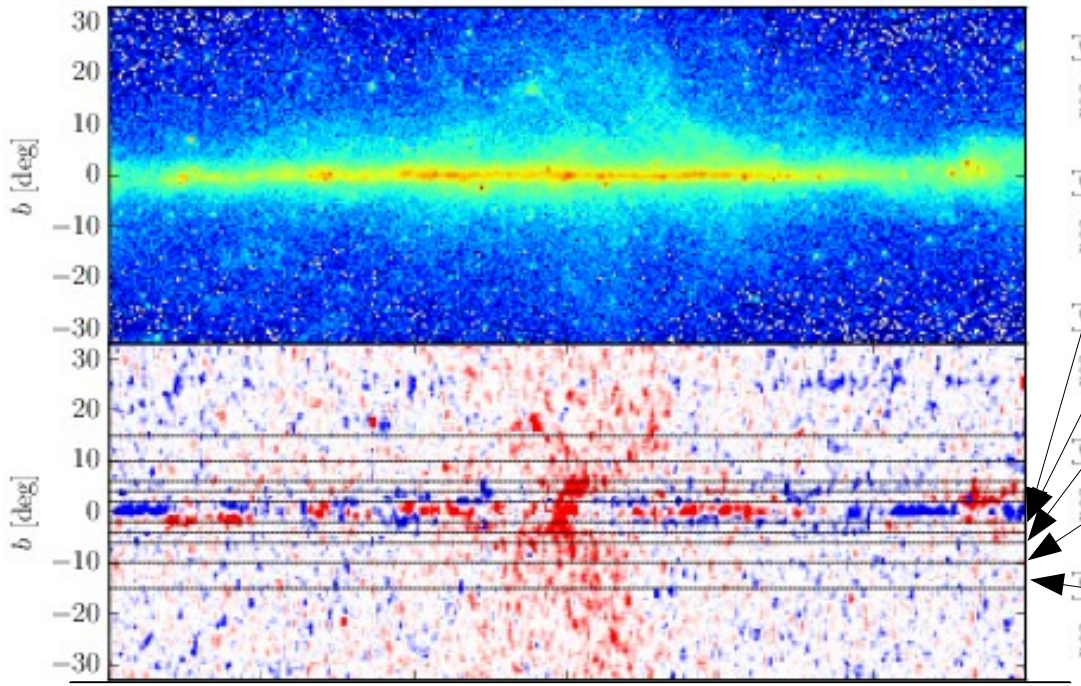

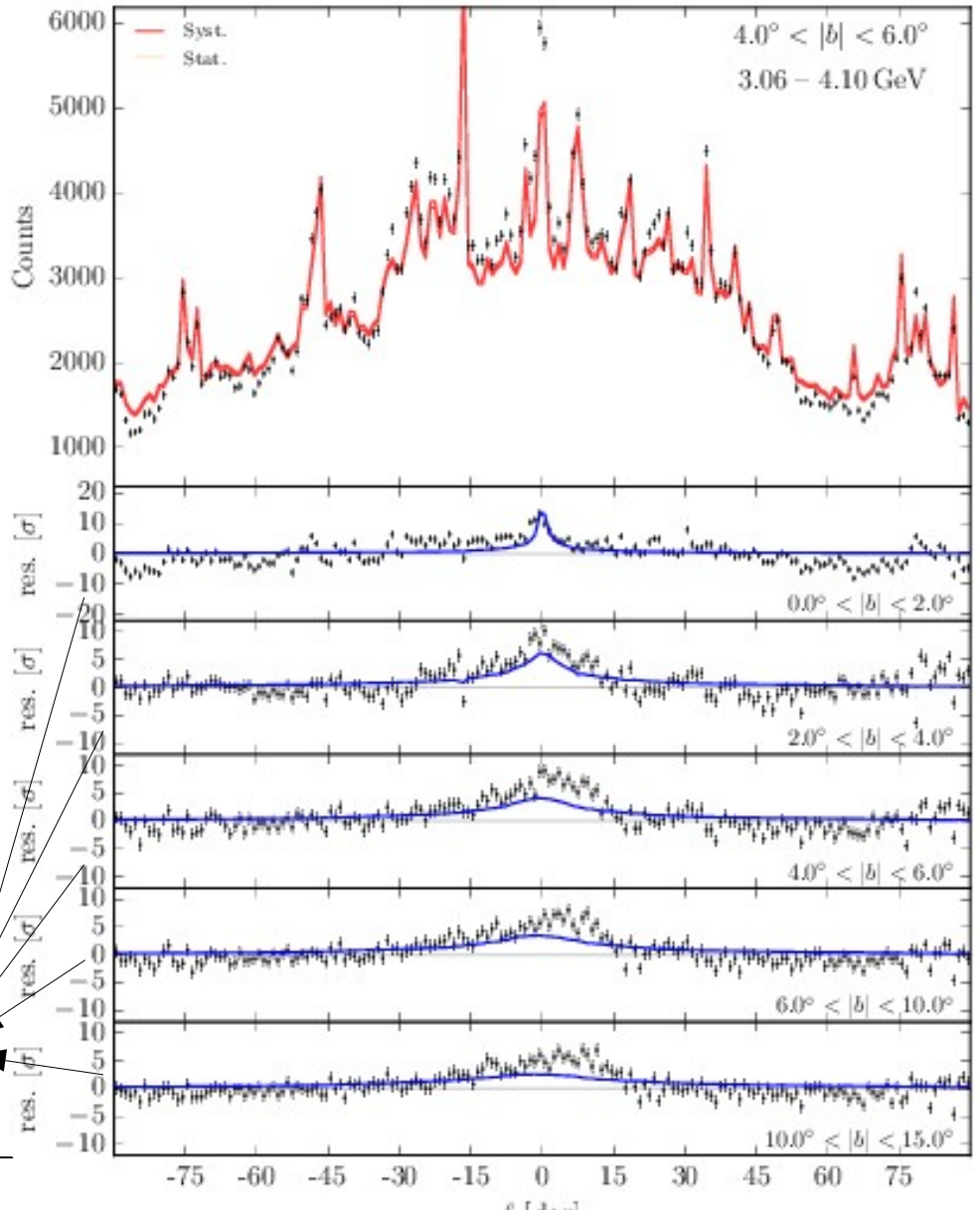

Blue: stacked MSP spectrum

The poor man version of the GeV excess

Bartels & CW

Residuals w.r..t. 300 MeV longitudinal morphology

$$RES(E,\ell,b) = \bar{D}(E,\ell,b) - \mathcal{R}(b)\bar{D}(300\ \mathrm{MeV},\ell,b)$$

Point-source correction:

$$\bar{D}(E,\ell,b) = D(E,\ell,b) - \mathrm{PSC}(E,\ell,b)$$

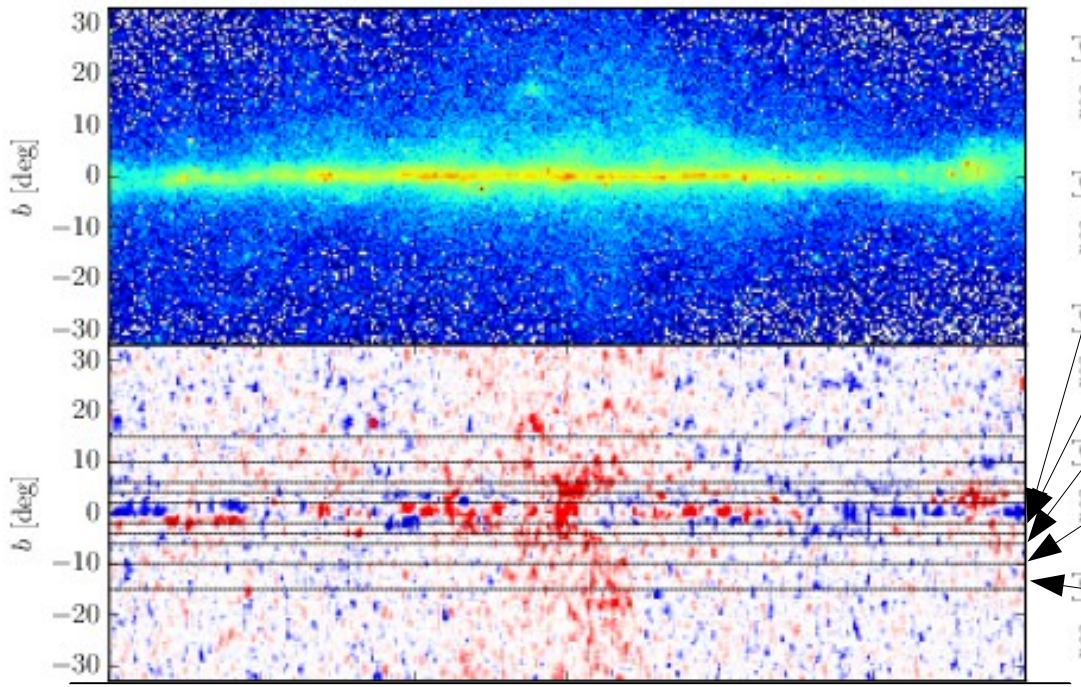

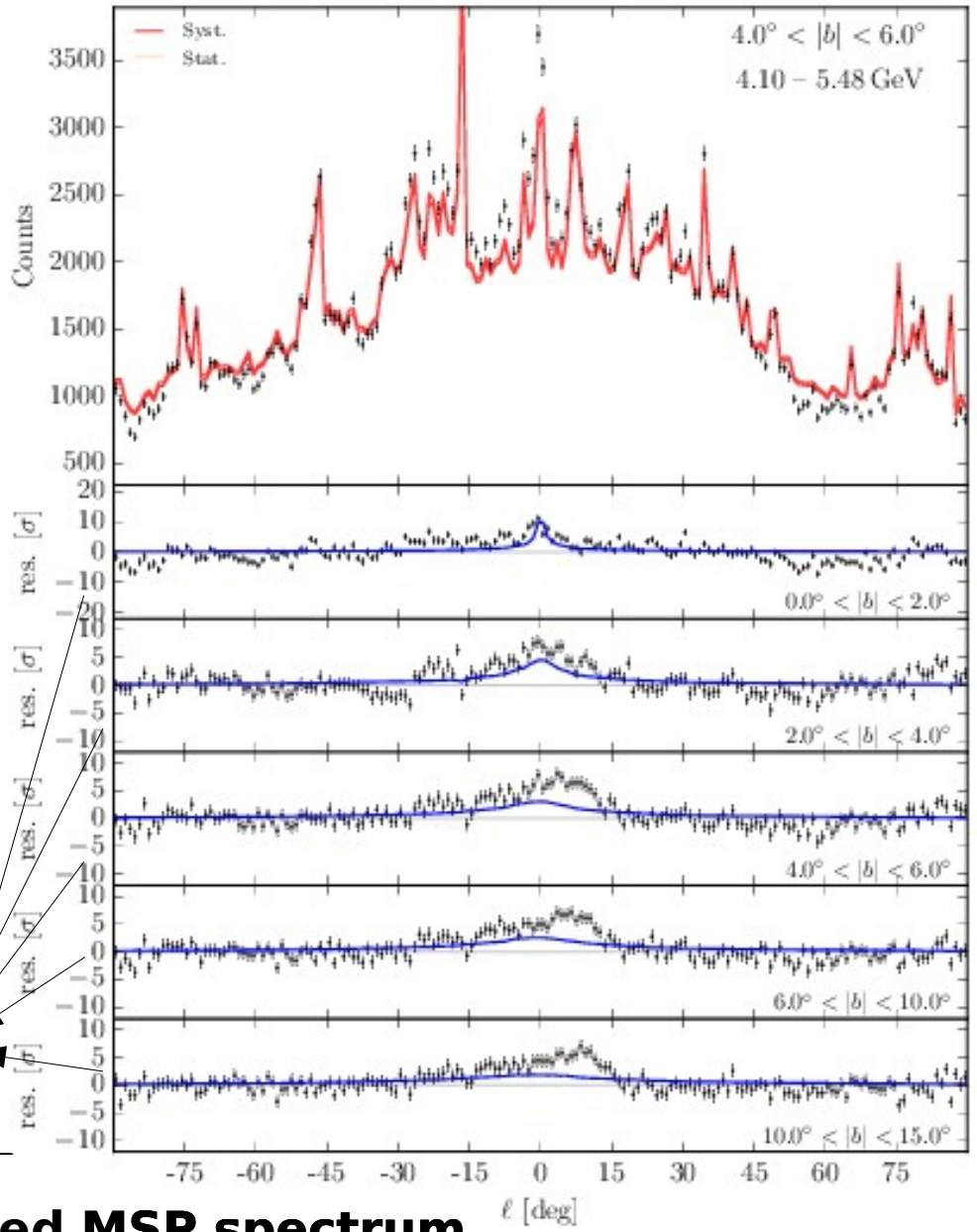

Blue: stacked MSP spectrum

The poor man version of the GeV excess

Bartels & CW

Residuals w.r..t. 300 MeV longitudinal morphology

$$RES(E,\ell,b) = \bar{D}(E,\ell,b) - \mathcal{R}(b)\bar{D}(300\ \mathrm{MeV},\ell,b)$$

Point-source correction:

$$\bar{D}(E,\ell,b) = D(E,\ell,b) - \mathrm{PSC}(E,\ell,b)$$

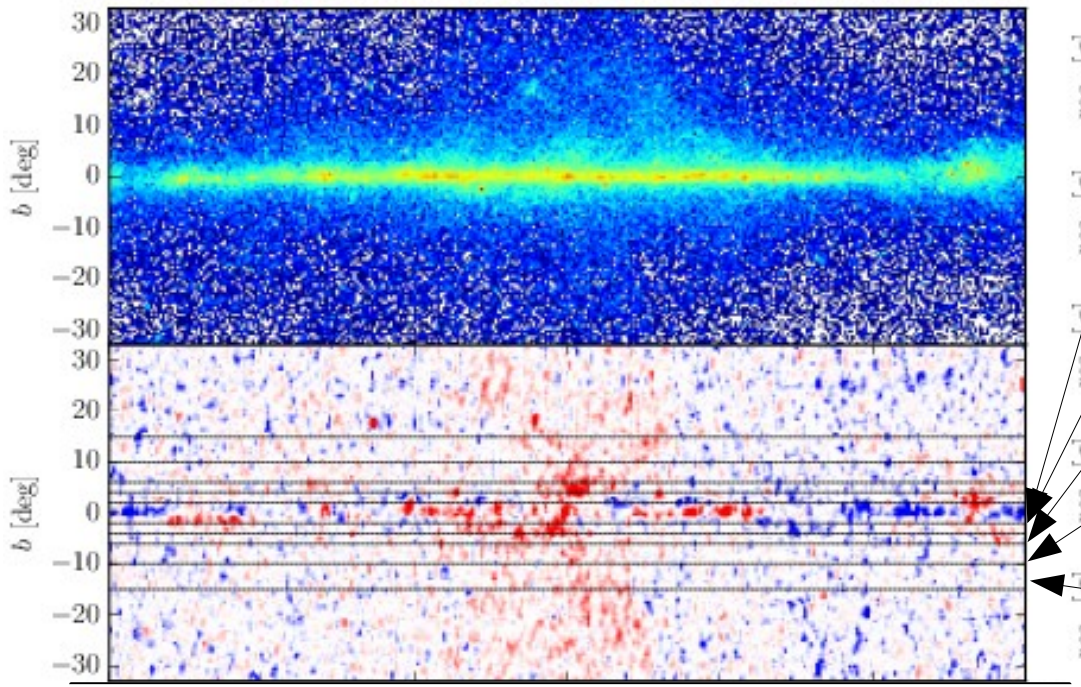

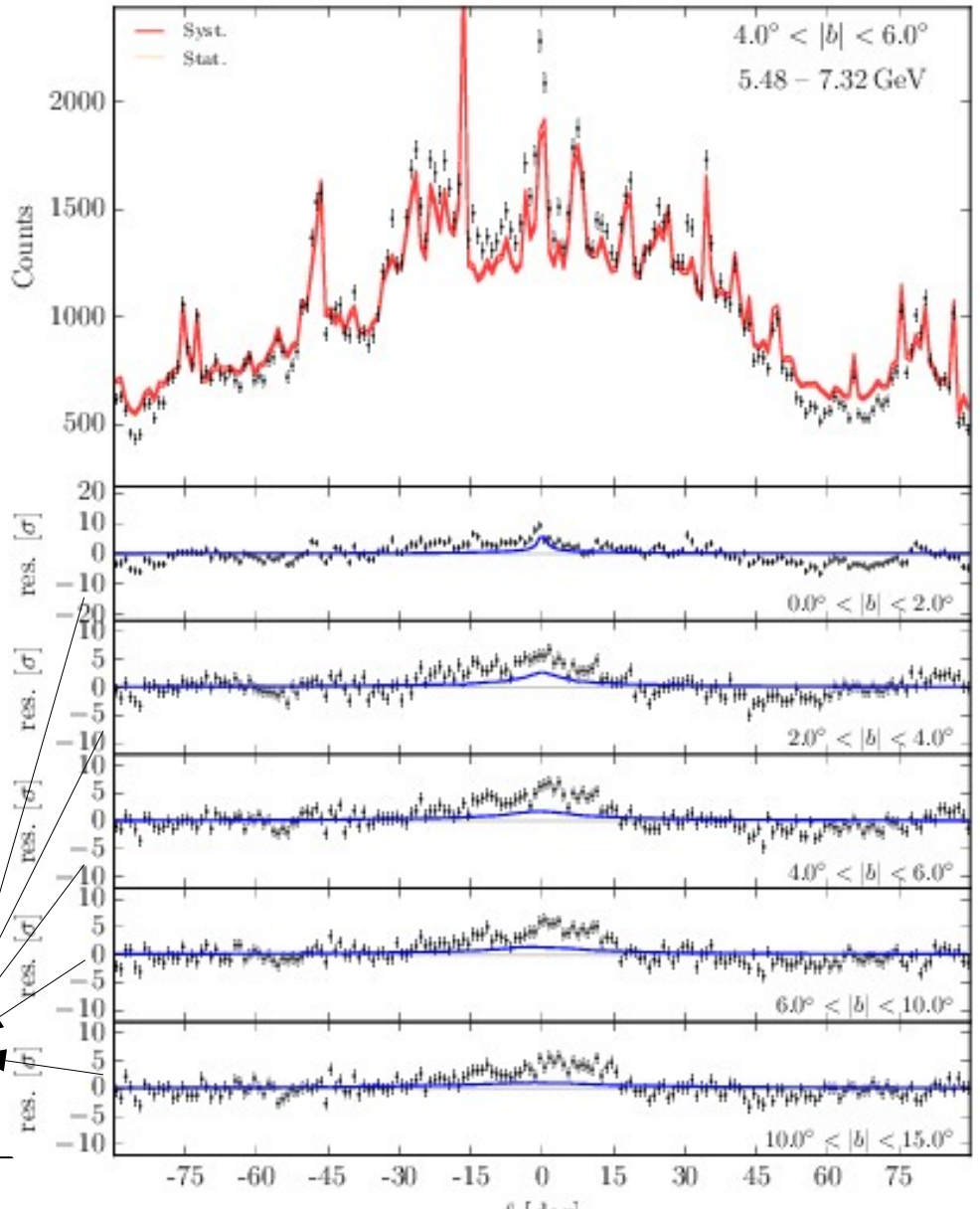

Blue: stacked MSP spectrum

The poor man version of the GeV excess

Bartels & CW

Residuals w.r..t. 300 MeV longitudinal morphology

$$RES(E,\ell,b) = \bar{D}(E,\ell,b) - \mathcal{R}(b)\bar{D}(300\ \mathrm{MeV},\ell,b)$$

Point-source correction:

$$\bar{D}(E,\ell,b) = D(E,\ell,b) - \mathrm{PSC}(E,\ell,b)$$

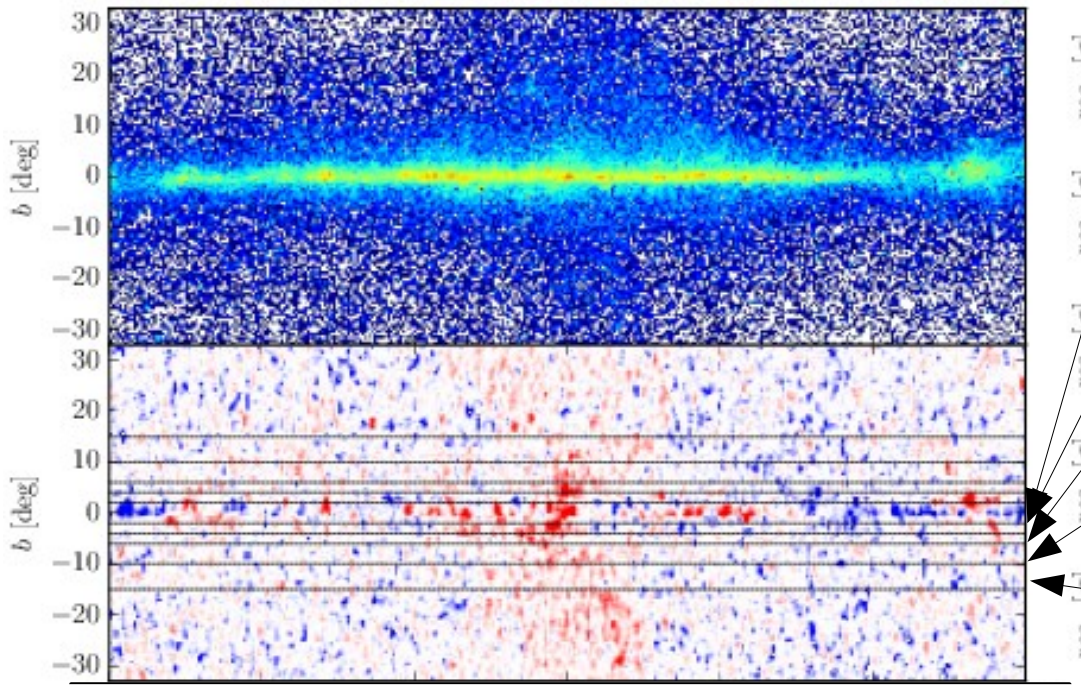

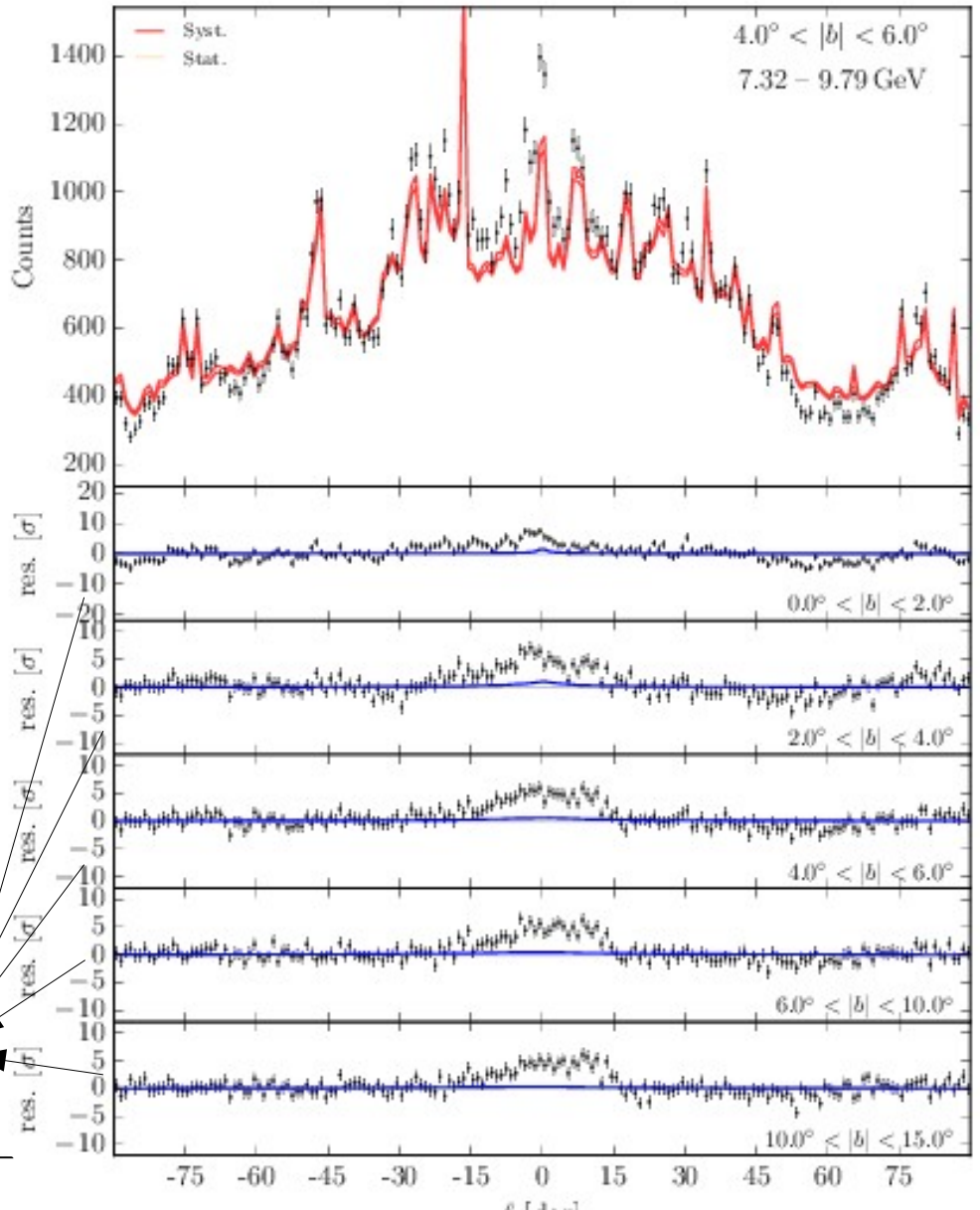

Blue: stacked MSP spectrum

The poor man version of the GeV excess

Bartels & CW

Residuals w.r..t. 300 MeV longitudinal morphology

$$RES(E,\ell,b) = \bar{D}(E,\ell,b) - \mathcal{R}(b)\bar{D}(300\ \mathrm{MeV},\ell,b)$$

Point-source correction:

$$\bar{D}(E,\ell,b) = D(E,\ell,b) - \mathrm{PSC}(E,\ell,b)$$

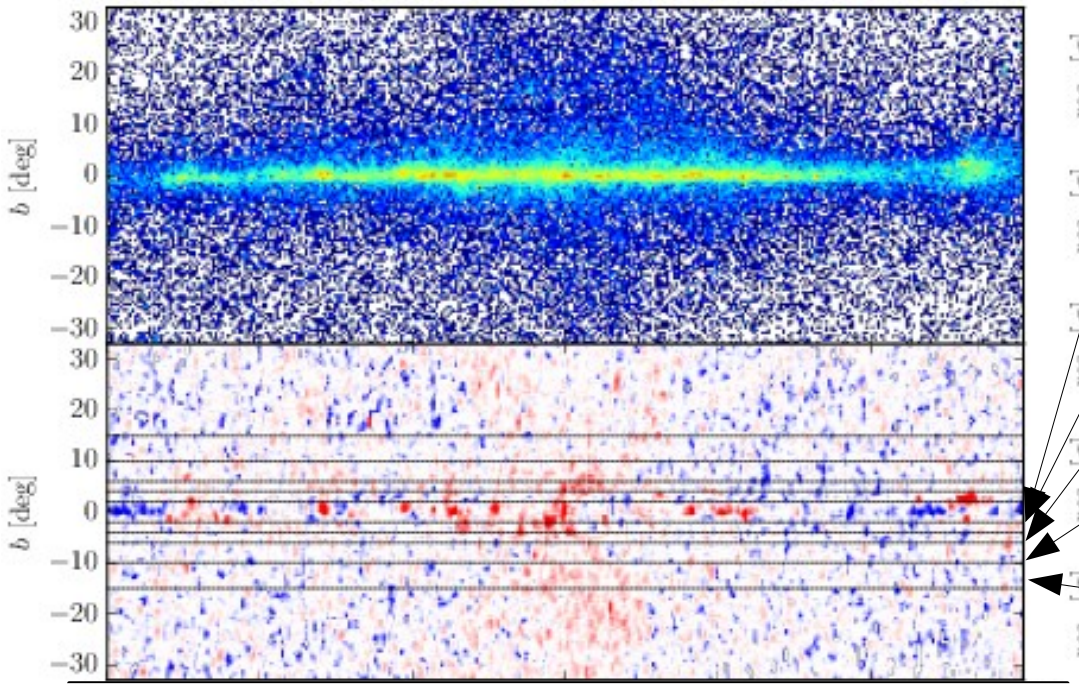

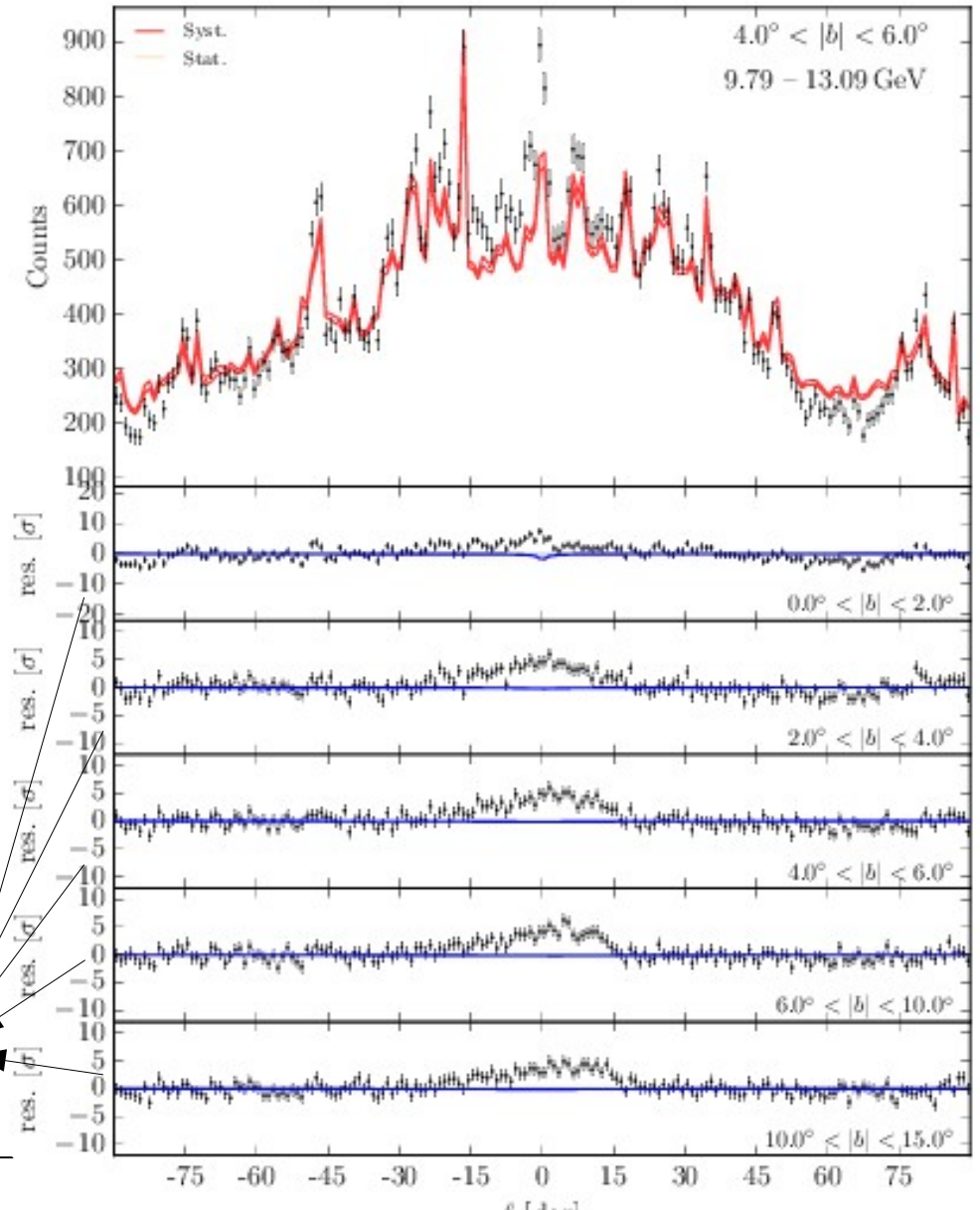

Blue: stacked MSP spectrum

The poor man version of the GeV excess

Bartels & CW

Residuals w.r..t. 300 MeV longitudinal morphology

$$RES(E,\ell,b) = \bar{D}(E,\ell,b) - \mathcal{R}(b)\bar{D}(300\ \mathrm{MeV},\ell,b)$$

Point-source correction:

$$\bar{D}(E,\ell,b) = D(E,\ell,b) - \mathrm{PSC}(E,\ell,b)$$

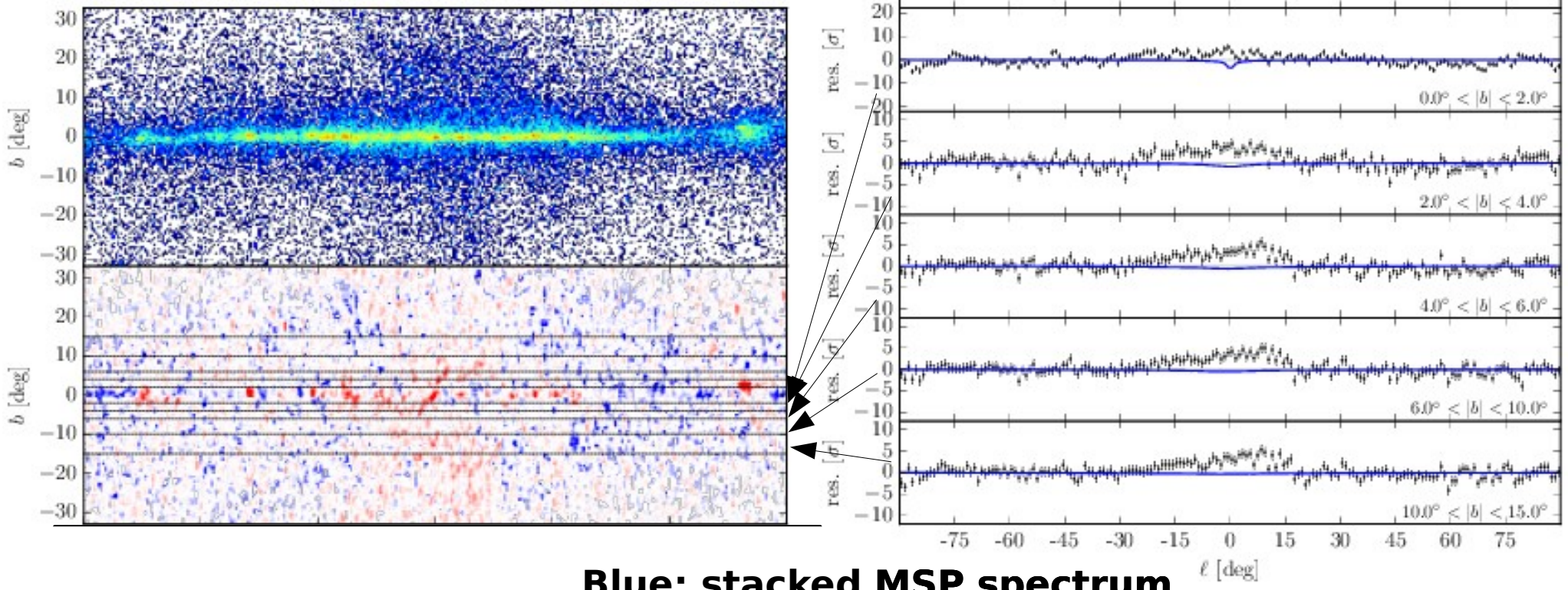

Blue: stacked MSP spectrum

The poor man version of the GeV excess

Bartels & CW

Residuals w.r..t. 300 MeV longitudinal morphology

$$RES(E,\ell,b) = \bar{D}(E,\ell,b) - \mathcal{R}(b)\bar{D}(300\ \mathrm{MeV},\ell,b)$$

Point-source correction:

$$\bar{D}(E,\ell,b) = D(E,\ell,b) - \mathrm{PSC}(E,\ell,b)$$

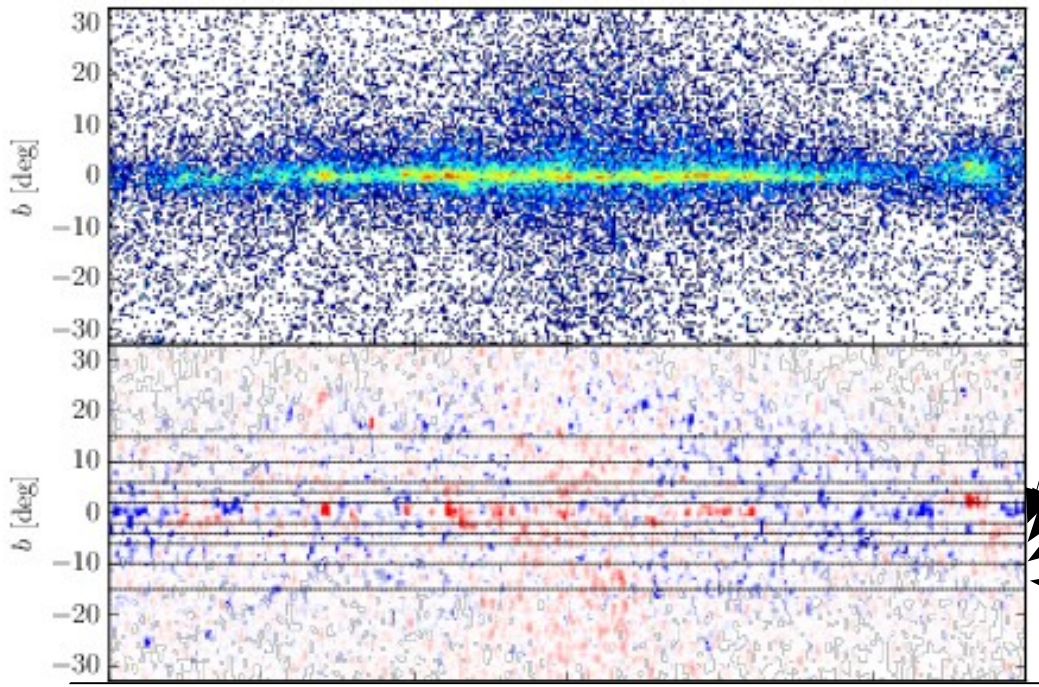

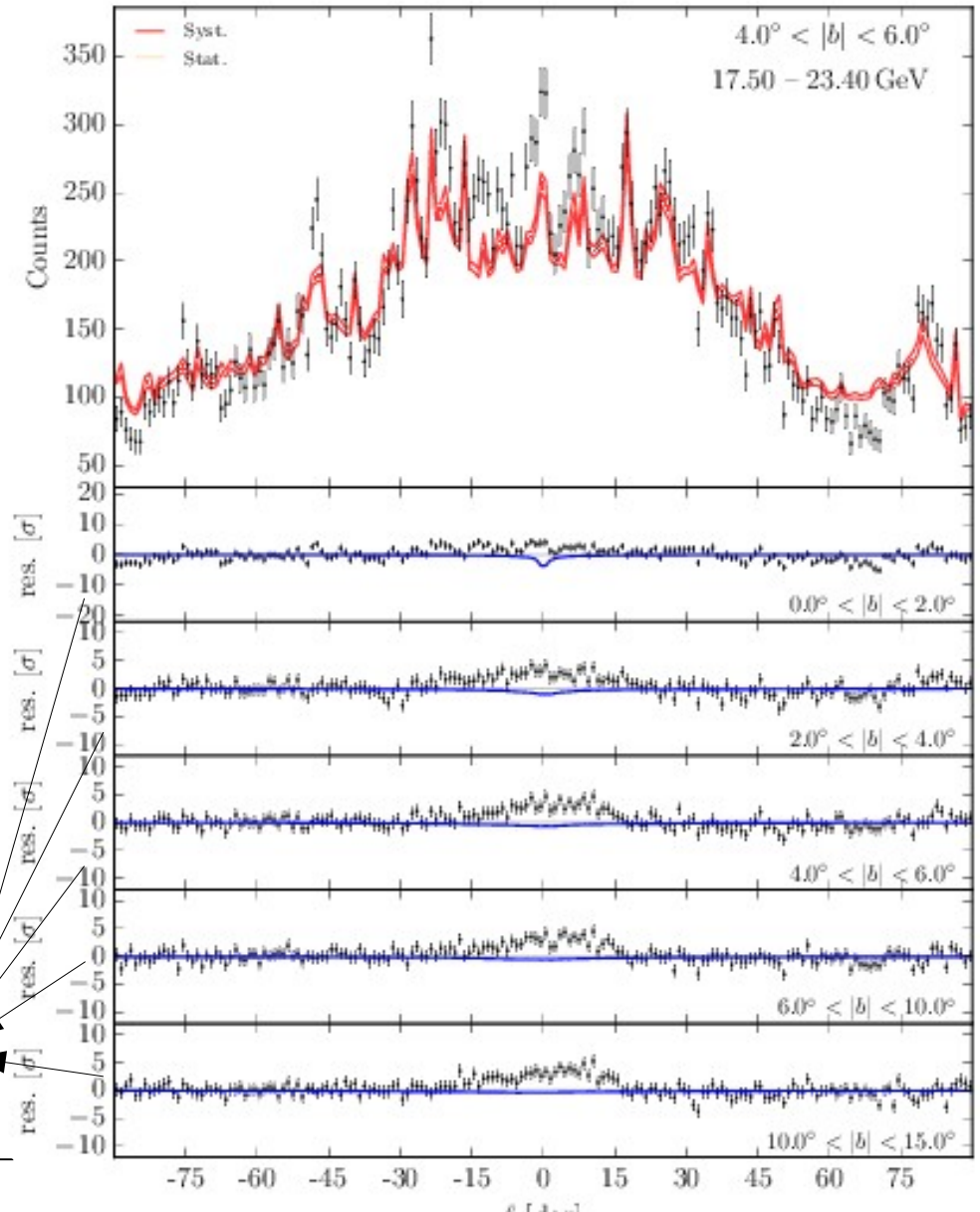

Blue: stacked MSP spectrum

The poor man version of the GeV excess

Bartels & CW

Residuals w.r..t. 300 MeV longitudinal morphology

$$RES(E,\ell,b) = \bar{D}(E,\ell,b) - \mathcal{R}(b)\bar{D}(300\ \mathrm{MeV},\ell,b)$$

Point-source correction:

$$\bar{D}(E,\ell,b) = D(E,\ell,b) - \mathrm{PSC}(E,\ell,b)$$

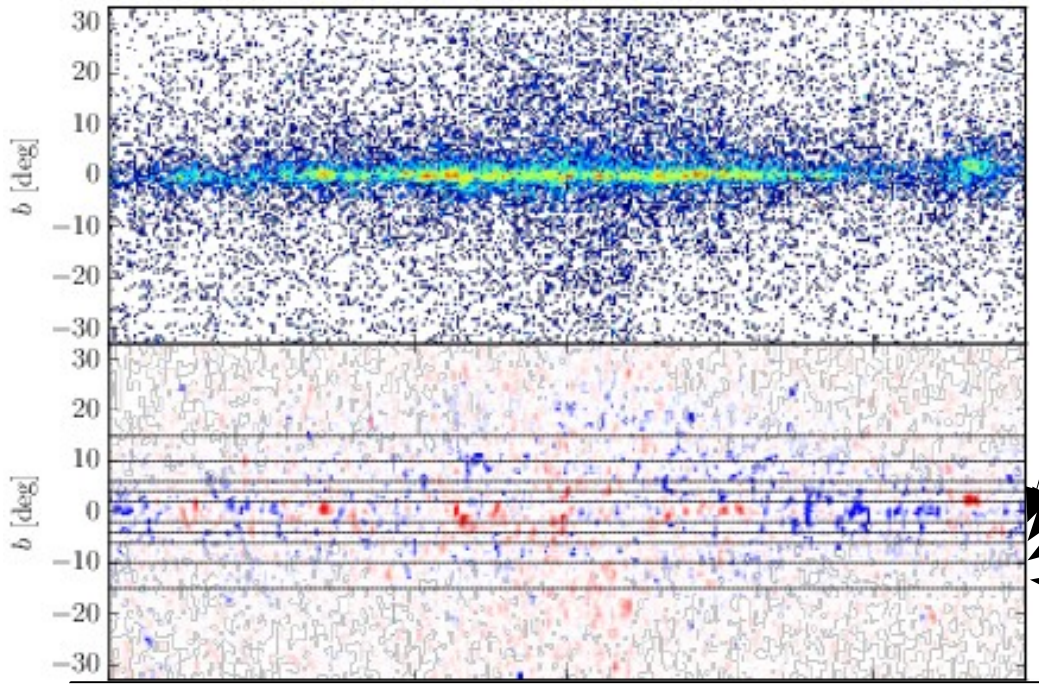

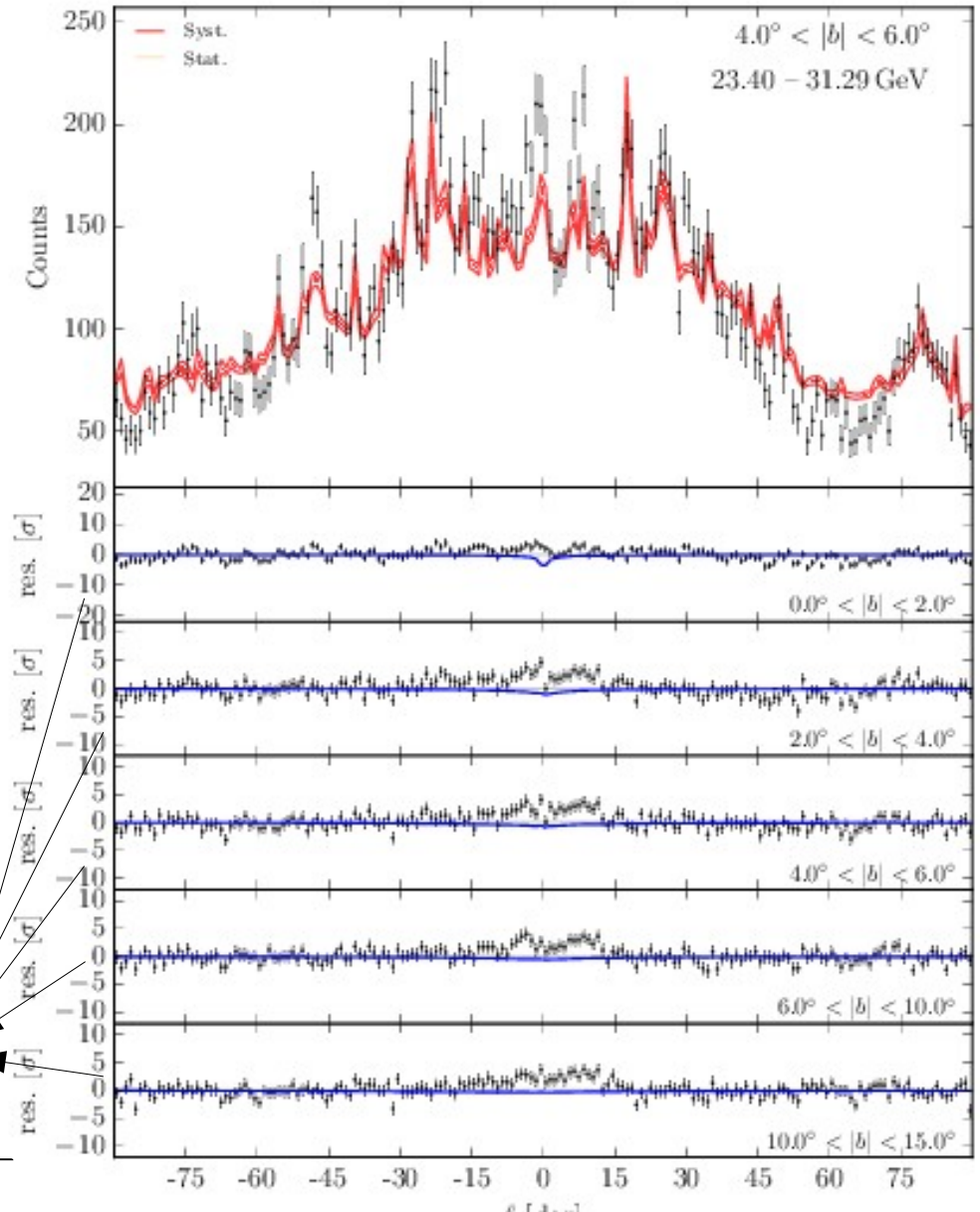

Blue: stacked MSP spectrum

The poor man version of the GeV excess

Bartels & CW

Residuals w.r..t. 300 MeV longitudinal morphology

$$RES(E,\ell,b) = \bar{D}(E,\ell,b) - \mathcal{R}(b)\bar{D}(300\ \mathrm{MeV},\ell,b)$$

Point-source correction:

$$\bar{D}(E,\ell,b) = D(E,\ell,b) - \mathrm{PSC}(E,\ell,b)$$

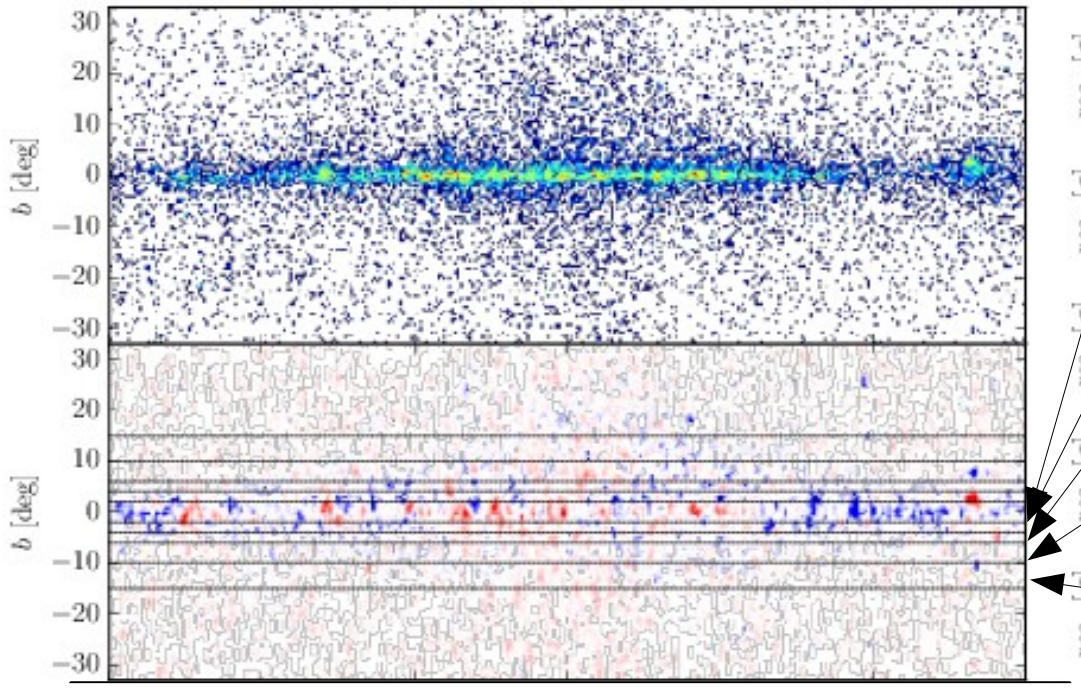

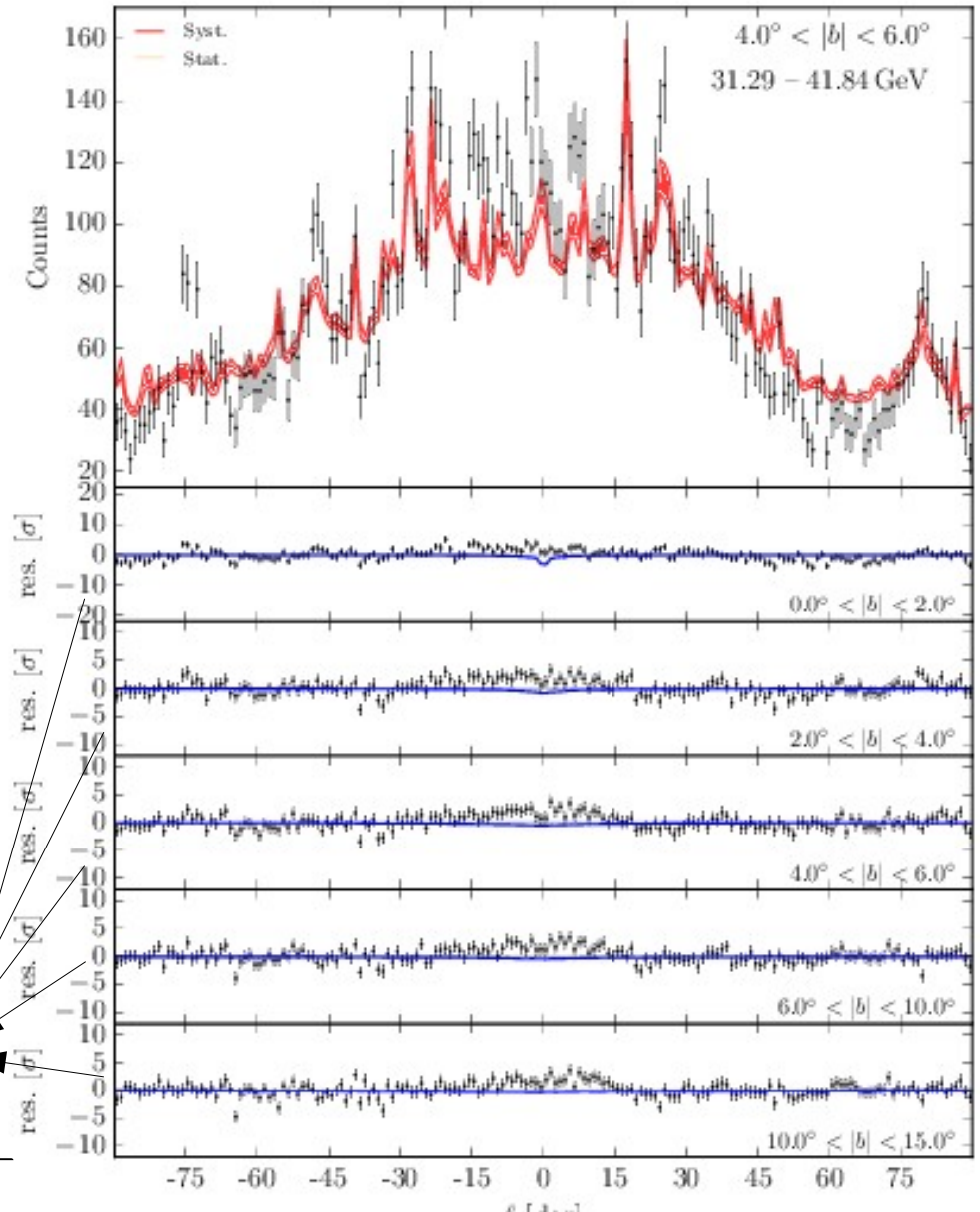

Blue: stacked MSP spectrum

The poor man version of the GeV excess

Bartels & CW

Residuals w.r..t. 300 MeV longitudinal morphology

$$RES(E,\ell,b) = \bar{D}(E,\ell,b) - \mathcal{R}(b)\bar{D}(300\ \mathrm{MeV},\ell,b)$$

Point-source correction:

$$\bar{D}(E,\ell,b) = D(E,\ell,b) - \mathrm{PSC}(E,\ell,b)$$

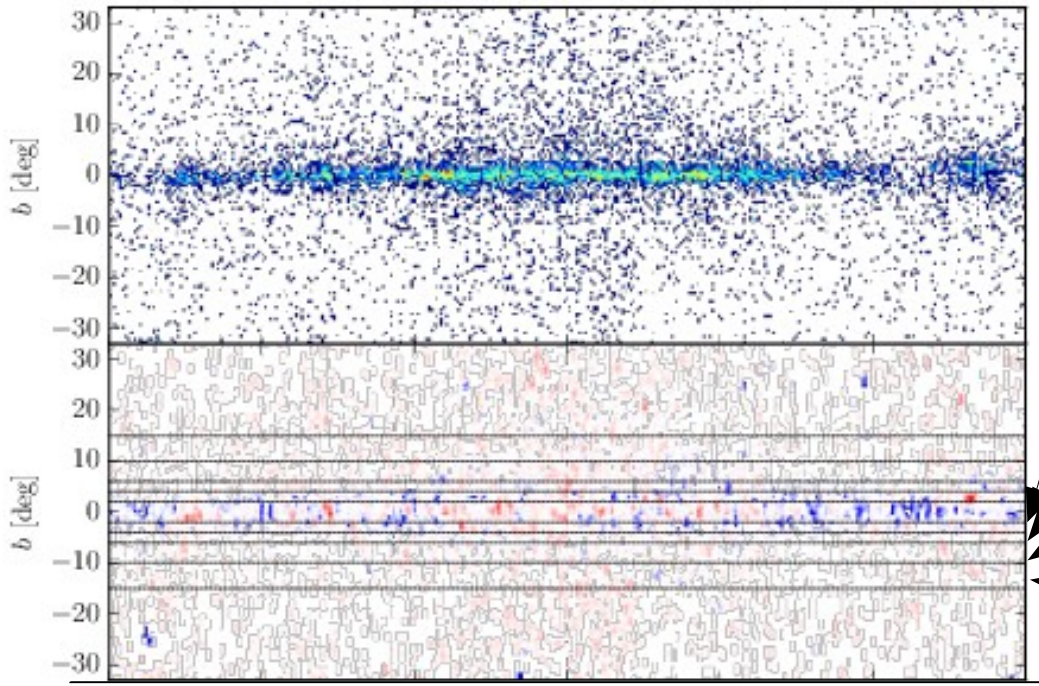

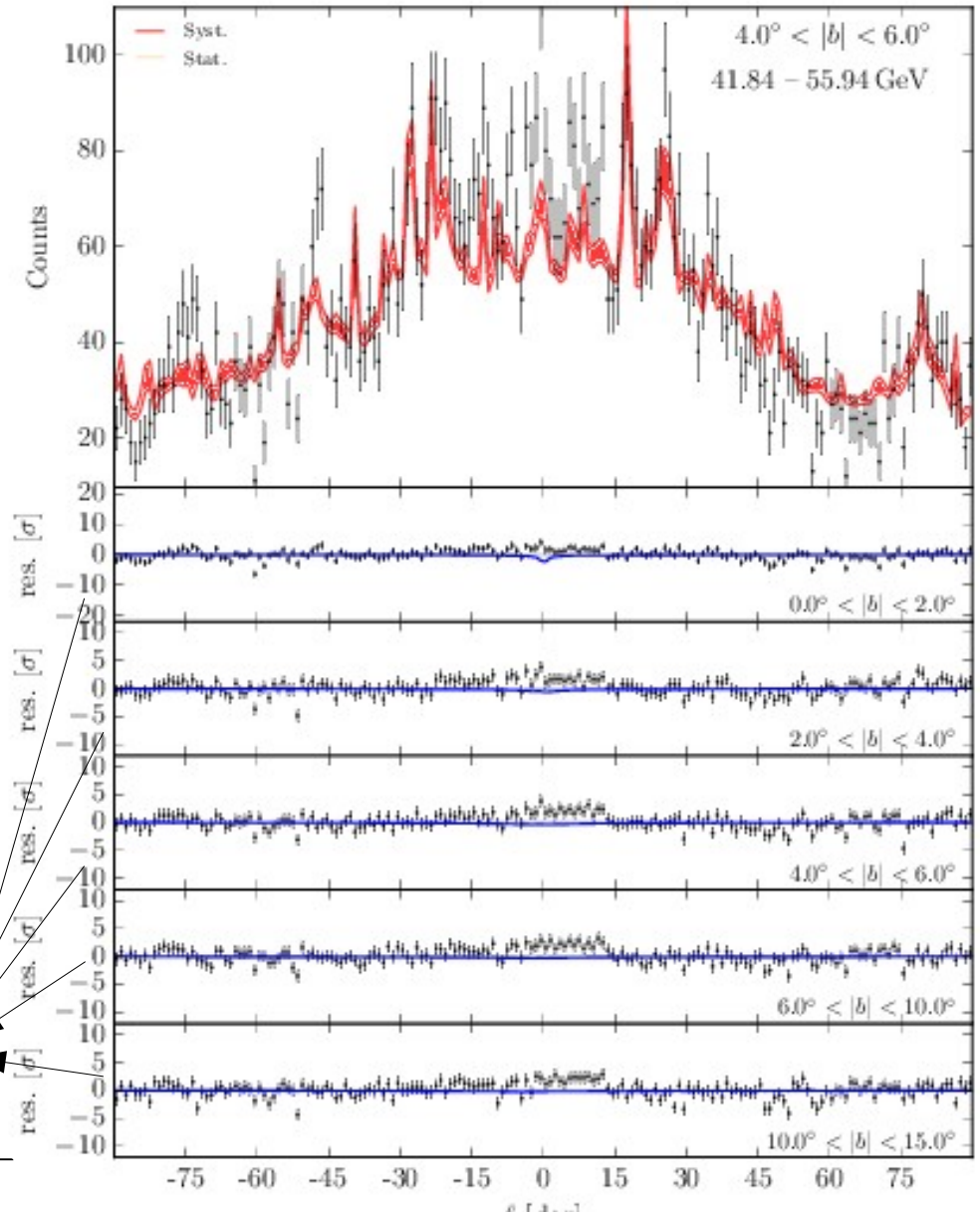

Blue: stacked MSP spectrum

Summary

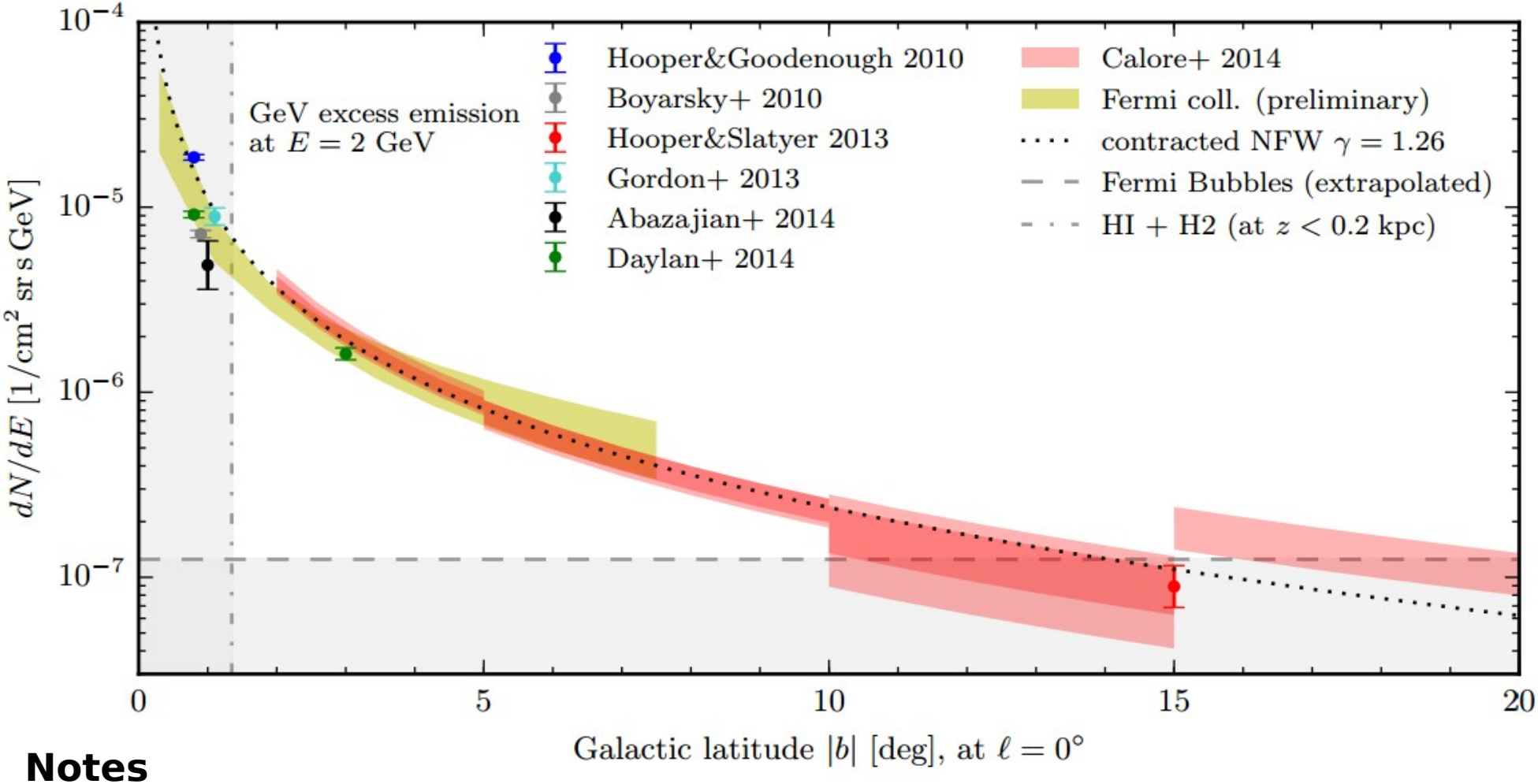

Notes

- What we call “excess” is most likely the gamma-ray emission from the Galactic bulge
  (this component is not included or modeled in most of the diffuse emission models)
- The emission is compatible with a uniform energy spectrum and spherically symmetric volume emissivity following an inverse power-law

$$E_{\rm peak} \sim 2\ {\rm GeV} \qquad \frac{dn}{dV} \propto r^{-2.5}$$

Star formation in the CMZ

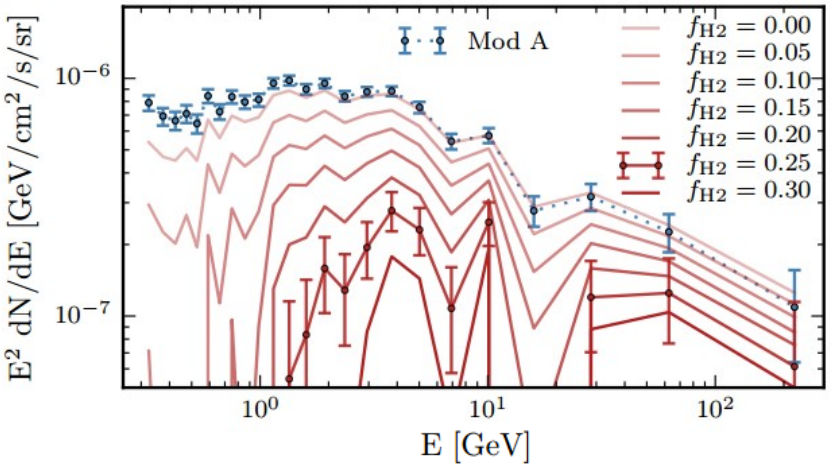

Carlson+ 2015

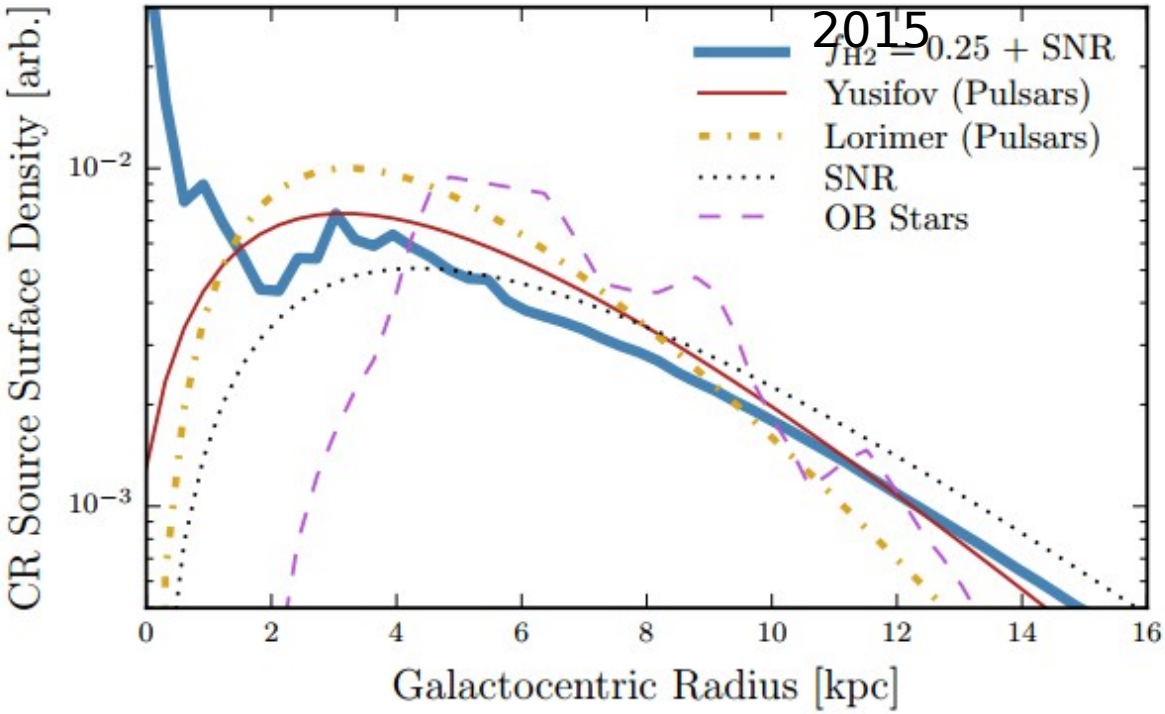

Note

- Previous Galactic diffuse emission models neglected CR injection in the inner Galaxy (with few exceptions, Ackermann+ 2013)
- Inverse Compton emission from electrons accelerated in the CMZ potentially accounts for a good fraction of the bulge emission
- However, the predicted spectra are usually too soft to fully account for the observations

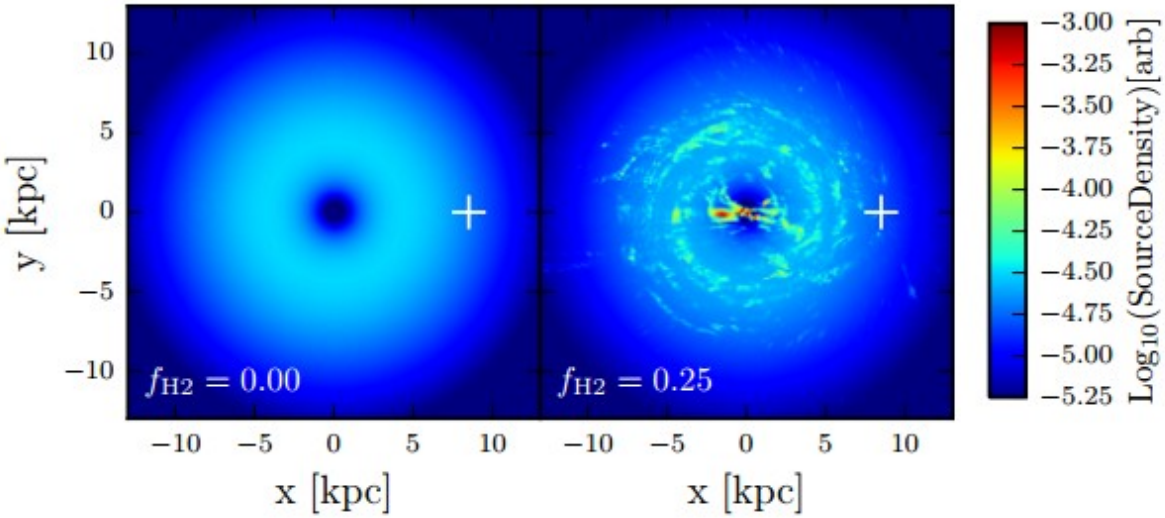

Two leptonic outbursts?

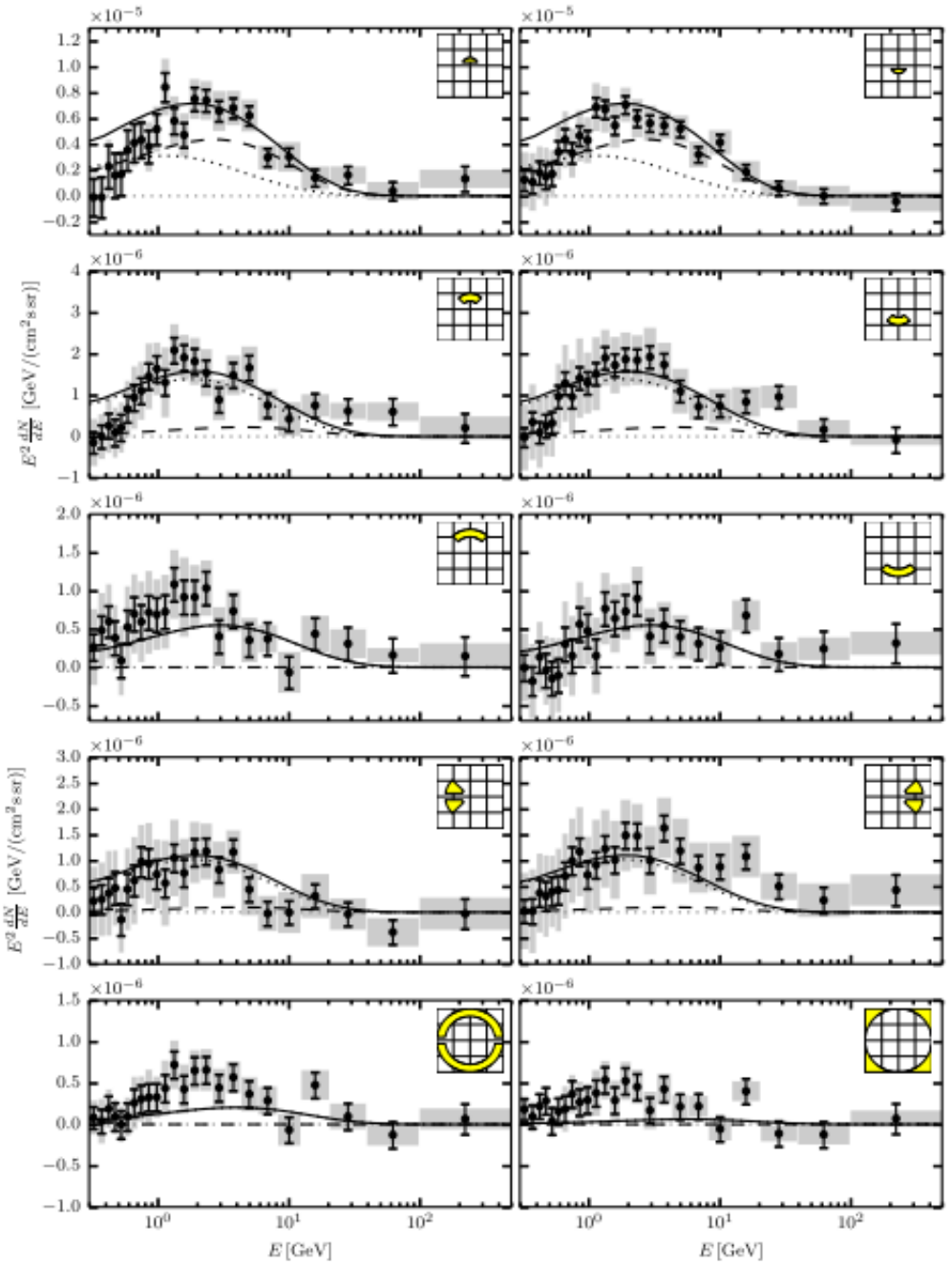

Parameter	Model A	Model B	Model C
α_1	1.2	2.0	1.1
α_2	NA	NA	1.0
$E_{\rm cut,1}$	1 TeV	1 TeV	20 GeV
$E_{\rm cut,2}$	NA	NA	60 GeV
τ_1 (Myr)	0.83	0.46	0.1
τ_2 (Myr)	NA	NA	1.0
N_1 (10^{51} erg)	2.89	9.87	0.1
N_2 (10^{51} erg)	NA	NA	0.88
δ	0.20	0.23	0.3
D_0 (10^{28} cm^2/s)	5.08	9.12	9.0
D_{zz}/D_{xx}	1.12	0.87	NA
v_A (km/s)	176	122	150
B_0 (μG)	11.5	11.5	11.7
r_c (kpc)	10.0	10.0	10.0
z_c (kpc)	2.0	2.0	0.5
dv_c/dz (km/s/kpc)	0.0	0.0	0.0
ISRF	1.0, 1.0	1.0, 1.0	1.8, 0.8
χ^2 ($p-$value)	277 (0.04)	317 (0.0004)	261 (0.14)

Some tuning is required to make it work reasonably well

- Extremely hard injection indices (<2)
- **One burst around 1 Myr**
- ~10^51 erg injected energy in CR e-
  (~1000 SN)
- Still, does not well reproduce the

[Cholis, Evoli, Calore, Linden, CW, Hooper 2015]

Even two bursts cannot explain everything

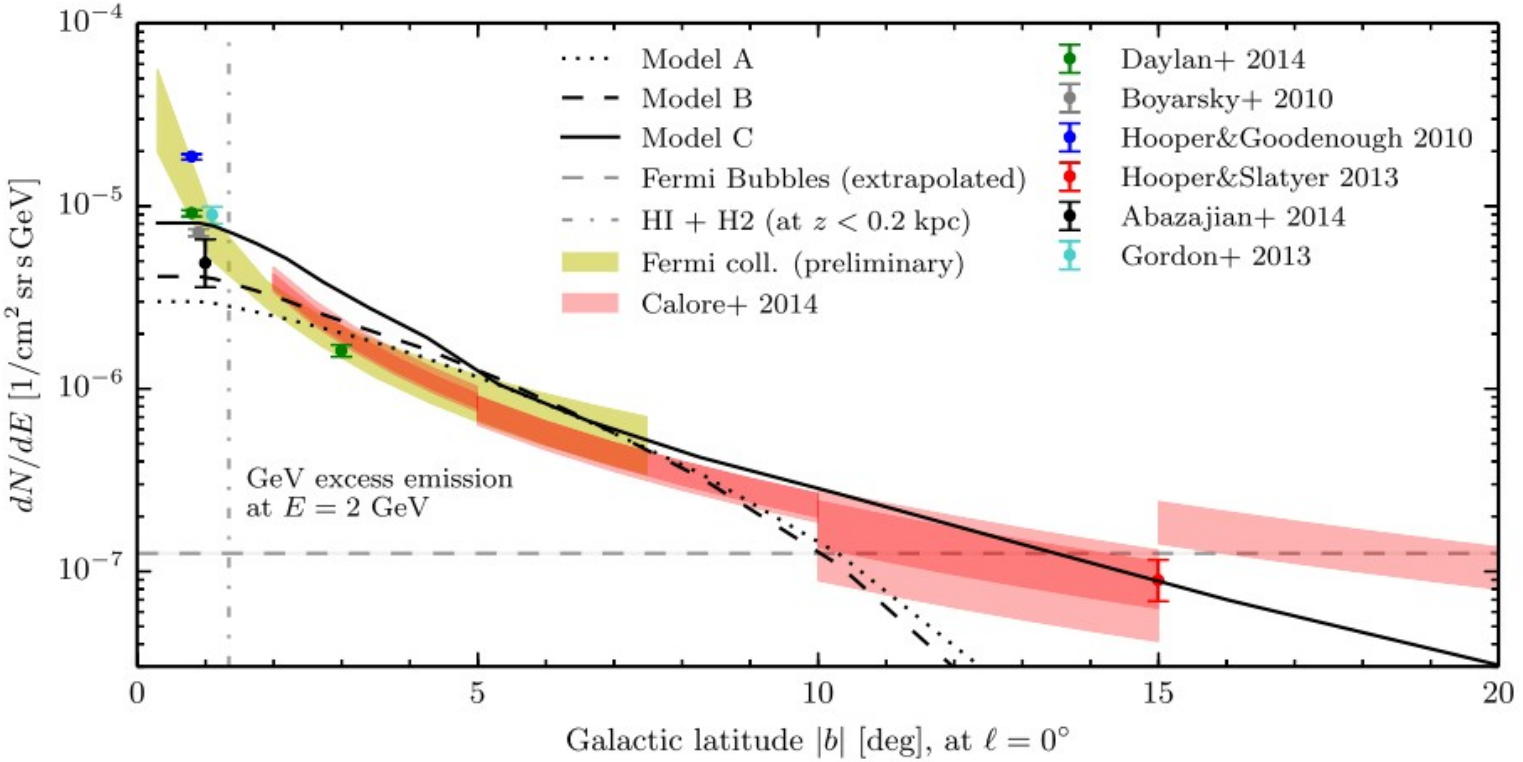

Summary

- It *is* possible to achieve a reasonable description of the data by using two bursts and tuning injection and propagation parameters
- However, the rise of the emission towards the inner few 10 pc is not predicted
- **A series of leptonic bursts are observationally viable, but not likely to explain all of the excess emission**

[Cholis, Evoli, Calore, Linden, CW, Hooper 2015]

Gamma-ray detected pulsars

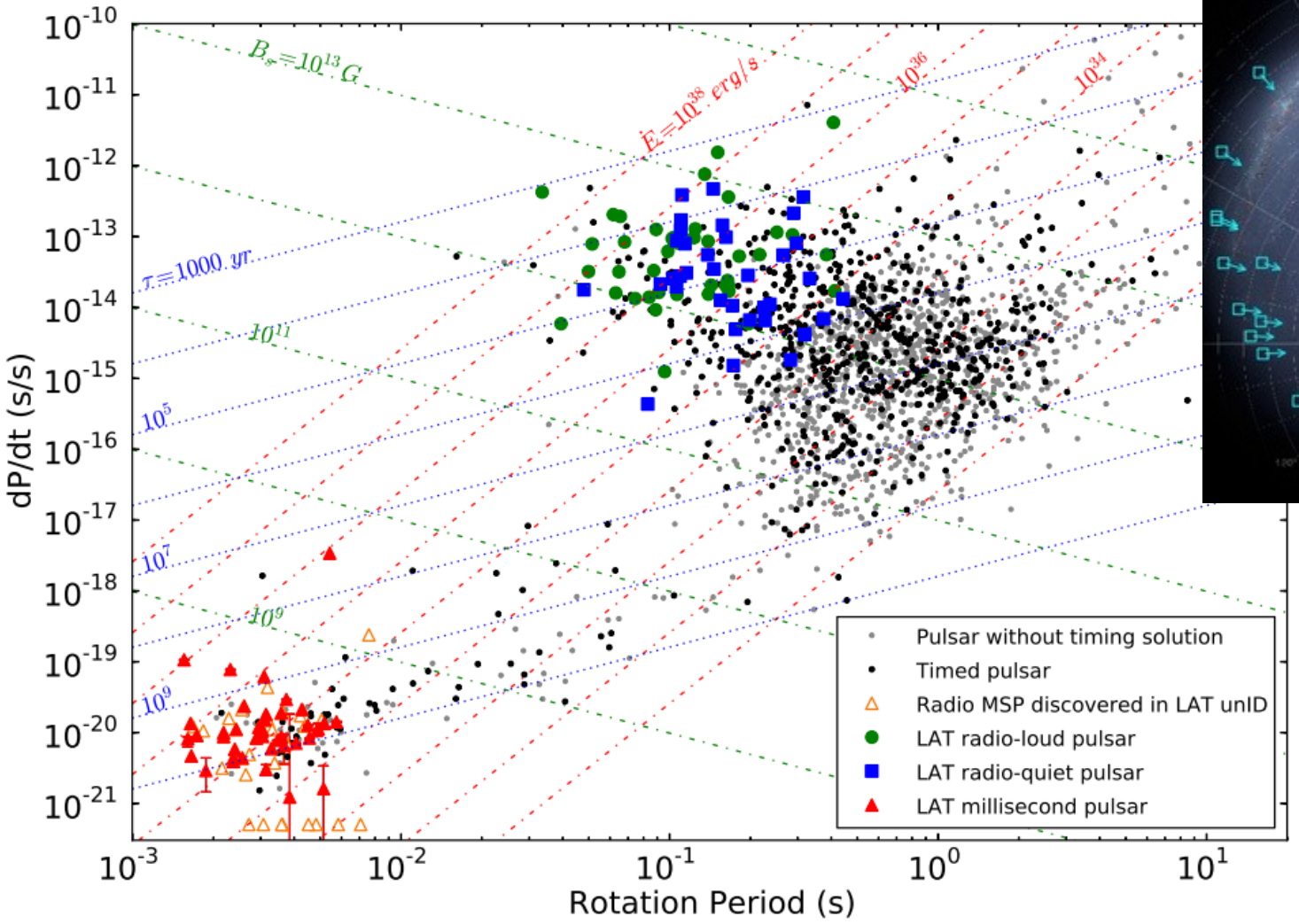

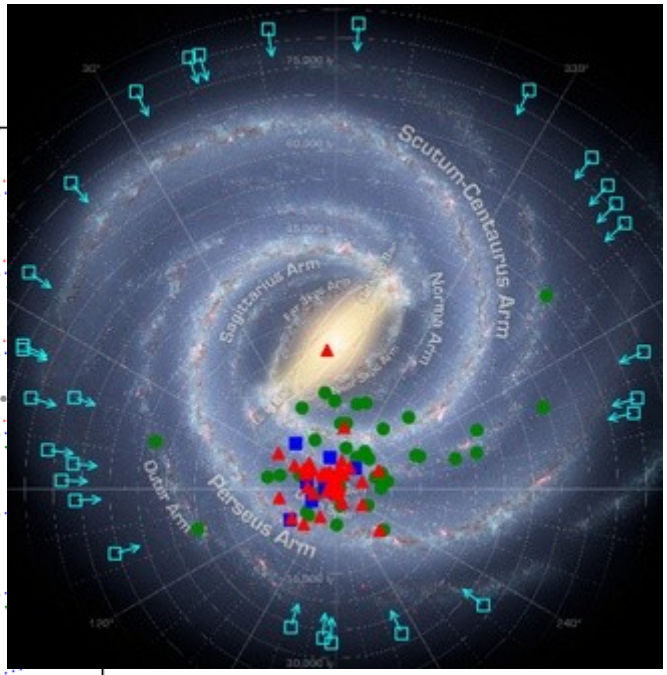

$$B_{\rm S} = (1.5 I_0 c^3 P \dot{P})^{1/2} / 2\pi R_{\rm NS}^3$$

$$\tau_c = P/2\dot{P}$$

[Abdo+ 2013, 2nd Fermi Pulsar catalog]

Young pulsars

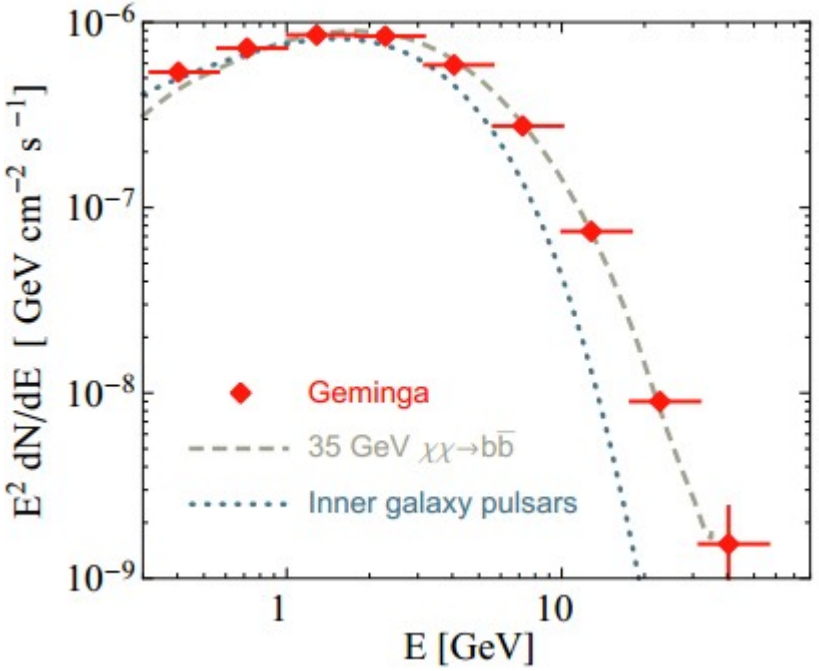

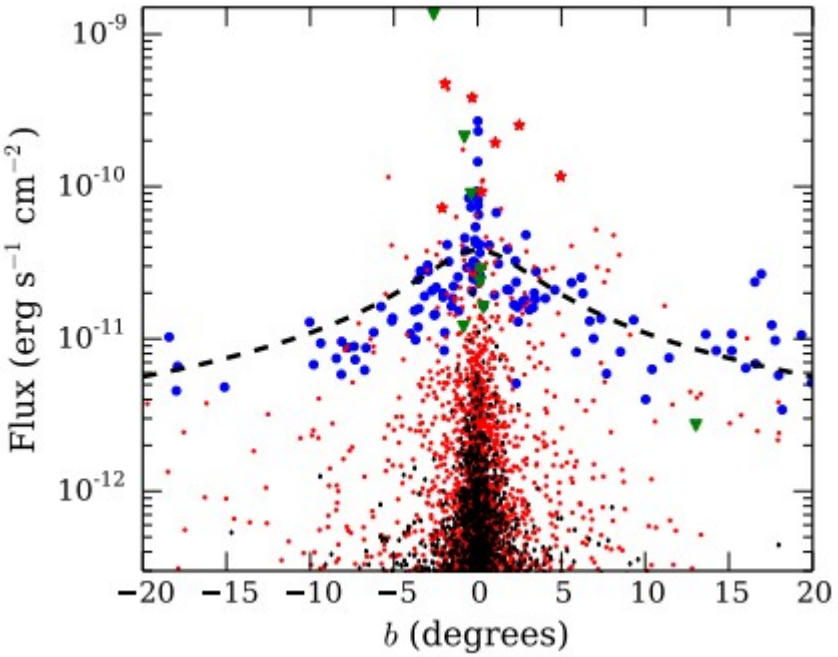

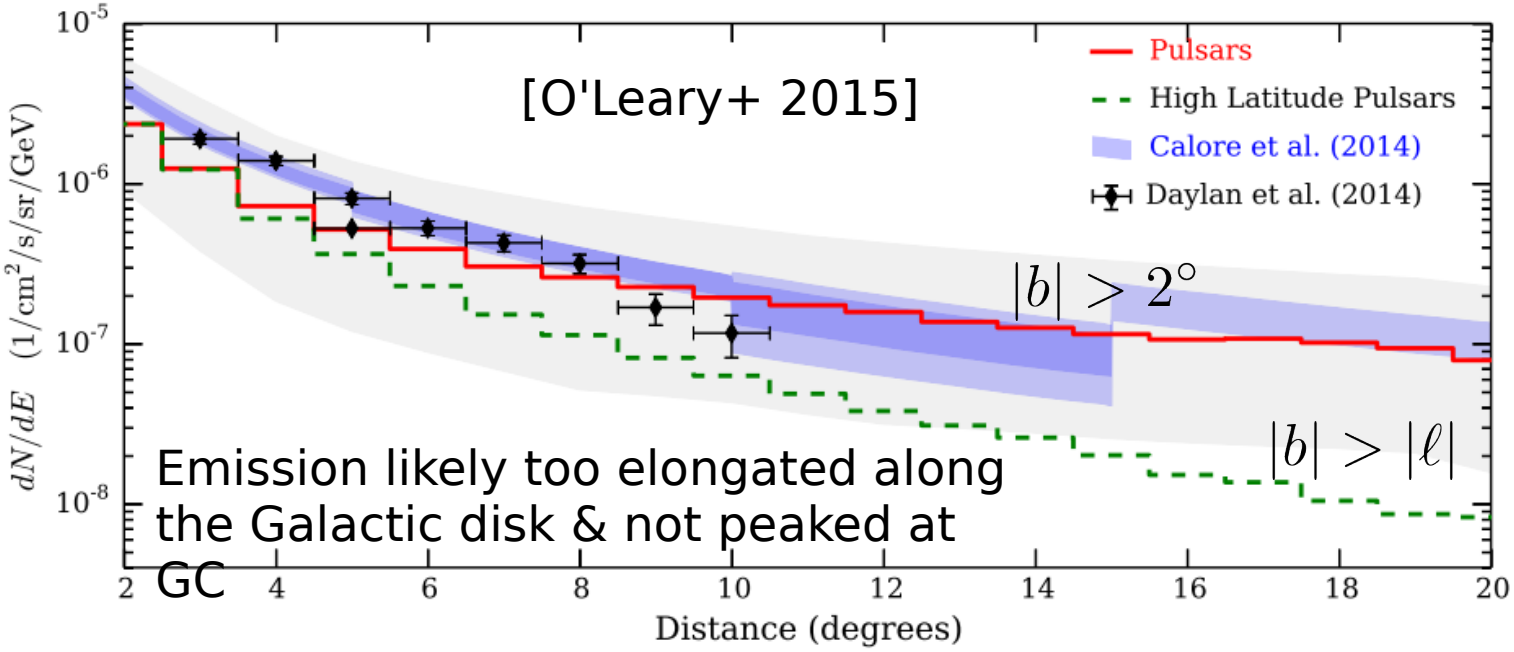

Millisecond pulsars

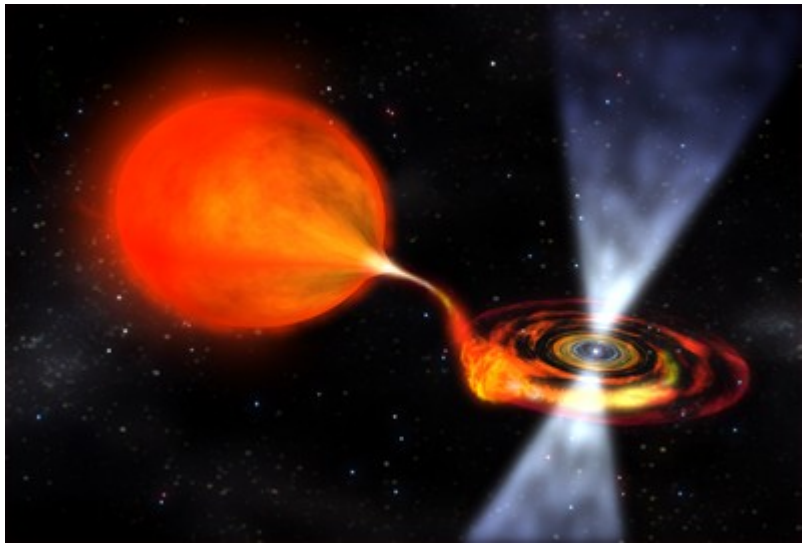

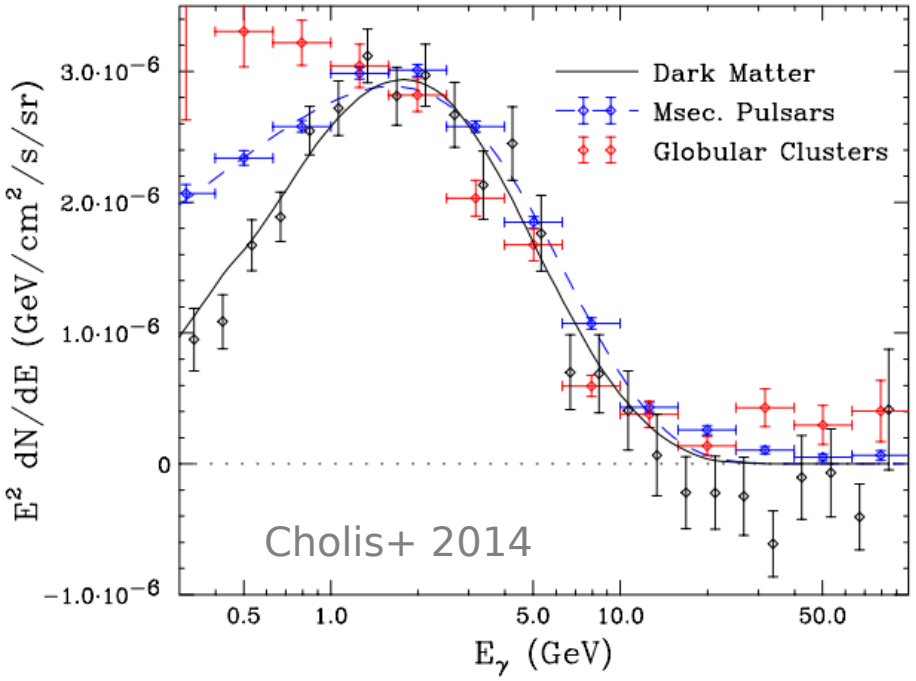

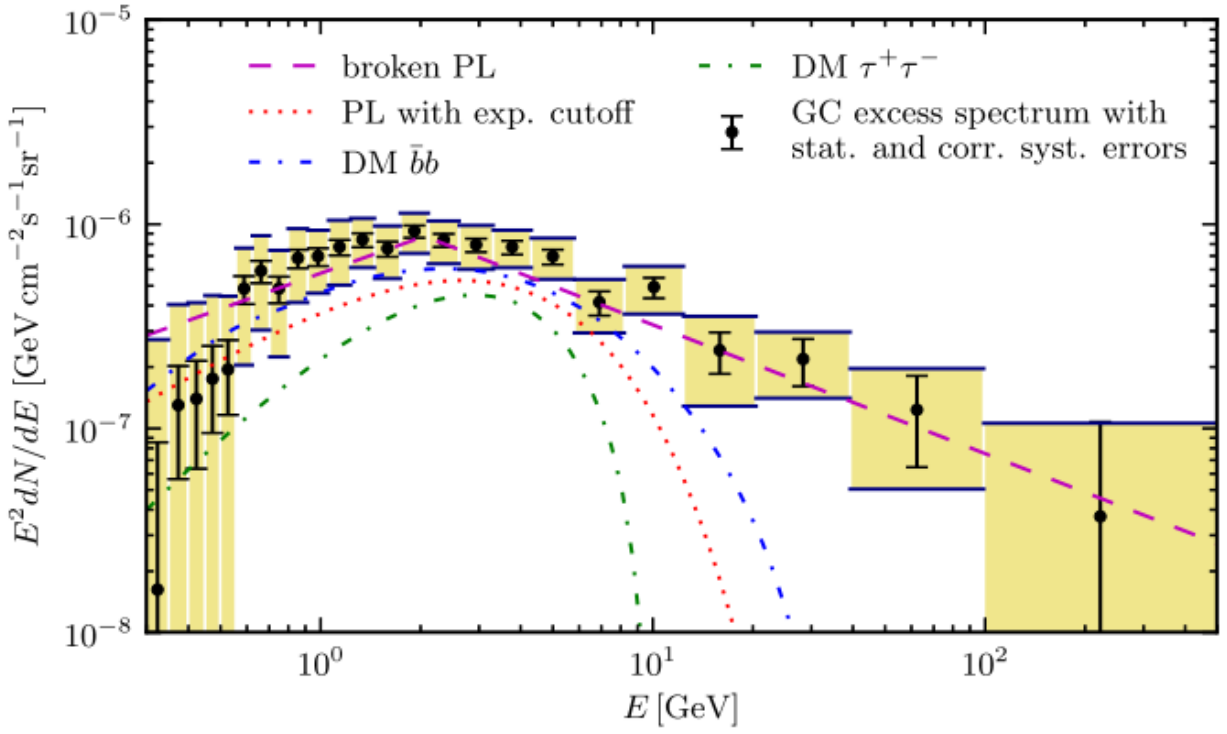

Millisecond pulsars from disrupted globular clusters

Brandt & Kocsis 2015

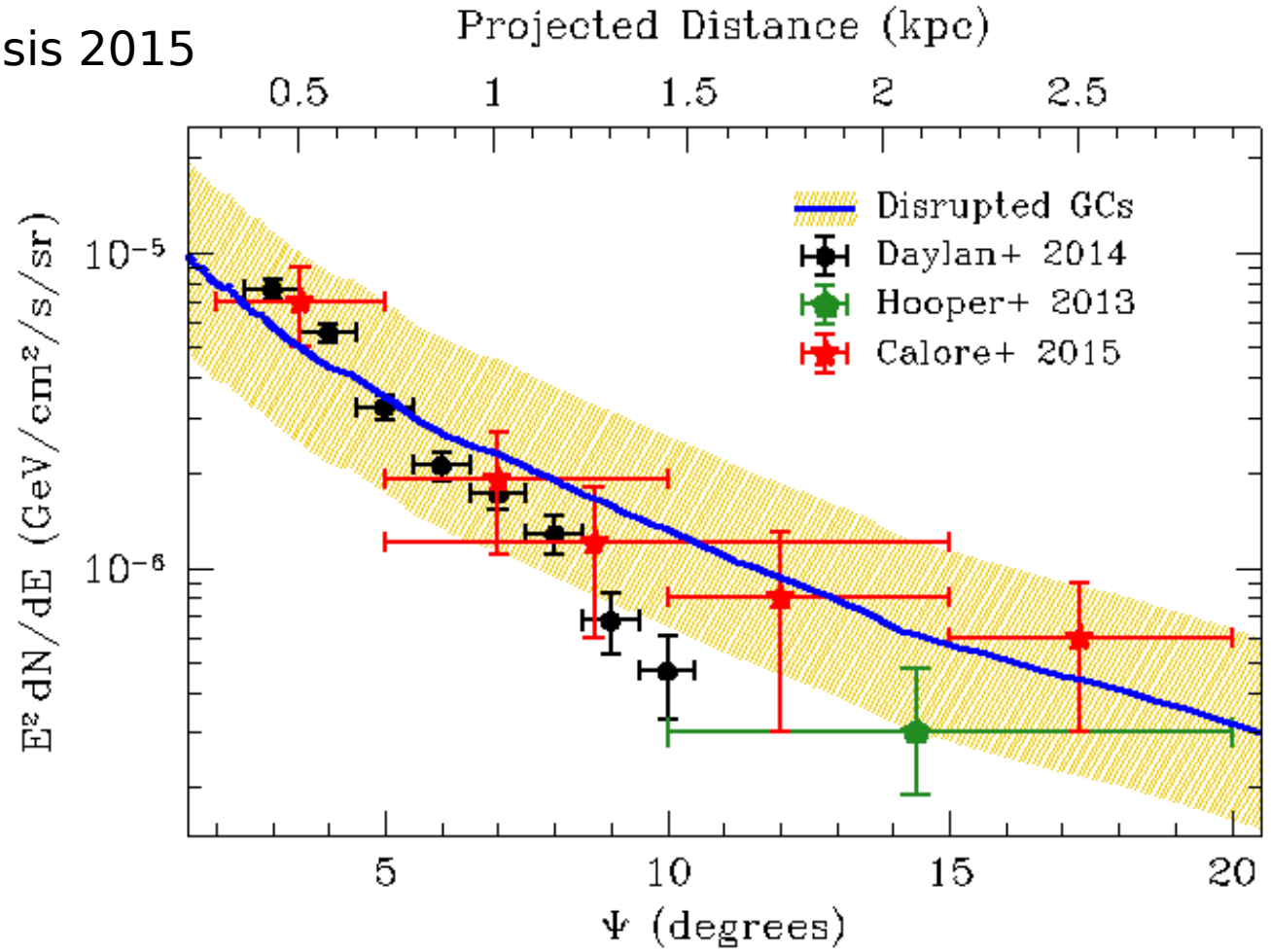

Possible formation history

- Field millisecond pulsars in the bulge could have been created in globular clusters that were tidally disrupted
- This scenario was suggested to explain both normalization and shape of the excess emission

An observational challenge

Point sources or diffuse emission?

- A signal composed of point sources would appear more "**speckled**" than a purely diffuse signal

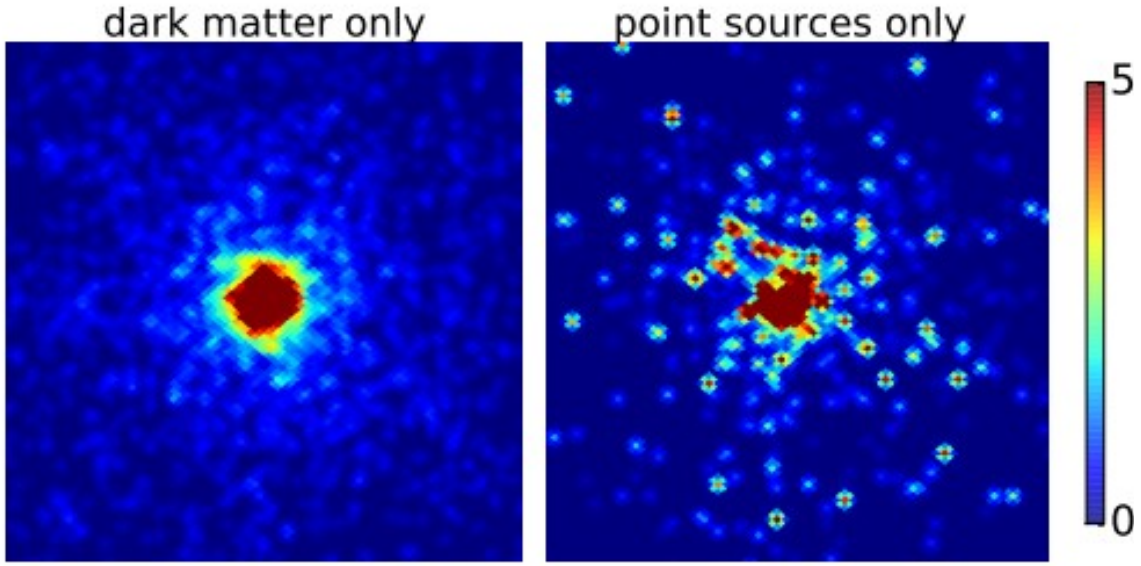

(Credit: Lee+ 2014)

Proposed methods

- *One-point statistics*
  - Random contribution of point sources to individual pixels leads to non-Poissonian noise [Lee et al. 2014] (successfully used at high latitudes byMalyshev & Hogg 2011)
  - **BUT**: Requires modeling / subtraction of backgrounds → Subject to systematics
- *Local maxima of normalized wavelet transform:*
  - *"Wavelet transform":* spatially constrained Fourier transform. Filters out structures of a specific size, like point sources. Removes diffuse emission.
  - *"Normalized":* Null hypothesis is equivalent to smoothed Gaussian random

Effective modeling of MSPs

Modeling of unresolved sources

- We assume that they are distributed like required to explain the GCE (with a radial index of -2.5 or so)
- We simulate PSCs that follow a luminosity distribution

$$\frac{dN}{dL} \sim L^{-1.5}$$

  up to some cutoff $L_{\max}$
- Main uncertainties: Slope, normalization and cutoff of the luminosity function. Here: slope fixed to -1.5

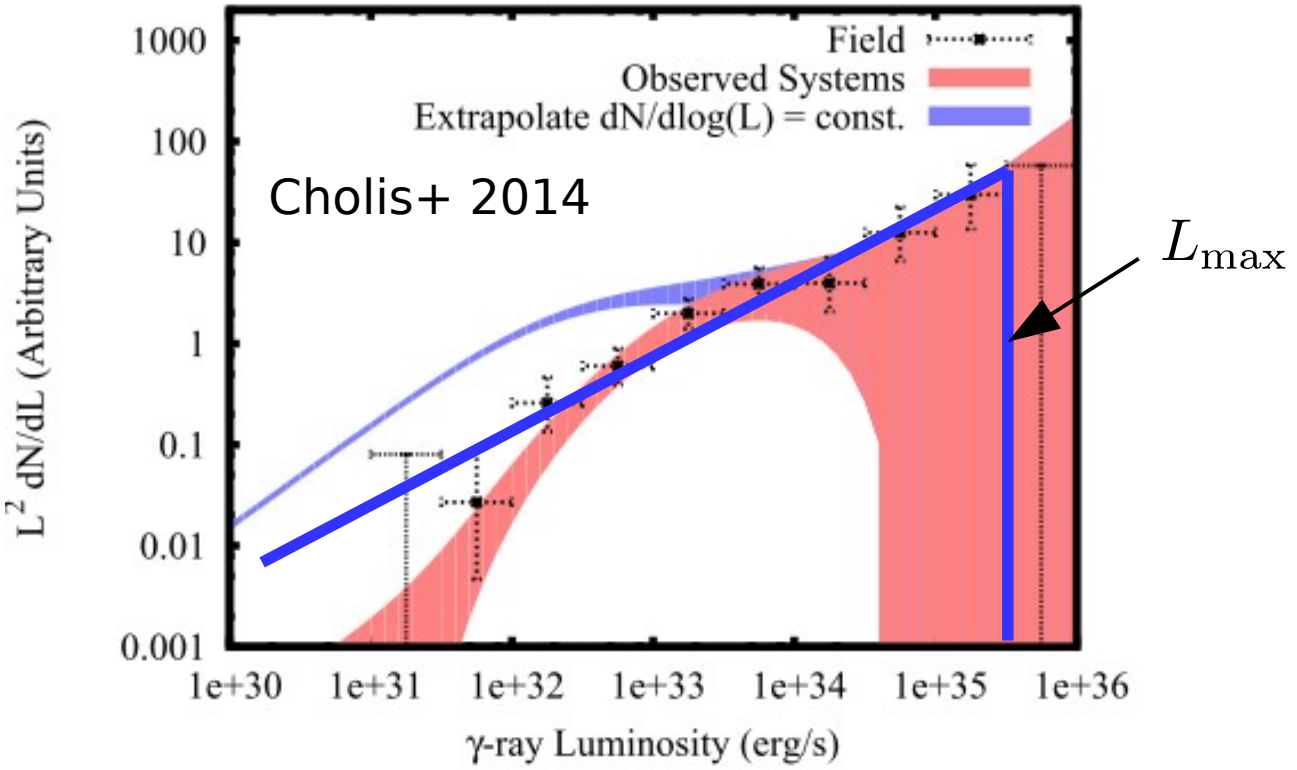

Peaks in the normalized wavelet transform

Definitions

- First we perform a standard wavelet transform

$$\mathcal{F}_{\mathcal{W}}[\mathcal{C}](\Omega) \equiv \int d\Omega\, \mathcal{W}(\Omega - \Omega')\mathcal{C}(\Omega')$$

Wavelet

Count map (1-4 GeV)

The Mexican Hat Wavelet Family

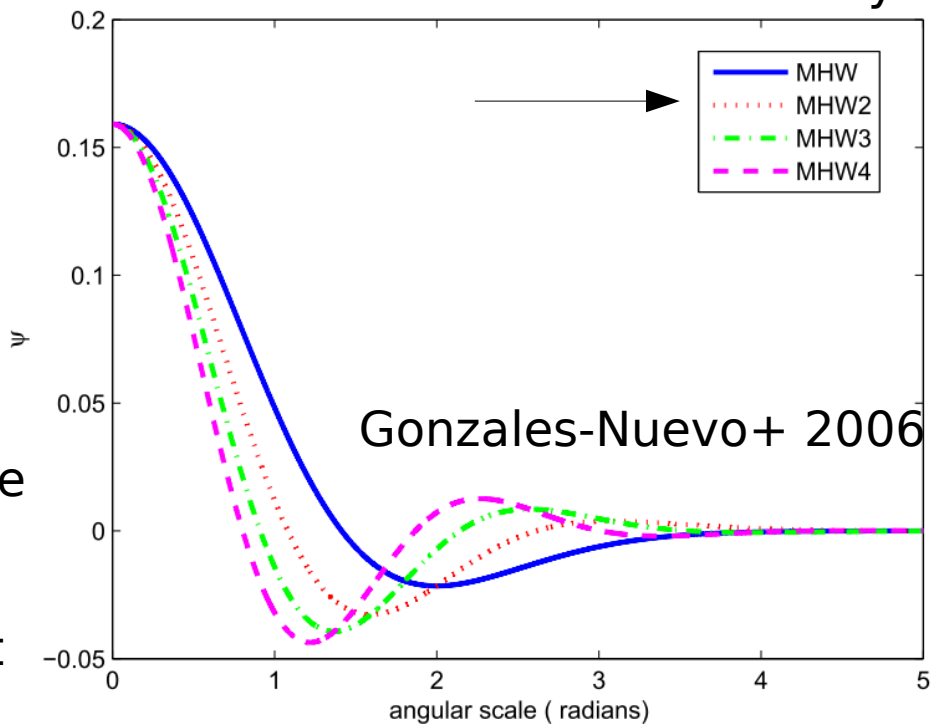

- We adopt the 2nd of the Mexican Hat Wavelet Family, which was shown to have a good performance w.r.t. background variations
  (used by Planck for detection of compact radio sources, Ade+ 2013)

- Instead of fluxes, we consider the signal-to-noise ratio (SNR) defined by

$$\mathcal{S}(\Omega) \equiv \frac{\mathcal{F}_{\mathcal{W}}[\mathcal{C}](\Omega)}{\sqrt{\mathcal{F}_{\mathcal{W}^2}[\mathcal{C}](\Omega)}}$$

On sufficiently smooth data sets, and for a large number of photons, this behaves approximately like a normal distribution
→ Smoothed Gaussian random

- Peak identification is numerically

Wavelet transform of inner Galaxy data

Image color: Value of normalized wavelet transform
Black circles: Wavelet SNR peaks with values above 2 (circle area ~ *S*)
Red circles: 3FGL sources for comparison (circle area ~ sqrt(TS) in 1-3 GeV band)
Green crosses: Unmasked sources (MSP-like)
Dashed lines: Spatial bins for likelihood analysis

Bartels, Krishnamurthy, CW 2015

Based on:
Pass8 Fermi LAT data
Ultraclean events
Front+back converted
6 ½ years of data
1-4 GeV range

Masked disk
|b|>2 deg

Artifacts around bright sources (removed in later analysis)
→ Except for bright sources (where noise estimates includes source flux), we find good agreement between sqrt(TS) and S.

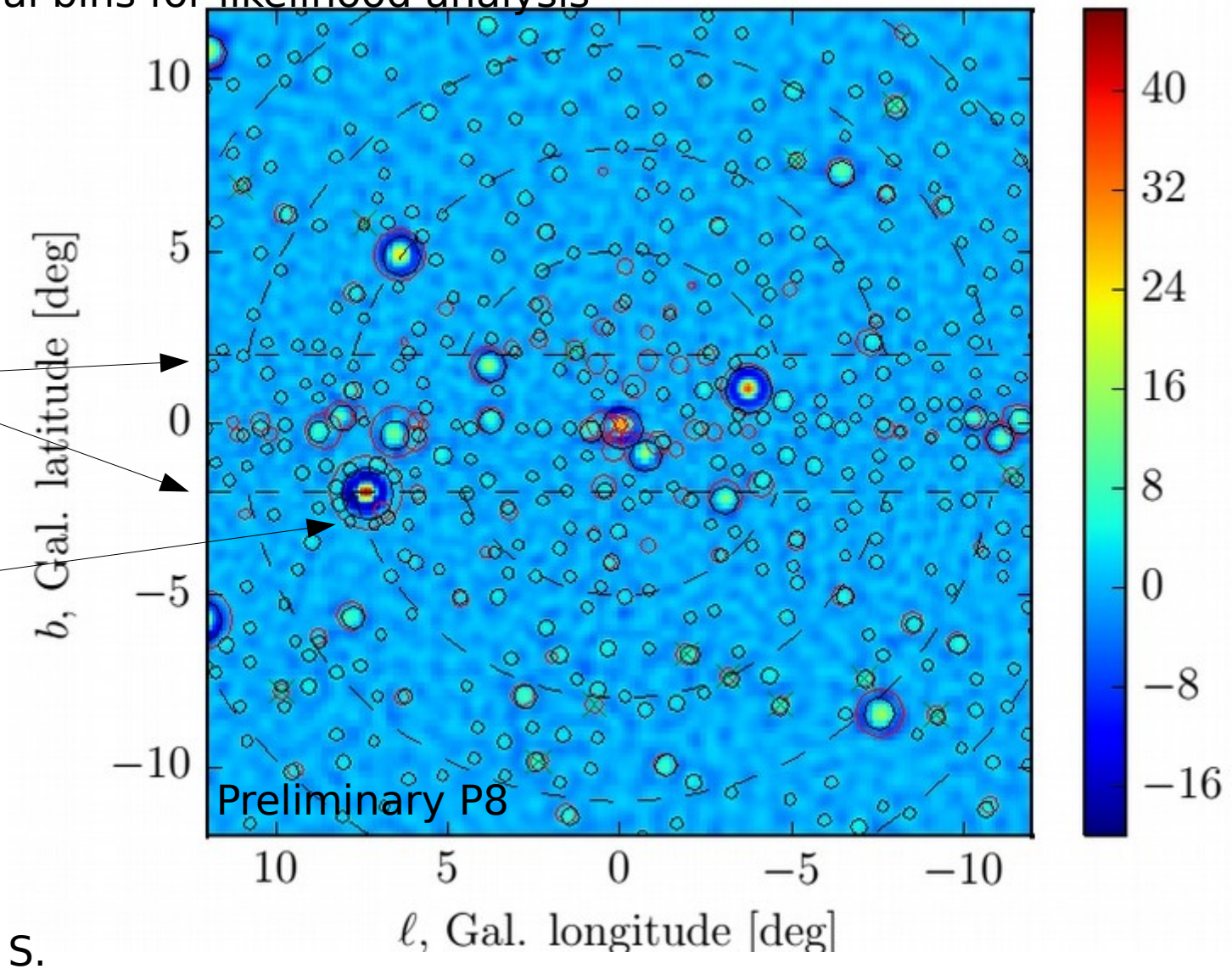

Histogram of peaks and MC results

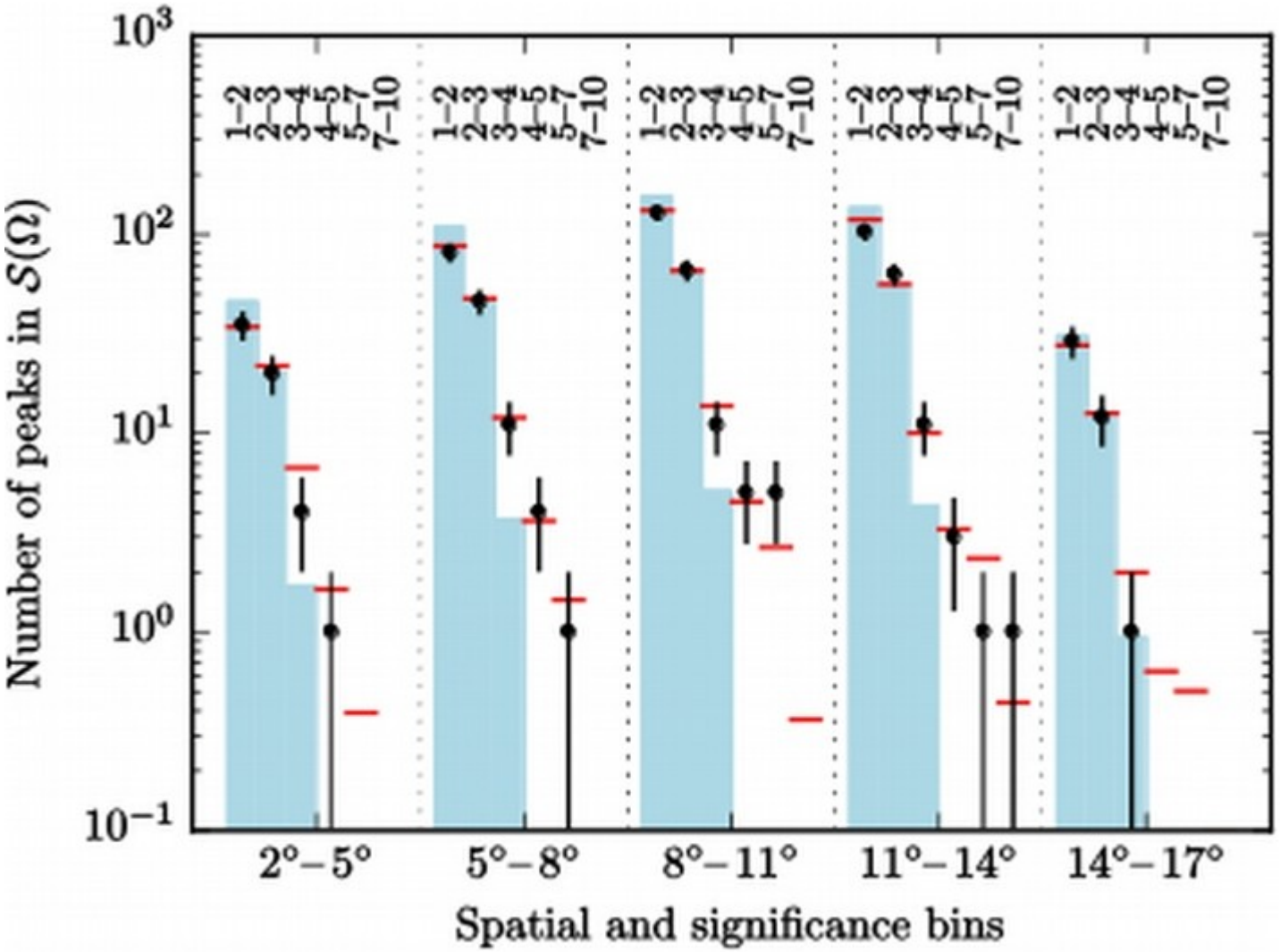

Histogram

- **Error bars:** inner Galaxy data

Null-hypothesis

- **Red**: null-hypothesis
- **Gray**: Control region results

Fit for norm and Lmax

- **Green**: best-fit

→ 8.3 sigma significance

MC predictions + simple estimates for disk population

We use a common maximum likelihood analysis (assuming that peaks are Poissonian distributed) to perform parameter estimation for the luminosity function:

$(L_{\max}, n_{\mathrm{MSPs}})$

Best-fit contours agree with MSP expectations

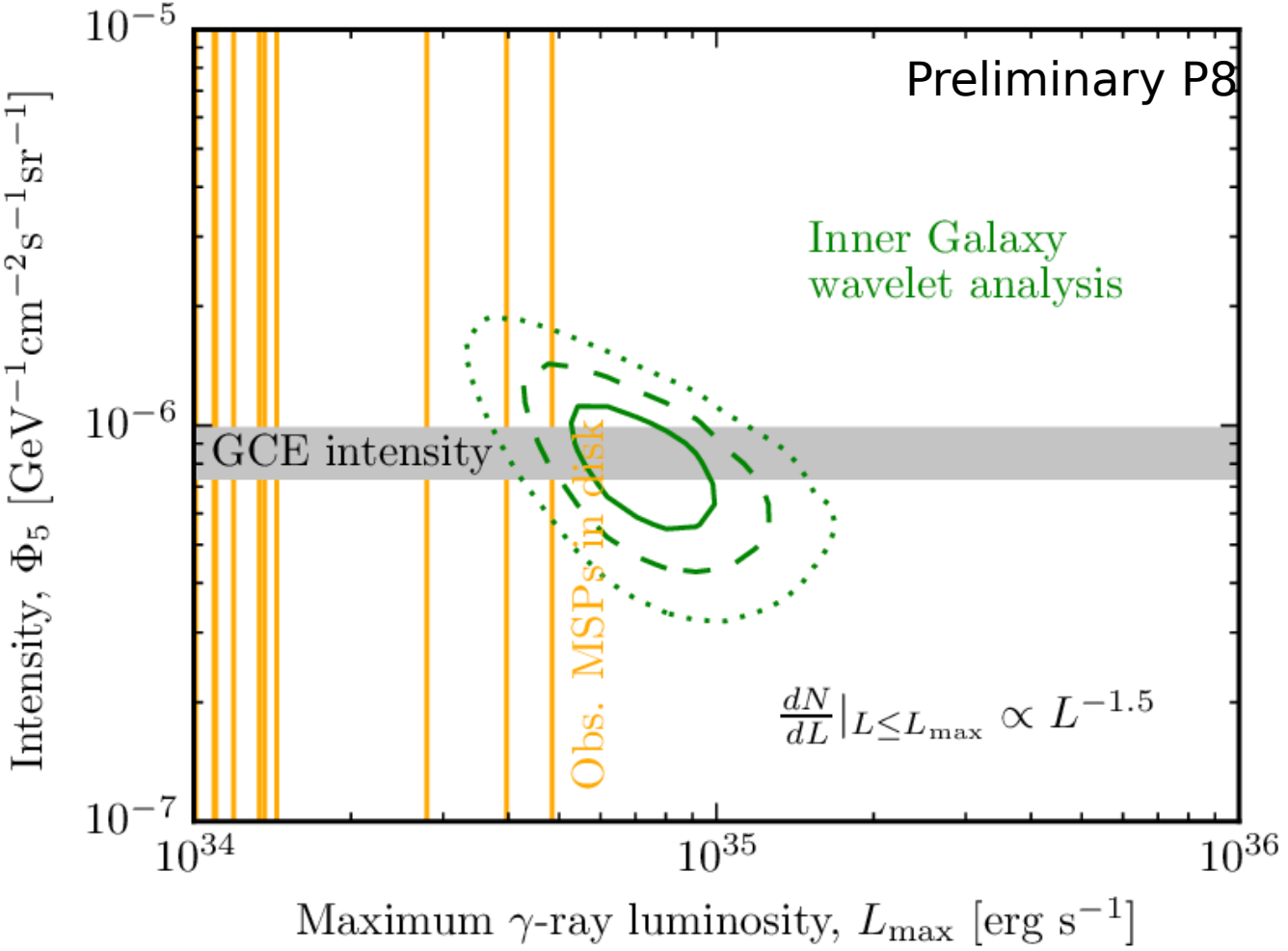

Results

- For a luminosity function index around 1.5, a MSP population with the best-fit normalization would reproduce 100% of the excess emission
- The best-fit cutoff luminosity is compatible with gamma-ray emission from detected nearby MSPs (beware of large uncertainties due to uncertainties in the distance measure, Petrovic+ 2014, Brandt & Kocsis 2015)

Many things that one can check

Concentrated inner Galaxy

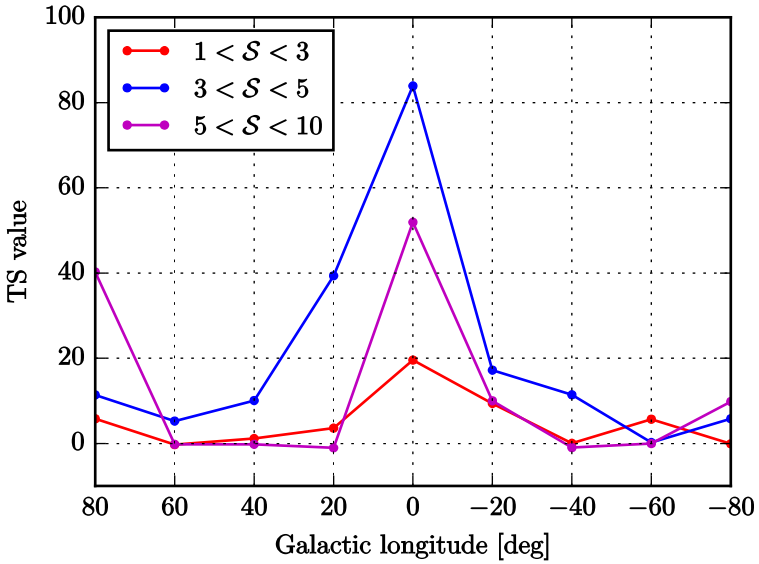

Likely MSPs

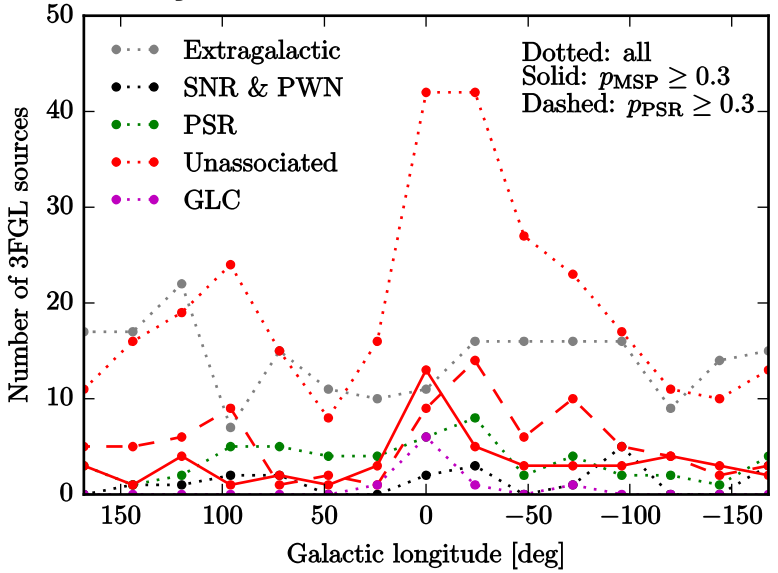

Weak dependence on dN/dL

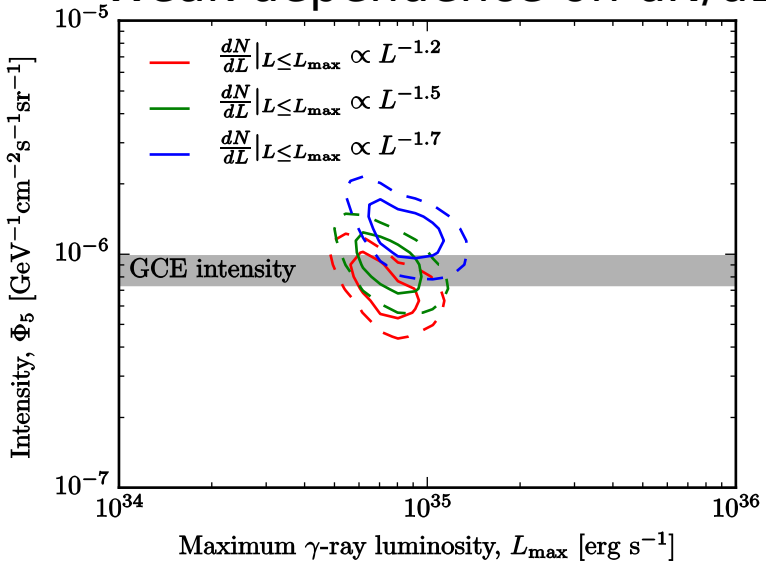

Self consistent in sub ROIs

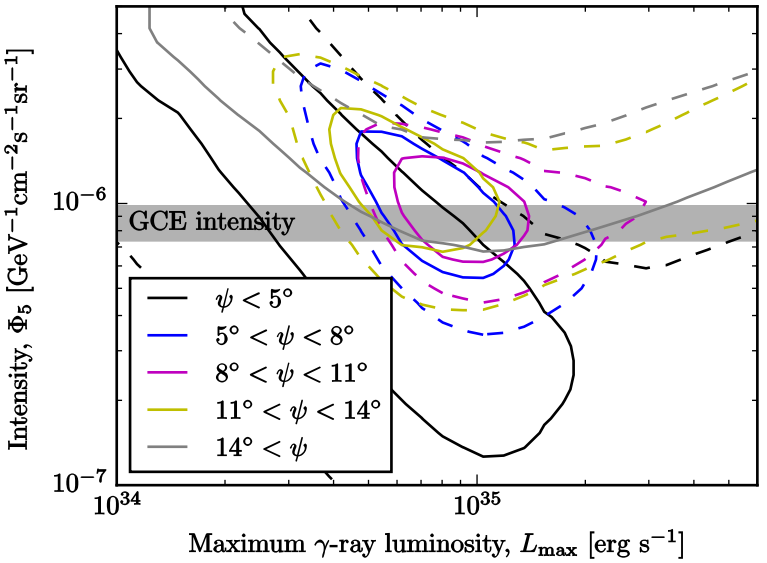

Conclusions

- There *is* a strong excess of ~GeV gamma-rays in the inner Galaxy, above expectations from *a priori* diffuse emission models (i.e. without CR sources in the inner Galaxy)

- Excess emission could be partly due to standard diffuse emission (e.g. associated with the central molecular zone), and partly to other components

- The excess as a whole resembles very well a vanilla signal from DM annihilation

- Millisecond pulsars
  - are the arguably most likely explanation of a large part of the excess emission
  - corroborating evidence for this is found by dedicated searches for sub-threshold source populations in the inner Galaxy
  - → Next thing is to try to find them in radio